# Student Poster Book of Abstracts

***201ψ IEEE Power and Energy Society***

***Transmission and Distribution Conference and Exhibition***

***Chicago, Illinois April 14-17 201ψ***

## IEEE PES Student Activities Subcommittee

**Chair**
Dr. Anurag K Srivastava
Assistant Professor
School of Electrical Engineering and Computer Science
Washington State University
PO Box 642752
EME 102
Spokane St Pullman
Washington 99164-2752, USA
asrivast@eecs.wsu.edu

**Vice-Chair**
Dr. Jignesh M. Solanki
Assistant Research Professor
Lane Department of Computer Science and Electrical Engineering
West Virginia University
395 Evansdale Drive,
Morgantown, WV 26506-6109, USA
jmsolanki@csee.wvu.edu

**Secretary**
Dr. Aaron St. Leger
Assistant Professor
Department Electrical Engineering and of Computer Science
United States Military Academy
646 Swift Road
West Point, NY 10996-1905, USA
Aaron.StLeger@usma.edu

**Webmaster**
Dr. Jignesh M. Solanki
Assistant Research Professor
Lane Department of Computer Science and Electrical Engineering
West Virginia University
395 Evansdale Drive,
Morgantown, WV 26506-6109, USA
jmsolanki@csee.wvu.edu

## Smart Sensors, Communication and Control in Energy Systems

| No. | Student Reg. No. | T & D Reg. No. | Title of Posters | Student Name | Grad/Undergrad |
|---|---|---|---|---|---|
| 1 | 1110 | 14-7976 | Real-Time HIL Simulation of Shipboard Power System (SPS) and Energy Storage Devices (ESD) Management | Dingyi Li | MS |
| 2 | 1123 | 14-8303 | Designing An Open-Source Phasor Measurement Unit with C37.118 Compliance | Brad Tuffley | BS |
| 3 | 1078 | 14-6641 | Optimal PMU Placement for Fault Observability in Distributed Power System by Using Simultaneous Voltage and Current Measurements | Hamidreza Nazaripouya | PhD |
| 4 | 1087 | 14-7157 | A MATLAB Based Fault Detection in Phasor Measurement Unit (PMU) Measurements | Anupam Mukherjee | MS |
| 5 | 1140 | 14-8591 | Distributed Excitation Control for Future Cyber Physical Energy Systems | Meimanat Mahmoudi | PhD |
| 6 | 1143 | 14-8708 | Investigating Synchrophasor Data Quality Issues | Kenta Kirihara | MS |
| 7 | 1091 | 14-7430 | PMU Based Proportional-Integral Damping Controller To Enhance Power System Stability | Saad Elasad | BS |

## Smart Grid Technology

| No. | Student Reg. No. | T & D Reg. No. | Title of Posters | Student Name | Grad/Undergrad |
|---|---|---|---|---|---|
| 8 | 1117 | 14-8027 | Coordinated Electric Vehicle Charging Solutions Using Renewable Energy Sources | Kumarsinh Jhala | MS |
| 9 | 1017 | 14-4856 | An Optimal Framework for Residential Load Aggregators | Qinran Hu | PhD |
| 10 | 1086 | 14-6509 | Agent based State Estimation in Smart Distribution Grid | S M Shafiul Alam | PhD |
| 11 | 1107 | 14-7952 | Burns & McDonnell - K-State Smart Grid Laboratory: Protection, Communication & Power Metering -Integrated Smart Grid Laboratory | Emilio C.Piesciorovsky | PhD |
| 12 | 1137 | 14-8618 | Incentive Based Demand Response in WECC 240-Bus System to Minimize Price Variation | Ailin Asadinejad | PhD |
| 13 | 1166 | 14-8825 | Benefits of using PEV vehicles in PRT systems and modifying vehicle routing problem | Ali Dehghan Banadaki | PhD |

## Cyber and Physical Security of Smart Grid

| No. | Student Reg. No. | T & D Reg. No. | Title of Posters | Student Name | Grad/Undergrad |
|---|---|---|---|---|---|
| 14 | 1162 | 14-8807 | False Data Attack on State Estimation in Smart Grid | Deepak Tiwari | PhD |
| 15 | 1165 | 14-8828 | Effect of Stealth Data Attack on AC Optimal Power Flow | Behnam Khaki | PhD |
| 16 | 1170 | 14-8834 | Cyber-Security Valunerablity Assessment of the Smart Grids | Reza Kazemi | PhD |
| 17 | 1145 | 14-8297 | NISTIR 7628 Visualization Model | Matthew Harvey | BS |

## Geometric Disturbance in Electric Power Systems

| No. | Student Reg. No. | T & D Reg. No. | Title of Posters | Student Name | Grad/Undergrad |
|---|---|---|---|---|---|
| 18 | 1100 | 14-7970 | Effects of Micro-Structured Surface Geometries on Condensation Heat Transfer | Andrés Martínez | BS |

## Advanced Computational Methods for Power System Planning, Operation, and Control

| No. | Student Reg. No. | T & D Reg. No. | Title of Posters | Student Name | Grad/Undergrad |
|---|---|---|---|---|---|
| 19 | 1073 | 14-5852 | Optimal Strategy for Minimizing Load Shedding in Microgrids subsequent to Fault-Triggered Islanding | Shanshan Ma | MS |
| 20 | 1013 | 14-3206 | A Hybrid Dynamic Optimization Approach for Stability Constrained Optimal Power Flow | Guangchao Geng | PhD |
| 21 | 1026 | 14-4967 | Reactive Power Planning Considering High Penetration Wind Energy | Xin Fang | PhD |
| 22 | 1032 | 14-4907 | Interval Power Flow Using Linear Relaxation and Optimality-based Bounds Tightening (OBBT) Methods | Tao Ding | PhD |
| 23 | 1033 | 14-5003 | Exploration of Multifrontal Method with GPU in Power Flow Computation | Xue Li | PhD |
| 24 | 1036 | 14-4904 | Multi-objective Robust Optimization Model for Microgrids Considering Tie-line Power Constraints and Wind Uncertainty | Linquan Bai | PhD |
| 25 | 1105 | 14-8063 | Impact of Load Models on the Statistics of Voltages in Stochastic Power Systems | Goodarz Ghanavati | PhD |
| 26 | 1126 | 14-8396 | Power Management of Remote Microgrids Considering Stochastic Behavior of Renewable Energy Sources | Santosh Chalise | PhD |
| 27 | 1146 | 14-8654 | Flue Gas Desulfurization Wastewater Treatment Using Constructed Wetlands | Jose M. Paredez | BS |
| 28 | 1157 | 14-8798 | Optimal Power Flow Including Magnetic Amplifier by Using Sequential Quadratic Programming | Xiaohu Zhang | PhD |

## Emerging Software Needs for the Restructed Grid

| No. | Student Reg. No. | T & D Reg. No. | Title of Posters | Student Name | Grad/Undergrad |
|---|---|---|---|---|---|
| 29 | 1150 | 14-8777 | NMSU Power Generating Capacity: Vision and Roadmap for 2050 | Aaron Rosenthal | MS |

## System-Wide Events and Analysis Methods

| No. | Student Reg. No. | T & D Reg. No. | Title of Posters | Student Name | Grad/Undergrad |
|---|---|---|---|---|---|
| 30 | 1159 | 14-8804 | Power System Events Identification using Feature Selection and Extraction Techniques | Prem Alluri | MS |
| 31 | 1011 | 14-3077 | Locating Sub-Cycle Faults in Distribution Network Applying Half-Cycle DFT Method | Po-Chen Chen | PhD |
| 32 | 1175 | 14-8840 | A Lyapunov Function Based Remedial Action Screening Tool Using Real-Time Data | Mohammed Benidris | PhD |

## Intelligent Monitoring and Outage Management

| No. | Student Reg. No. | T & D Reg. No. | Title of Posters | Student Name | Grad/Undergrad |
|---|---|---|---|---|---|
| 33 | 1004 | 14-3041 | Development of an FPGA based controller for islanding and anti-islanding of microgrid | Kumaraguru Prabakar | PhD |
| 34 | 1080 | 14-6797 | Development of Graphical User Interface for Reactive Power Planning and VAR Benefit Assessment for Power Systems with High Penetration of Renewable Energy | Riyasat Azim | PhD |
| 35 | 1183 | 14-14831 | Synchrophasor monitoring of line outages in WECC with an angle across an area | Atena Darvishi | PhD |

## Integrating Renewable Energy into the Grid

| No. | Student Reg. No. | T & D Reg. No. | Title of Posters | Student Name | Grad/Undergrad |
|---|---|---|---|---|---|
| 36 | 1181 | 14-8717 | Optimization Active Power Curtailment (APC) with Load Tap changing (OLTC) Regulators to Control Voltage fluctuating in Renewable supply | Hameed R. Atia | PhD |
| 37 | 1031 | 14-3842 | A Wavelet-Based Method for High Resolution Multi-Step PV Generation Forecasting | Ahlmahz Negash | PhD |
| 38 | 1042 | 14-4901 | Emission-based Optimal Dispatch Framework with DR and Volatile Wind Power | Hantao Cui | PhD |
| 39 | 1055 | 14-3212 | Energy Resource Scheduling in Real Time Considering a Real Portuguese Generation and Demand Scenario | Pedro Faria | PhD |
| 40 | 1089 | 14-7142 | Renewable Energy Forecasting using Hybrid Artificial Neural Network Technique | Chiranjeevi Bharadwaj Kotharu | MS |
| 41 | 1124 | 14-8255 | Harmonic Analysis in Distribution System with Electric Vehicles and Wind Generators | Ritam Misra | MS |
| 42 | 1125 | 14-8369 | Optimization of a Solar-Diesel-Battery Hybrid Energy System for Remote Regions | Mu Chai | BS |
| 43 | 1131 | 14-8480 | Integration of Photovoltaic with Hydro only System in an Isolated Network | Pratiksha Tiwari | MS |
| 44 | 1149 | 14-8177 | Locational Dependence of PV Hosting Capacity | Kyle Coogan | MS |
| 45 | 1179 | 14-8843 | An Analytical Method for Constructing a Probabilistic Model of a Wind Farm | Samer Sulaeman | PhD |

## Substation and Distribution Automation

| No. | Student Reg. No. | T & D Reg. No. | Title of Posters | Student Name | Grad/Undergrad |
|---|---|---|---|---|---|
| 46 | 1034 | 14-4886 | Dynamic Compensation of Electronic Transformer Phase Delay | Can Huang | PhD |
| 47 | 1070 | 14-5870 | A Multi-Agent Design for Power Distribution Systems Automation | M. Jawad Ghorbani | PhD |
| 48 | 1184 | 14-14660 | An Online Algorithm for Health Diagnosis and Prognosis of Circuit Breaker | Saugata Biswas | PhD |

## Dynamic Performance and Control of Power Systems

| No. | Student Reg. No. | T & D Reg. No. | Title of Posters | Student Name | Grad/Undergrad |
|---|---|---|---|---|---|
| 49 | 1127 | 14-8429 | Improvement of Transient Stability of PV-Hydro System Using Virtual Synchronous Machines | Ujjwol Tamrakar | MS |
| 50 | 1156 | 14-8543 | An Out-Of-Step Detection of Multi-machine Power System using PMU Data | Yawei Wei | MS |
| 51 | 1164 | 14-8816 | Sequential Learning Function applied to the design and tuning of a Fuzzy Controller for VSC | Ivan Riaño | BS |
| 52 | 1039 | 14-5078 | PMU-Based Wide Area PSSs to Enhance the Damping of Inter-Area Oscillations | Duaa Abumaali | MS |

## Market Interactions in Power Systems

| No. | Student Reg. No. | T & D Reg. No. | Title of Posters | Student Name | Grad/Undergrad |
|---|---|---|---|---|---|
| 53 | 1035 | 14-4988 | LMP Step Pattern Detection based on Real-Time Data | Haoyu Yuan | PhD |
| 54 | 1098 | 14-7931 | Customer Incentive Pricing Mechanism in the Smart Grid | Timothy Hansen | PhD |
| 55 | 1132 | 14-8483 | Distribution Locational Marginal Price using Optimal Three-phase Current Injection Power Flow | Jie Wei | MS |

## Asset Management

| No. | Student Reg. No. | T & D Reg. No. | Title of Posters | Student Name | Grad/Undergrad |
|---|---|---|---|---|---|
| 56 | 1173 | 14-8750 | Discharge Energy Based Stage Classification of Cavity Partial Discharge in Oil-Paper Insulation | Zhenze Long | MS |
| 57 | 1101 | 14-5279 | Impact of Voltage Reduction and Ambient Temperature on Power Consumption, Line Loss and Generation | Sushanta Paul | PhD |

## Flexible AC Transmission Systems

| No. | Student Reg. No. | T & D Reg. No. | Title of Posters | Student Name | Grad/Undergrad |
|---|---|---|---|---|---|
| 58 | 1029 | 14-4895 | Adaptive PI Control of STATCOM for Voltage Regulation | Yao Xu | PhD |

## Power Electronics

| No. | Student Reg. No. | T & D Reg. No. | Title of Posters | Student Name | Grad/Undergrad |
|---|---|---|---|---|---|
| 59 | 1046 | 14-3464 | Control of Hybrid Tripole HVDC Based on LCC and F-MMC | Feng Xu | PhD |
| 60 | 1088 | 14-7154 | A Total Harmonic Distortion (THD) computation using improved Shunt Active Power Filter Design in Energy Management Systems | Ranganath Vallakati | MS |
| 61 | 1171 | 14-8714 | PV Current Harmonic Suppression Under Unbalanced Fault Based on Factor Selection Control | Xiaoxuan Lou | MS |

## Electric Machine and Drives

| No. | Student Reg. No. | T & D Reg. No. | Title of Posters | Student Name | Grad/Undergrad |
|---|---|---|---|---|---|
| 62 | 1079 | 14-6719 | Harmonic filtering phenomenon in single phase induction motors | Gaurav Singh | PhD |

## Power System Modeling and Simulation

| No. | Student Reg. No. | T & D Reg. No. | Title of Posters | Student Name | Grad/Undergrad |
|---|---|---|---|---|---|
| 63 | 1054 | 14-0404 | Modeling and Simulation of a High-Head Pumped Hydro System | Hang Li | MS |
| 64 | 1108 | 14-8075 | Developing Integrated Load Modeling Framework for Campus Microgrids with Large Buildings | Sayonsom Chanda | PhD |
| 65 | 1172 | 14-8837 | Dynamic Modeling and Analysis on Cut-in Grid of Doubly-fed Induction Wind Power System | Sibei Mi | MS |

# Real-Time HIL Simulation of Shipboard Power System (SPS) and Energy Storage Devices (ESD) Management

Dingyi Li and Dr. Noel N. Schulz
Department of Electrical and Computer Engineering
Kansas State University
Manhattan, KS
Email: dingyi@ksu.edu

***Abstract* - There are many situations that can cause a fault on a shipboard power system, especially in naval battleships. Batteries and ultra-capacitors are simulated to be the backup energy storage devices (ESDs) to power the shipboard power system when an outage and damage happen. ESDs are commonly being used for electrical ship applications, due to carious advantages, such as: guaranteed load leveling, good transient operation and energy recovery during braking operation. To fulfill these requirements converters with specific control algorithm are required to connect the ESDs to the dc link of the motor drive system. SPS is required to function in three different modes namely: steady-state (normal) mode, acceleration mode and braking (regenerative) mode. During acceleration mode the power flow is from ESDs to SPS whereas during regenerative mode the kinetic energy of the motor is converted into electrical energy and fed back to battery. Also, generators inside of SPS can charge the battery packs under normal mode when the State-Of-Charge (SOC) level of battery packs are below the standard level. The SPS and ESDs which include battery packs and ultra capacitors are simulated and verified through the simulations by using Matlab Simulink. In this research, the real-time hardware-in-the-loop (HIL) simulation of shipboard power system (SPS), bidirectional DC-DC converter, and ESDs are being designed, implemented and controlled on OPAL-RT simulator to test the performance of SPS and ESDs in different fault locations.**

***Key words* – HIL; real-time; SPS; ESDs management; bidirectional DC-DC converter**

# Designing An Open-Source Phasor Measurement Unit with C37.118 Compliance

Brad Tuffley, *Student Member*, *IEEE*
Douglas Rapier, *Student Member*, *IEEE,*
Anurag K. Srivastava, *Senior Member*, *IEEE*
Smart Grid Demonstration and Research Investigation Lab, Washington State University

*Email: btuffley@eecs.wsu.edu, drapier@eecs.wsu.edu, asrivast@eecs.wsu.edu*

***Abstract*— IEEE Standard C37.118 outlines standards for collecting time aligned voltage and current phasors by using a Phasor Measurement Unit (PMU). Some of the performance criterion include Total Vector Error (TVE), Frequency Error (FE), and Rate of Change of Frequency Error (RFE) are defined by this Standard. However, due to technologically different approaches, each manufacturer uses different estimation algorithms to derive their PMU data. The purpose of this project is to develop a prototype of advanced open source PMU, which can be used as a platform to test various phasor estimation algorithms for different power system operating conditions. The open source nature will allow for versatile PMU testing given unique algorithms and specifications. Support for this project comes from Washington State University (WSU) and the U.S. Department of Energy (DOE).**

## I. Key Equations

Total Vector Error (TVE).

$$\mathrm{TVE(n)} = \sqrt{\frac{(\hat{X}_r(n)-X_r(n))^2+(X_i(n)-X_i(n))^2}{(X_r(n))^2+(X_i(n))^2}}. \quad (1)$$

Frequency Measurement Error (FE).

$$\mathrm{FE} = |f_{ture} - f_{measured}| = |\Delta f_{ture} - \Delta f_{measured}| \quad (2)$$

ROCOF Measurement Error (RFE).

$$\mathrm{RFE} = |(df/dt)_{ture} - (df/dt)_{measured}| \quad (3)$$

## II. Key Figures

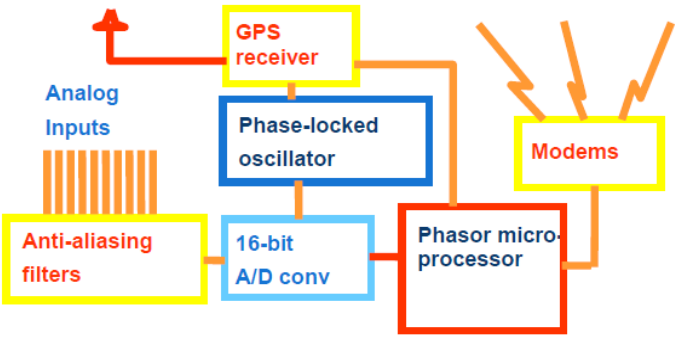


Figure 1 Shows the typical PMU components used today in order to capture and relay phasor data.

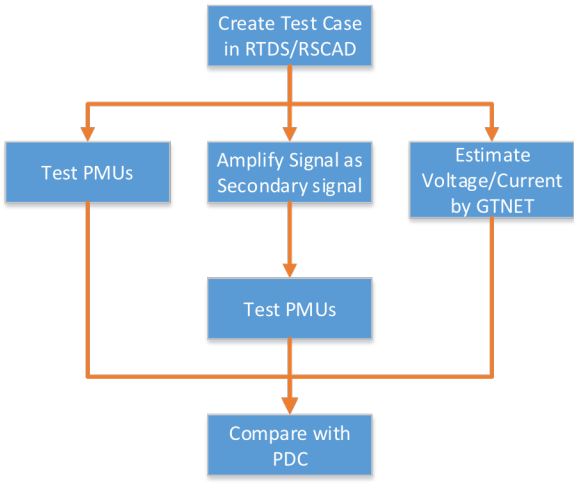


Figure 2. Outlines the basic process diagram that is currently used for PMU Testing.

# Optimal PMU Placement for Fault Observability in Distributed Power System by Using Simultaneous Voltage and Current Measurements

H. Nazaripouya[1] and S. Mehraeen[2], *Member, IEEE*

***Abstract*—This paper proposes a new strategy to achieve fault observability of power systems while aiming minimum required number of Phasor Measurement Units (PMUs) in the network. The proposed method exploits the nodal voltage and mesh current analyses where the impedance and admittance matrices of the network and its dual circuit are developed and utilized for fault location. The criterion of determining the number and the places of PMUs is to be able to obtain the fault location and impedance in a unique manner (i.e., without multi estimation.) In addition, the method considers faults along the lines as opposed to the faults only on system buses available in the literature. The proposed approach provides an economical solution to decrease measurement costs for large power networks, distributed generation networks, and micro grids. Simulation results for IEEE 7-bus, 14-bus, and 30-bus systems verify the effectiveness of the proposed approach.**

***Index Terms* – Fault Location, Phasor Measurement Unit (PMU), Optimal Placement, Fault Observability.**

## I. Methodology

PMU placement at each bus helps measure the voltage phasor at that bus and the current phasors in all the branches connected to that bus. When a fault occurs in the system, according to the location and impedance of the fault all voltages and currents of the network change including at PMU nodes (busses.) But the problem arises when more than one fault (with possibly different impedances and locations) cause the same change in the voltages and currents at PMU busses. This problem is called multi estimation. The focus of this paper is to find the proper locations for PMUs that reduce multi estimation when faults occur, and to use measured voltage and current changes at the PMU locations to uniquely identify a fault as opposed to the available methods that only rely on voltage measurement/estimation. Here, the concept of "mesh impedance," namely $Z'$, matrix is developed and the mesh equations of the network are obtained. Introducing current measurement can reduce the number of required PMUs.

Authors are with the school of Electrical Engineering and Computer Science, Louisiana State University, Patrick F. Tailor Hall, Dr., Baton Rouge, LA 70803. Contact authors: [1]hnazar1@tigers.lsu.edu. [2]smehraeen@lsu.edu,

This work was supported in part by NSF CAREER ECCS#1151141

## II. Key Figures

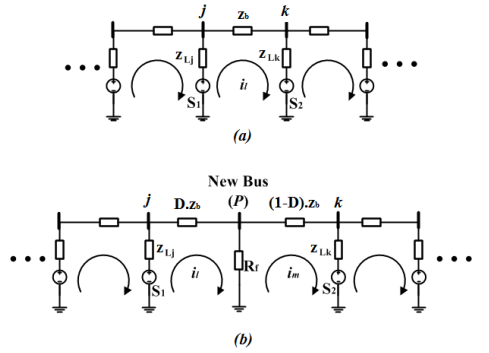


Fig. 1. Power network a) before the fault b) after the fault on point *p*

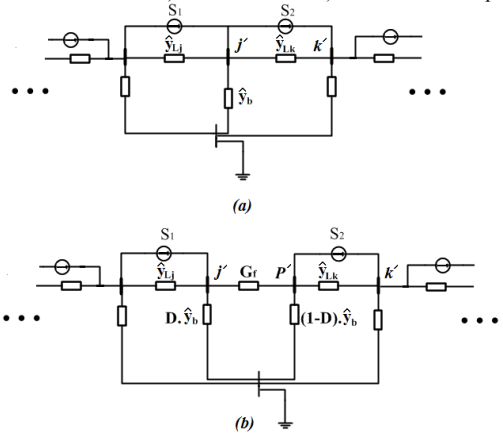


Fig. 2. Part of dual circuit of the power system a) before the fault b) after the fault on point *P*

## III. Key Results

Table I. Results of applying proposed approach

| Test System | Based on Voltage change only | Based on both Voltage and current change | | |
|---|---|---|---|---|
| | # undesired sectors | # undesired sectors | # PMUs | Location |
| **IEEE 7 Bus** | 30 | 2 | 1 | Bus 1 or 2 or 4 or 5 or 7 |
| **IEEE 14 bus** | 115 | 40 | 1 | Bus 1 or 2 or 4 or 5 |
| **IEEE 30 bus** | 405 | 162 | 2 | Bus 10 and 25 |

Table II. Comparison between proposed approach and prior approach

| Test System | Number of PMUs | |
|---|---|---|
| | Prior Approach | Proposed Approach |
| **IEEE 7 Bus** | 5 | 1 |
| **IEEE 14 bus** | 8 | 1 |
| **IEEE 30 bus** | 17 | 2 |

# A MATLAB Based Fault Detection in Phasor Measurement Unit (PMU) Measurements

Anupam Mukherjee, *IEEE student member* and Prakash Ranganathan, *IEEE Senior Member*
Electrical Engineering Department, University of North Dakota, Grand Forks, USA
email: anupam.mukherjee@my.und.edu

***Abstract*—Fault detection, isolation and correction in an electrical grid have always been the critical tasks for ensuring maximum transfer of electric power to loads. The phasor measurement units (PMU) or Digital Fault Recorders (DFR) has been in the forefront to monitor the phasor voltages, current and frequency parameters in the transmission lines for detection faults[1]. With increase in frequency of outages, weather related disturbances; the percentage of fault occurrence has increased dramatically. This poster work focuses on the detection of transmission line errors using the PMU data set. A MATLAB based PMU testbed is developed, and tested for generation and detection of faults affecting an electric signal [2]. The design parameters include 1) amplitude, 2) frequency and 3) phase deviations.**

**Keywords: PMU, Fault detection, MATLAB**

## I. Introduction

In our experiments, simulation test beds were developed to detect deviation of the PMU parameters. The simulations have been discussed briefly.

### *A. Amplitude Deviation Setup*

A functional representation of the three phase AC signal can be shown as in (1) and (2).

$$V = V_a * \sin(2\pi f t + \theta) \quad (1)$$

$$I = I_a * \sin(2\pi f t + \theta) \quad (2)$$

We consider the voltage signal $(V)$, where $(V_a)$ is the amplitude, $(f)$is the frequency and$(\theta)$is the phase angle. In the transmission line $(V_a)$ can be monitored for any deviation from a reference value$(V_{ref})$, which is considered to be value of $(V_a)$under no fault condition.

If, $|(V_a - V_{ref})| \geq 0.05 * (V_{ref})$ at any instance, then the deviation is considered to be due to a fault in the line. Here, $0.05 * (V_{ref})$ is a randomly chosen value.

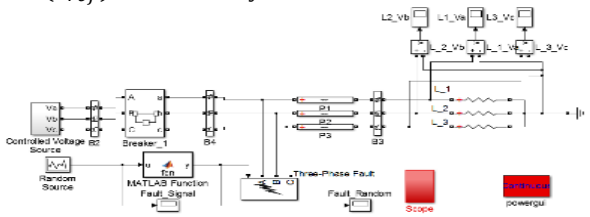

Fig 1. Test Bed to monitor amplitude deviation

### *B. Frequency Deviation Setup*

Faults in the system can cause the frequency of the signal to deviate from the acceptable value$(f_{ref})$. The frequency $(f)$ of the voltage signal can be obtained from the frequency domain representation of the time domain voltage signal. This can be achieved through the application of Fourier transfer function. In the frequency deviations of the voltage signal can then be monitored. The FFT tool of Simulink represents the voltage signal in the frequency domain. It represents the magnitude of the signal$(D_f)$ as a percentage of that of the fundamental frequency $(f_{ref})$ and plots it as a function of the varying frequency$(f)$. Value of $(D_f)$ is constant for a given frequency. If the value of $(D_f)$ at $(f_{ref})$is considered to be$(D_{fref})$, then any deviation of$(D_f)$from $(D_{fref})$will give us an equivalent deviation of $(f)$from$(f_{ref})$, as shown in (3).

$$(D_f - D_{fref}) \equiv (f - f_{ref}) \quad (3)$$

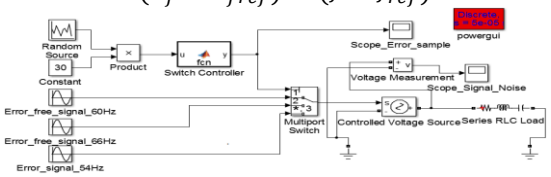

Fig. 2 Test Bed to monitor frequency deviation

### *C. Phase Deviation Setup*

The deviation in phase $(\Delta\theta)$ can be calculated by performing a cross correlation function between the line voltage signal $(V)$ and a reference voltage signal $(V_{ref})$, shown in (4).

$$V_{ref} = V_{aref} * \sin(2\pi f_{ref} + \theta_{ref}) \quad (4)$$

Considering (f= $f_{ref}$) and$V_a = V_{aref}$, the cross correlated signal can be represented as shown in (5).

$$R_{xy} = (V_{aref} * V_a/2) * [\cos(\theta_{ref} - \theta) - \sin(2 * 2\pi f t + \theta_{ref} + \theta] \quad (5)$$

From this signal, the higher order frequencies can be filtered using a low-pass filter (LPF). Let us denote the resulting frequencies by $(S_\theta)$. The term remaining after filtering is$(V_a * V_a/2) * \cos(\theta_{ref} - \theta)$. Thus, the phase deviation $(|\Delta\theta|)$can be calculated as shown in (6).

$$|\Delta\theta| = arcos(2 * S_\theta/(V_a * V_a/2)) \quad (6)$$

.

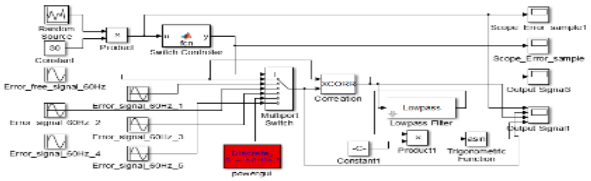

Fig, 3. Test Bed to monitor Phase Deviation

## II. References

[1] A.G.Phadke and Bogdan Kasztenny, "Synchronized Phasor and Frequency Measurement Under Transient Conditions," IEEE Trans. Power Delivery, vol. 24, no.1, pp. 89-95, 2009.
[2] www.mathworks.org

# Distributed Excitation Control for Future Cyber Physical Energy Systems

Meimanat Mahmoudi, Kevin Tomsovic, Seddik Djouadi and Husheng Li
Department of Electrical Engineering and Computer Science
University of Tennessee, Knoxville, 37996

***Abstract*--Integration of cyber technologies capable of monitoring, communicating, and controlling the electric power system, renders the smart grid one of the most complex cyber physical systems. For the smart grid to be resilient to disturbances, wide-area monitoring and control is a necessity. While local controllers are blind to the widespread effects of disturbances and centralized controllers are challenging to implement, distributed controllers can achieve a trade-off between performance and associated cost. In this work, the design and performance of two distributed excitation control schemes are presented. We show that distributed control can help prevent disturbances from propagating in large power networks. Moreover, we demonstrate the effectiveness of distributed control in damping inter-area oscillations. In order to highlight the advantages of the proposed controllers, results are compared with local and centralized control schemes.**

***Index Terms*--Cyber-physical systems, distributed control, smart grid, and wide-area control.**

## I. Introduction

THE next generation of electricity grid, also known as the "Smart Grid" , is one of the most complex cyber physical systems (CPS) due to its extreme dimension, geographic reach and high reliability requirements. For the smart grid to be resilient, wide-area monitoring and control is a necessity. The interconnected structure of the power grid poses a great risk of system-wide failures in the network. A local disturbance can influence the system over a wide area and lead to cascading failures and blackouts. Prior to the introduction of real-time phasor measurement units (PMUs) power system control was primarily local. Except for the very slowest of controllers and a few specialized schemes, engineers have designed systems largely through local decisions based on local measurements. Due to the lack of observability in local measurements of certain inter-area modes, existing control schemes may fail to deliver the expected performance and reliability. Therefore, using wide-area measurements becomes a key element in designing control.

The purpose of this research is twofold. First, we show that distributed control can help prevent disturbances from propagating in large power networks. In doing so, we used the continuum model test systems. Second, we demonstrate the effectiveness of distributed control in damping inter-area oscillations and compare the results with the performance of local and centralized control schemes. For this, we use a two-area four machine test system which has been widely used for analysis of inter-area modes. Due to the distributed nature of the design, communication between local controllers helps to improve the damping of inter-area modes, which are not readily apparent for the local controller. Moreover, there is no need to model a large-scale system as a whole and deal with the complexities arising in a centralized scheme.

## II. Distributed Excitation Control for Power Networks

### A. Distributed LQR Excitation Control Design

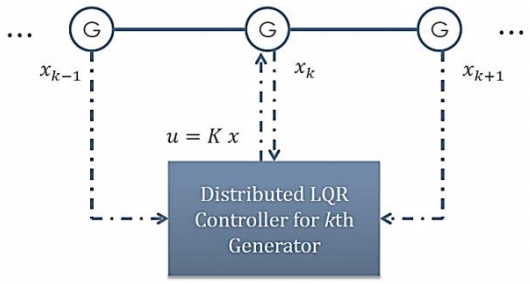


Fig. 1. Distributed LQR control agent and information exchanges for part of a radial structure.

### B. Distributed Excitation Control with $H_\infty$ Performance

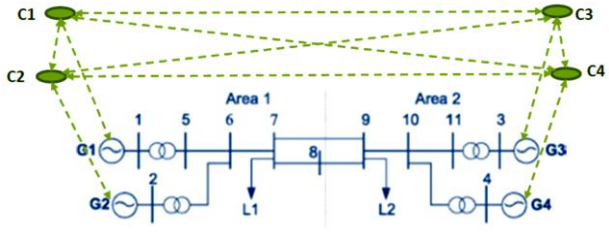


Fig. 2. Physical layer (in blue) and cyber layer (in green) for Two-area four machine test system.

## Acknowledgment

The authors gratefully acknowledge the support of the National Science Foundation through grant CNS-1239366 and support by the Engineering Research Center Program of the National Science Foundation and the Department of Energy under NSF Award Number EEC-1041877 and the CURENT Industry Partnership Program.

# Investigating Synchrophasor Data Quality Issues

Kenta Kirihara, *Student Member, IEEE*, Andy K. Yoon, *Student Member, IEEE*,
Karl E. Reinhard, *Student Member, IEEE*,and Peter W. Sauer, *Fellow, IEEE*
Department of Electrical and Computer Engineering
University of Illinois at Urbana-Champaign
Email: kirihar1@illinois.edu

***Abstract*—Synchrophasor data is a real-time measurement of electrical quantities from across the power grid taken by Phasor Measurement Units (PMUs), which can substantially improve real-time situational awareness and control of the events happening on the power system. Currently, more than 1000 PMUs are installed across North America, computing and storing synchrophasor data at select locations. However, the efforts to process the synchrophasor data to meet very high operator trust expectations has been challenging. This paper describes Synchrophasor Data Quality (SDQ) Activity, Trustworthy Cyber Infrastructure for the Power Grid (TCIPG) Project efforts to investigate synchrophasor data archived from American Transmission Company's system including both observations from the field and evolving efforts to characterize synchrophasor data quality. Methods to identify and utilize synchrophasor characteristics for systems events is investigated with the aid of statistical techniques.**

## I. Overview

Since April 2012, the SDQ Activity has been working with American Transmission Company (ATC) to investigate its archived synchrophasor data. Fig. 1 shows an example nominal synchrophasor data network from the point of measurement to the control room and data archive with four levels and connecting transmission paths. Each level has an identifiable role in computing, processing, and forwarding data to meet power system requirements and as such becomes a possible point of failure. Attributing defective synchrophasor data sources and corresponding error rates is key to prioritizing efforts to improve data quality.

During summer 2013, an SDQ Activity research student worked as an EMS intern working for ATCs synchrophasor system project engineer. His experience working with field synchrophasor data in the field highlighted fundamental challenges to providing very reliable, high integrity, and very accurate synchrophasor data to the system control room. The first challenge was analyzing synchrophasor data flow to identify and classify data error types. There were occurrences in which a single PMU data failed to report to the PDC, or when a group of PMUs that are associated with a PDC failed to report to the data archives. To aid understanding the issues, he developed and implemented an application showing real-time data status at each PMU location on a service area map. This tool enabled the control center to have continuous, real-time situational awareness of data availability.

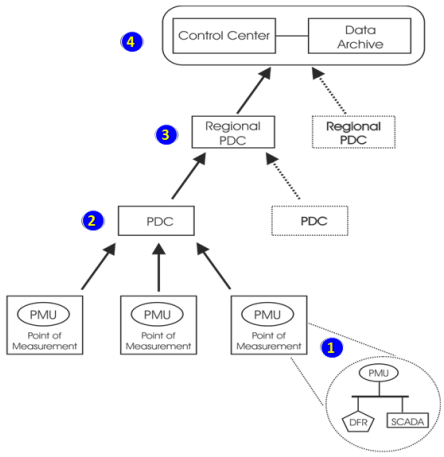


Fig. 1. Example PMU Data Flow [1]

Another challenge was productively using synchrophasor data. The volume of the PMU data collected, which is over 1GB of relevant measurement information per hour, contains a plethora of information. For instance, during an unusual event in a system, the voltage phase may present signature behavior. In order to investigate this, a tool to visualize the phase angle difference through system in both real-time and post-event was created. Having a tool which allows the information to be presented immediately adds value to the data. The tool was also used to compare the PMU angle measurements to the State Estimator derived from the SCADA measurements.

Although both of these solutions were significant steps in developing a utilization of PMUs, the full potential of synchrophasor measurements is far from fully trustworthy. Through the summer internship, ATC and TCIPG researchers gained valuable insights into ATC, which subsequently proved to be invaluable to setting up practical, secure data sharing arrangements between ATC and TCIPG that enable further investigation of synchrophasor data quality.

## References

[1] Research Activity Fact Sheet, Trustworthy Cyber Infrastructure for the Power Grid, Champaign, IL, 2012, pp. 57-59

3) Third, we have modeled the interactions between different decision making entities in energy markets, assuming a game-theoretic framework and considering different objectives for system operators and generation companies [5].
4) Fourth, a bi-level optimization problem that supports renewable energy integration and other social, physical, and technical stakeholders' objectives has been established.

To analyze the proposed CPSS framework, we are currently integrating these cyber, physical, and social aspects of the problems discussed. The development of this CPSS framework will further enhance our understanding of large-scale complex systems and thus build better mechanisms, strategies, and protocols to improve these systems' reliability and welfare.

The proposed framework will be used to analyze different scenarios, such as the analysis of consumer behavior. The main objective of the consumer behavior analysis scenario is to study the behavior of large scale consumers given energy market price fluctuations, under the CPSS framework. We assume that the objective of the consumer is to minimize a certain real-time cost function, that models a utility function of consumers (which encapsulates the social component of the model) when they backlog their energy consumption for a period of time. This cost function also incorporates the cost of energy paid to utilities in each time-period, given certain price and energy dynamics for each large-scale consumer. Furthermore, the control input in this scenario is the amount of energy to be backlogged in each time-period, which is a part of the possible shiftable demand. The cyber-physical component is depicted by the means of communication between the consumers and utilities, and different physical properties and dynamics that govern and characterize the operation of the grid. Under this framework, the following questions and analysis scenarios arise:

- For a consumer utilizing optimal control problem for energy backlogging, how does the consumer behavior change during subsequent time-periods in response to price signals from utilities or retailers?
- How are locational marginal prices affected by energy backlogging problems of large-scale consumers?
- How does the social utility function for consumers affect the optimal decisions from the energy backlogging problem, and what are different models of consumer utility function in terms of energy backlogging?

Furthermore, other research scenarios can be analyzed using this framework. Examples include a) *policy decision scenarios* such as the effect of subsidy prices on the optimal generation quantities from different plants on the stability of the power grid, and b) *system disturbances and robustness scenario* such as the effects of cyber-attack mechanisms in the DNCS level on the social welfare.

## III. Acknowledgment

The work presented in this abstract is funded in part by the NSF CMMI grant 1201114.

## References

[1] D. Hristu-Varsakelis and W. S. Levine (Ed.): Handbook of networked and embedded control systems, 2005
[2] International Energy Agency, "Technology roadmap, Smart Grids," IEA, Tech. Rep., 2011.
[3] A. Elmahdi, A. F. Taha, S. Hui and S. H. Żak ,"A hybrid scheduling protocol to improve quality of service in networked control systems," 2012 50th Annual Allerton Conference on Communication, Control, and Computing, pp. 98–105, 1–5 Oct. 2012
[4] A. Elmahdi, A.F. Taha, and Dengfeng Sun, "Observer Based Control of Decentralized Networked Control Systems". *Submitted* to the *IEEE Transactions on Automatic Control*. September, 2013. *Under Review.*
[5] Taha, A. and Panchal, J. H., "Multilevel decision-making in decentralized energy systems with multiple technologies and uncertainty, IEEE Transactions on Systems, Man and Cybernetics: Systems, 2013, in press.

# PMU Based Proportional-Integral Damping Controller To Enhance Power System Stability

Saad Elasad, *Member*, *IEEE* Ebrahim Al Agi, *Member*, *IEEE*
Ihab Aljayyousi, Member, *IEEE* Khaled Ellithy, *Senior Member*, *IEEE*
Department of Electrical Engineerinng, Qatar University

***Abstract*—With the mature of synchrophassor new technology, developing phasor measurement units (PMUs) based wide-area damping control system becomes feasible. PMUs are devices that provide synchronized measurements of real-time phasors of voltages and currents. Synchronization is achieved by same-time sampling of voltage and current waveforms using timing signals from the global positioning system satellite (GPS). A number of PMUs are already installed in several power utilities around the world for various applications. Real-time information from remote PMUs offers the power system operators the opportunity to avoid catastrophic outages, improve system stability, and predicts the status of the system under varying conditions. The objective of this study is to design a Proportional-Integral (PI) damping controller based on PMU to enhance power systems stability. The remote PMUs with satellite synchronized clock will generate the stabilizing signal with high speed and accuracy to the PI controller. The PI controller was tuned through pole-placement technique. The impact of the designed PI damping controller on the system dynamic performance is assessed using modal analysis (eigenvalues analysis) and nonlinear time-domain simulations. The salient significance of this study is to gain experience on this new technology and its applications to smart power systems. The power system shown in Fig. 1 was used to study the effectiveness of the proposed PMU-based PI damping controller. Fig. 2 shows the developed architecture of the overall system. The system state-space representation was formed and the dominant eigenvalues corresponding to the electro-mecanical oscillation mode were obtained as listed in Table 1. It can be seen that the damping of electro-mecanical oscillation mode was improved with the proposed PMU-based PI controller. The system dynamic model was developed using Real-Time Digital Simulator (RTDS). Time-domain simulations using the RTDS model was carried out to verify the the eigenvalues results and to test the performance of the proposed PI controller under large disturbances. Fig. 3 shows the system time-response with and without the designed PI controller; it can be seen that the proposed PMU-based PI controller improves the damping of the poorly damped oscillation modes and hence enhancing the system stability***

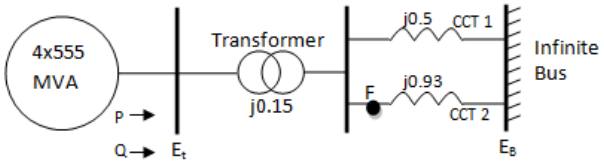


Fig. 1 Single-line diagram of power system under study

This project was sponsored by Qatar National Resarch Fund-Undegradute Research Experience Program UREP 15-148-2- 046

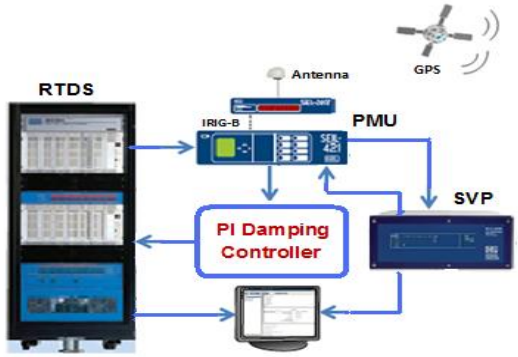


Fig.2 Real-time system modeling using RTDS with PMUs

Table 1: Eigenvalues of electro-mechanical osccilations mode

| Test Power System | Eigenvalues | |
|---|---|---|
| | Operating Point 1<br>P = 0.9pu, Q= 0.3pu | Operating Point 2<br>P = 0.6pu, Q= 0.3pu |
| Without Controller | 0.5318 ± j7.2102 | −0.0899 ± j7.705 |
| With PI Based PMU | −2.7285 ± j15.0657 | −3.8022 ± j13.7008 |

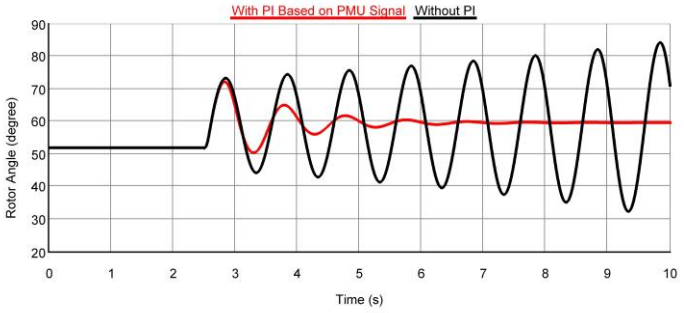


Fig. 3 System time-response for a three phase fault at point F (Operating point 1: P = 0.9 pu , Q= 0.3pu)

## REFERENCES

[1] Aboul-Ela, A. Sallam, J. McCalley, and A. Fouad, "Damping controller design for power system oscillations using global signals," *IEEE Trans. On Power Syst.*, vol. 11, No. 2, pp. 767–773, May 1996.

[2] Jaime De La Ree, Virgilio Centeno, James S. Thorp, and A. G. Phadke, "Synchronized Phasor Measurement applications in Power Systems IEEE Trans. On Smart Grid, pp. 20-27,Vol. 1, No. 1, June 2010.

[3] C. W. Liu, "Phasor Measurement Applications in Taiwan" Proc.. Transmission and Distribution Conference and Exhibition, IEEE - Asia Pacific, pp. 490-493, 2002.

# Coordinated Electric Vehicle Charging Solutions Using Renewable Energy Sources

Kumarsinh Jhala, *Student Member, IEEE*, Balasubramaniam Natarajan, *Senior Member, IEEE*
Anil Pahwa, *Fellow, IEEE* and Larry Erickson
WiCom Group, Department of Electrical and Computer Engineering, Kansas State University
Manhattan, KS-66502, USA
kumarsinh@k-state.edu, bala@k-state.edu

***Abstract*—The growing concerns about global warming, air pollution and oil shortage have motivated the research and development of electric vehicles (EVs), which are energy efficient. The US government has stated its goal of putting 1 million EVs on the road by 2015. Due to the anticipated increase in number of EVs, EV charging is emerging as a significant challenge for customers and utilities. In this work, we propose coordinated EV charging strategies for residential chargers and commercial charging stations at parking lots. In residential charging, the main focus is on the investigation of distribution transformer overloading. In commercial charging stations, the focus is on minimizing energy drawn from grid while utilizing energy from renewable energy resources in order to maximize benefits to the parking lot owners. We propose an optimal control strategy for EV charging that maximizes the use of renewable energy sources. The coordination strategies are discussed for both of these scenarios.**

## I. Introduction

Electric vehicle charging poses significant challenges due to the anticipated increase in number of electric vehicles on the road. The anticipated increased penetration of EVs, if not properly managed, can have an adverse impact on the operation and stability of the power system. While it is evident the EVs can reduce $CO_2$ emissions and improve air quality, it is important to note that emissions are actually shifted from a vehicle tailpipe to the electric power generation that supports EV charging. Therefore, to have a tangible environmental impact, we have to consider renewable energy (RE) sources (e.g., wind and solar) and their role in EV charging solutions. Therefore, developing the charging strategy to incorporate maximum use of renewable energy is one of the major goals of this research. In this work, we are interested in two primary challenges related to EV charging.

1) *Residential charging - Distribution transformer overloading:*

According to [1], the current distribution system is incapable of supporting large number of EVs. In [1], a typical residential situation with worst-case uncoordinated charging scenario is considered where all users charge their EV simultaneously. In such cases, as few as two charging EVs can force transformer to operate above it's rating. This may eventually result in transformer failures. A probabilistic model of EV charging was developed in [2]. It considers the case that not all EVs need a full recharge and they will not be charging at the same time. The results in [2] show that uncoordinated charging can exceed the transformer rating. So, we need some method of coordination to avoid transformer's loss of life. The goal of this research is to develop charging strategies that avoid transformer's overloading while ensuring fairness to customers. Some charging methods that prevents transformer's overloading and loss of life like *Staggered Charging* and *Proportional Charging* are presented in this poster.

2) *Commercial Parking lot charging - Coordinating Distributed Generation (DG) and EVs:*

We consider a parking lot with $M$ charging stations. In addition to grid power the lot also uses solar and wind energy to charge plug-in EVs. EV charging at commercial parking lots need to have variable charging rates as time available for charging is random. We assume that, each charging station is capable of charging vehicles at five distinct charging rates. The goal of our work is to coordinate the charging rate in order to minimize the power drawn from grid while providing the desired level of charging within the available time frame. The charging rate of each vehicles is the control variable in this model. The constraints on the control problem include; (1) the *time available for charging*; (2) *demand of charge* for each vehicle in the charging station, and (3) the amount of renewable energy available from DGs(solar or/and wind generators). We propose an optimal control strategy for EV charging while maximizing the use of renewable energy sources in order to provide for maximum benefit to the charging station operator/lot owner.

## Acknowledgement

This work is supported in part by a grant awarded by The K-State Electric Power Affiliates Program.

## References

[1] M. Rutherford and V. Yousefzadeh, "The impact of electric vehicle battery charging on distribution transformers," in *Applied Power Electronics Conference and Exposition (APEC), 2011 Twenty-Sixth Annual IEEE*, 2011, pp. 396–400.

[2] S. Argade, V. Aravinthan, and W. Jewell, "Probabilistic modeling of ev charging and its impact on distribution transformer loss of life," in *Electric Vehicle Conference (IEVC), 2012 IEEE International*, 2012, pp. 1–8.

# An Optimal Framework for Residential Load Aggregators

Qinran Hu, Fangxing Li
The Department of Electrical Engineering and Computer Science, the University of Tennessee, Knoxville, TN 37996, USA,
Email: {qhu2, fli6}@utk.edu

***Abstract*— With the development of intelligent demand-side management with automatic control, distributed populations of large residential loads, such as air conditioners (ACs), have the opportunity to provide effective demand-side ancillary services while reducing the network operating costs. This work presents an optimal framework for residential load aggregators. Under this framework, the load aggregators are able to: 1) have an optimal control strategies over ACs and electrical water heaters (EWHs); 2) quickly and automatically response to the request from load serving entities. To residents, the framework is designed with probabilistic model of comfortableness, which ensures the residents' daily life will not be affected. Also, the framework fairly and strategically rewards residents who participated in the demand response program, which may stimulate the potential capability of loads optimized and controlled by the load aggregator. In addition, the proposed framework will be validated on several numerical case studies.**

## I. Motivation

The development of communication and sensor technologies provide the platform for consumers and suppliers to interact with each other. This creates an opportunity for load aggregators to play an increasingly vital role in demand response by applying optimal control strategies over loads. According to Monthly Energy Review April 2012 made by U.S. Energy Information Administration, the residential electricity use in US in 2011 is 1,423,700 million kWh consisting 38% of the total electricity use. Therefore, it is reasonable to consider designing an optimal framework for residential load aggregators to provide effective demand-side ancillary service by strategically controlling the residential loads and rewarding the residents.

Based on several pilot trial runs by utilities, ACs and EWHs are especially critical here, because they are increasingly predominant and can provide fast responses with minimal impact to residents in a short time period. Moreover, in most of the countries, ACs and EWHs typically account for one half of the total peak demand in residential aspects. Therefore, this work considers the aggregate demand of populations of ACs and EHWs.

## II. Introduction and Pre-study

There are several assumptions for the proposed framework, 1)ACs and EWHs have two-way communication with load aggregators; 2) Users provide a temperature range in which they feel comfortable with; and 3) Users decide whether they are willing to compromise about the temperature range. Following the above assumptions, the load aggregator is able to use the proposed framework to dispatch the loads need to be reduced without affecting residents daily life, while sending out the rewards to residents according to the contributions they made.

Fig.1 is the brief schematic figure of the control and rewards mechanism. Based on the proposed framework, some preliminary studies have been carried out. For example, here Fig.2 and TABLE I show the preliminary results of a 10-user case study regarding the residents' satisfaction as well as the reward distribution.

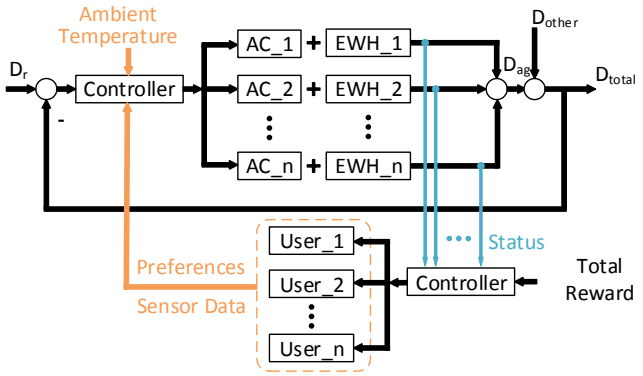


Fig.1 Schematics of the control and rewards mechanism

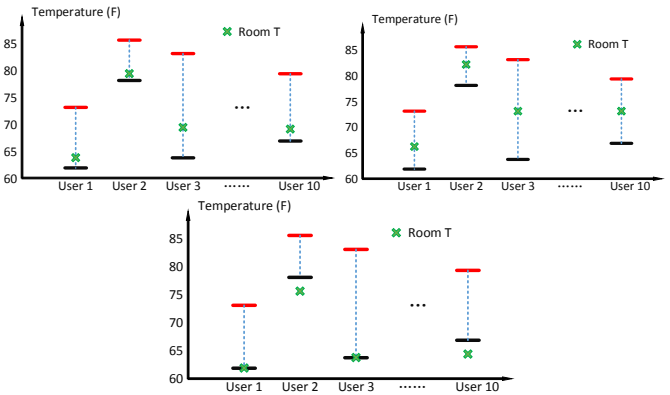


Fig 2. The operating points of ACs under some typical scenarios

TABLE I. Preliminary Result (length: one week)

| User | Temperature (F) | Compromise | Satisfaction (%) | Rewards ($) |
|---|---|---|---|---|
| 1 | 62-73 | No | 100 | 3.2 |
| 2 | 78-85 | Yes | 84 | 3.0 |
| 3 | 64-82 | No | 100 | 4.5 |
| 10 | 67-80 | Yes | 96 | 3.7 |

## III. Content To Include In The Work

With the above motivation, introduction and pre-study, this work proposes an optimal structure for residential load aggregators with both effective demand-side ancillary service and strategic rewarding mechanism. Also, the detailed of the framework design, including optimization problem formulation, probabilistic comfortableness model, and the rewarding mechanism will be detailed in the work. In addition, the proposed framework will be validated on numerical case studies.

# Agent based State Estimation in Smart Distribution Grid

S M Shafiul Alam, *Student Member, IEEE* Balasubramaniam Natarajan, *Senior Member, IEEE*
and Anil Pahwa, *Fellow, IEEE*

WiCom Group, Department of Electrical and Computer Engineering, Kansas State University
Manhattan, KS-66502, USA
alam@k-state.edu, bala@k-state.edu, pahwa@k-state.edu

***Abstract*—In this paper, a novel agent based static state estimation strategy is proposed. Electric power distribution network is well modeled using decentralized measurements and distributed state-space formulations. In such systems, sensor nodes acting as agents estimate only a subset of states, instead of evaluating local estimates of global states. We consider the case when for each agent, (1) the local measurement model is underdetermined and (2) all state elements for a particular agent is completely shared with its neighbors. We propose a state estimation strategy, which effectively integrates the principles of local consensus and least squares solution through the use of system specific binary projection matrices. The potency of the proposed method is illustrated using a radial power distribution network. A rigorous analysis of convergence is also presented to motivate its application for smart grid with arbitrary topology.**

***Index Terms*—Nonlinear underdetermined system, distributed state estimation, local consensus.**

# Burns & McDonnell - K-State Smart Grid Laboratory: Protection, Communication & Power Metering - Integrated Smart Grid Laboratory

Emilio C.Piesciorovsky and Noel N. Schulz
Electrical and Computer Engineering Department
College of Engineering, Kansas State University
Manhattan, U.S.A.

***Abstract*— The Burns & McDonnell - Kansas State University Smart Grid Laboratory was created because of the need of the energy industry (electrical utilities, equipment manufacturers, and contractors) and engineering universities to recruit highly skilled power engineers and develop a state-of-the-art educational program. The smart grid laboratory integrates communication, protection, metering and control equipment together to demonstrate engineering and electric power concepts for smart grid research and educational activities. The smart grid lab objectives are defined for pre-college, undergraduate, and graduate students based on Bloom's taxonomy levels, providing hands-on experiences and demonstrations. By coupling the laboratory experiences with computer-based simulations, students gain a deeper understanding of the engineering principles and real-world challenges.**

## I. Smart Grid Laboratory Objectives

The Burns & McDonnell - K-State Smart Grid Laboratory objectives are defined for pre-college, undergraduate, and graduate students based on Bloom's taxonomy levels, as shown in Figure 1.

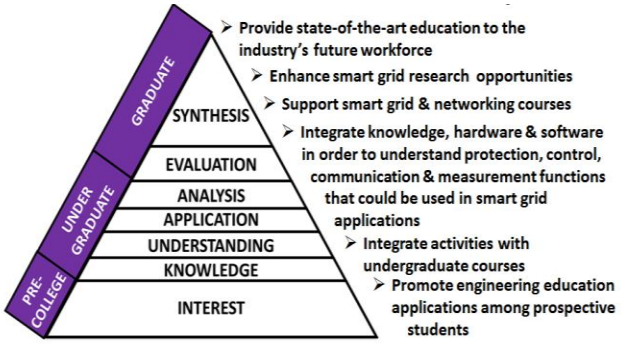


Figure 1. Smart Grid Laboratory Objectives.

## II. Network Arquitectures & Equipment

The smart grid laboratory is based on three smart grid architectures used in research and education. They are the substation-power system, power meter K-State facility and communication system. The Burns & McDonnell - K-State Smart Grid Laboratory is a multidisciplinary laboratory integrating power and protection systems at the substation-power system area, communications at the networking area, and power meters at the power meter K-State facility. Figure 2 shows the network (A), protection (B, E, and F), control (C), and computer-based simulator (D) panels.

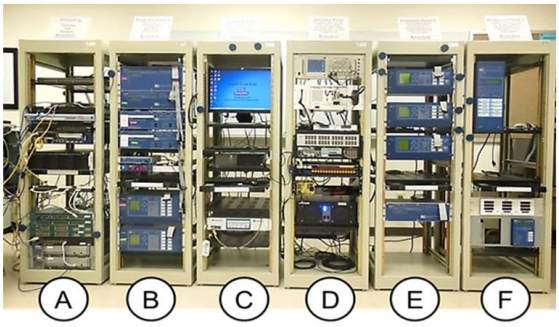


Figure 2. Smart Grid Laboratory Panels.

## III. Computer-Based Simulators, Activities & Results

This laboratory allows visitors and students to explore different issues in power system protection, communications and control. By coupling the laboratory experiences with computer based simulations, students gain a deeper understanding of the engineering principles and real-world challenges. The smart grid laboratory was integrated to university and college events, engineering courses, research and projects, and KSU facilities, for educational outreach and scholarly advances. The smart grid laboratory is an integrated facility focusing on the combination of protection, communication, and power metering areas to educate the public, to spark the interest of K-12 students in engineering careers, and to advance knowledge for current K-State students. In this laboratory, students can integrate equipment and software with course knowledge to better understand electric utility challenges in smart grid applications.

The authors gratefully acknowledge the contributions of Burns & McDonnell, Schweitzer Engineering Laboratories Inc., Fishnet Security, NovaTech, and Biotronics.

# Incentive Based Demand Response in WECC 240-Bus System to Minimize Price Variation

Ailin Asadinejad
Electrical and computer science engineering dept.
University of Tennessee
Knoxville, US
aasadine@utk.edu

Kevin Tomsovic
Electrical and computer science engineering dept.
University of Tennessee
Knoxville, US
tomsovic@utk.edu

*Abstract*

In this poster, an incentive based DR program is proposed. The required load reduction and adequate incentive payment are designed by a Load Serving Entity (LSE). This program is simple to implement for both customer and LSE while it brings considerable saving. To equitably share the benefits of DR, LSE can decrease the wholesale price for all customers, including those who do not participate in DR program. Different thresholds above market variable price are considered as trigger for DR programs. We compare a constant threshold and an optimal threshold based on a analysis of historical load and generation. In this optimization savings for both LSE and the customer are optimized but consumer inconvenience is limited by constraining the number of interruptions per day and season. Results show a constant threshold has a greater impact on average LMP and price volatility in the summer (peak summer load system) while greater value of DR can be realized throughout the year by optimizing the threshold.

Data and parameter that are required for numerical test is derived from a WECC 240 bus reduced model. Note that the load profiles of each device in residential and commercial sectors are used to find reducible part of load at each hour.

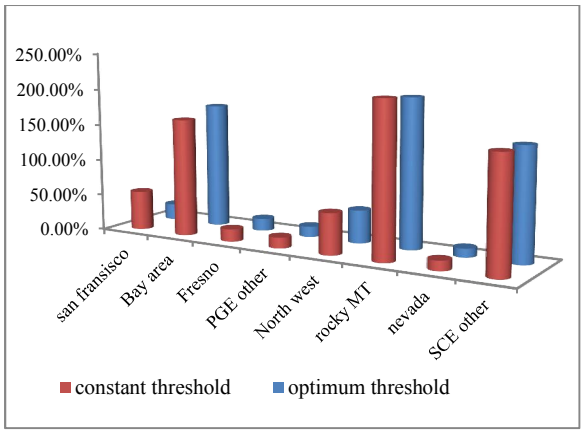


Figure1: LSE benefit from both methods

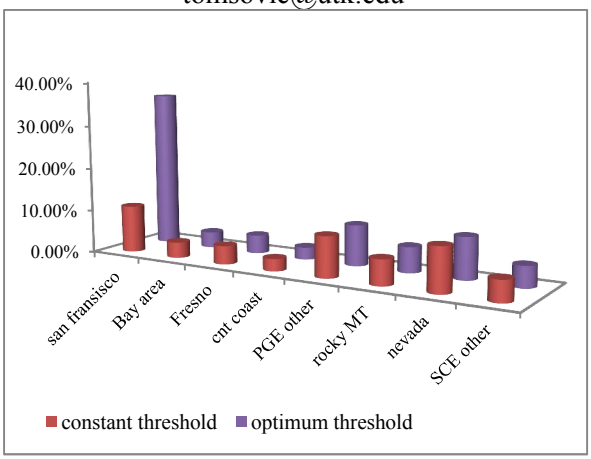


Figure 2: costumer saving from DR

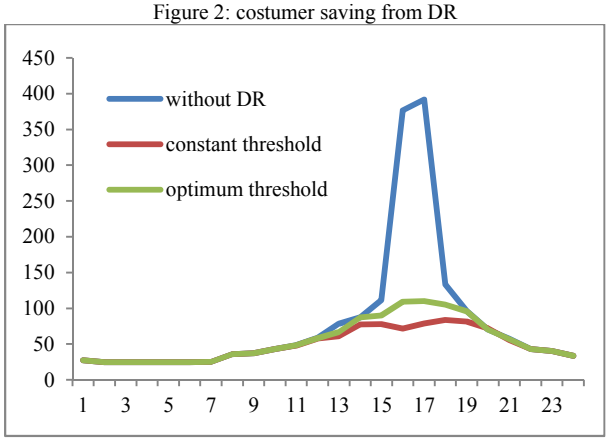


Figure 3: LMP curve in worse day of summer in Nevada region

References:

[1] U.S. Government Accountability Office, "Electricity Markets: Consumers could benefit from demand programs, but challenges remain," Report to Senate Committee on Governmental Affairs, 2004.

[2] The Brattle Group, "Quantifying Demand Response Benefits in PJM" report for PJM Interconnection and Mid Atlantic Distributed Resource Initiative (MADRI), 2007.

[3] Talukdar, Sarosh, "The Power Systems Engineering Research Center and Some Grand Challenges," Seminar presented to the Carnegie Mellon Electricity Industry Center, 2002, available at http://www.cmu.edu/electricity.

# Benefits of using PEV vehicles in PRT systems and modifying vehicle routing problem

Ali Dehghan Banadaki, Student Member, IEEE,
Co-Author: Venkata Satish Kasani, Student Member, IEEE
Dr. Sarika Khushalani-Solanki, Member, IEEE, Dr. Jignesh Solanki, Member, IEEE

Figure 1 – PRT in Morgantown

*Abstract* — **Personal Rapid Transit (PRT) is a public driverless transport system which has been used since 1975 in Morgantown. These small vehicles are controlled by computer center, therefore, eliminating human errors made them safer than usual transport systems like buses or taxies. Moreover PRT is based on demand response unlike the other mass transit vehicles which work on scheduled time; therefore, they are more energy efficient systems. Safety and energy efficiency are two important factors that made these vehicles to be more common these days and spreading through other countries like England and Netherlands. PRT uses electricity power instead of gas which is another privilege of PRT systems but still researchers propose new methods to make this kind of transportation even better than today. In this poster I try to show that converting power rail propelling to battery vehicle would make this transport system better for two reasons. First, if we model each vehicle of PRT as a current load, each power supply as a voltage source and each line with resistors, then we understand that in this kind of system some portion of power are always lost in the resistors of lines, therefore, by using battery vehicles there is no power loss in the lines and it improves the efficiency.**

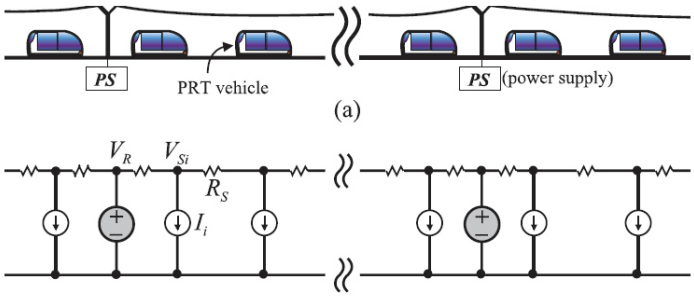


Figure[1] 2 - Physical structure and the corresponding electrical model of PRT

**Second, if we analyze the demand response of all stations of PRT in Morgantown we realize that the peaks are occurred around the daily peak in the morning and evening. Again we can handle this situation by using battery vehicles and setting the time for charging them in the hours which is not the peak load.**

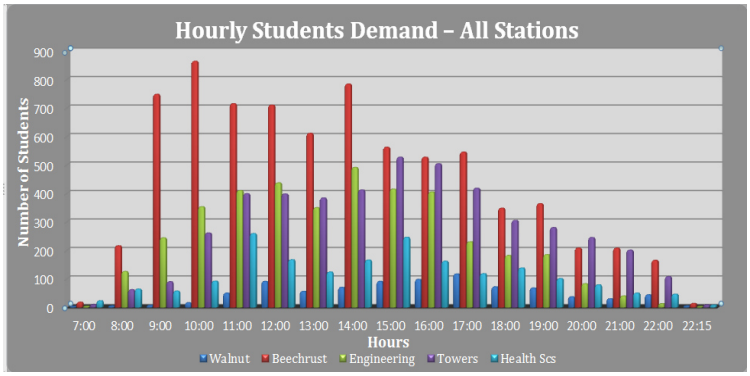


**In this case we should not forget to add a constraint to vehicle routing problem which makes a new optimization formula. This constraint limits the number of vehicles in each cycle to those who are not in charge station, i.e., we do not always have all of our vehicles ready to use. Thus a new constraint will be added to the formula to optimize the new vehicle routing problem.**

Reference:
1- Optimal Position Finding Algorithm for the Power Sources in the PRT system; IEEE Industry Applications Conference; 2003

# False Data Attack on State Estimation in Smart Grid

Deepak Tiwari, *Student Member, IEEE*, Jignesh Solanki, *Member, IEEE* and Sarika Khushalani Solanki, *Member, IEEE*

***Abstract*—Analysis of vulnerability of power grid is done in case of malicious data attack on state estimation. State estimation plays very vital role in determining the power grid variable through meter measurements and the available power system model, which is very important for the reliable operation of power grid. A special class of attack goes unobserved by the bad data detection algorithm, which is also discussed here in this poster. Main aim of the attacker is to construct such an attack vector which bypasses the detection algorithm.**

***Index Terms*—Malicious Data Attack, Optimization Technique, Smart grid.**

## I. Introduction

Measurement of vulnerability is defined by the impact of an attack and difficulty of detecting the attack. Smart grid is a transformed electrical grid which includes advanced censors, robust two way communication, and distributed computers. In a power grid, the Supervisory Control and Data Acquisition (SCADA) plays and important role. The state estimator takes the measured data from SCADA, which are power flows, bus power injections etc.

This poster also discusses the class of cyber security problem in smart grid [1]. In this paper, analysis of vulnerability of power grid to false data is done considering the cyber security problem as a cardinality minimization problem. Also the modeling of attacks have been done by various authors [2], [3]. In [3], the attack is considered as the two cases 1) random false data injection attack 2) targeted false data injection attack and construct an attack vector for both cases. The malicious measurements $Z_a$ can bypass the bad data detection (BDD) test if and only if attack is a linear combination of measurement matrix.

[4]- [6] discuss the unobserved coordinated attack as cardinality minimization problem, the optimal solution to which eases the task of vulnerability analysis of network. To detect the presence of bad data, the two norm of the residual calculated and limited by a threshold. If the residual is too big, the BDD alarm will be on.

## II. Key Equations

### A. Cardinality minimization problem

$$\min_{\Delta\theta \in R^n} \|H\Delta\theta\|_0$$
$$subject\ to\ \ H(k,:)\Delta\theta = 1$$

There are certain 'I' meters which could not be attacked due to the protection, so this model becomes

$$\min_{\Delta\theta \in R^n} \|H\Delta\theta\|_0$$
$$subject\ to\ \ H(k,:)\Delta\theta = 1$$
$$H(I,:)\Delta\theta = 0$$

### B. False data attack model

The measurement vector.

$$Z = h(x) + e$$

a is the attack vector injected into the system..

$$Z_a = h(x) + e + a$$

## III. Summary

This work is based on the solution to false data attack problem on the state estimation in smart grid. This cyber security problem was considered as cardinality minimization problem. Also the various optimization tools for the cyber-security needs to be developed in near future for the efficient operation of smart grid.

## IV. References

[1] Kin Cheong Sou, Henrik Sandberg, and Karl Henrik Johansson "On the exact solution to a smart grid cyber-security problem," IEEE Trans. Smart Grid, vol. 4,no 2, June 2011

[2] Jinsub Kim and Lang Tong, "On Topology Attack of a Smart Grid" IEEE Trans. Smart Grid Communication, vol 31,issue 7, pp 1294-1305, June 2013

[3] Y. Liu, M. K. Reiter, and P. Ning, "False data injection attacks against state estimation in electric power grids," 16th ACM Conf. on Computer and Communications Security, New York, NY, USA, 2009.

[4] H. Sandberg, A. Teixeira, and K. H. Johansson, "On security indices for state estimators in power networks," First Workshop on Secure Control Systems, Stockholm, Sweden, April 2010.

[5] Oliver Kosut, Liyan Jia, Robert J. Thomas , and Lang Tong, "Malicious Data Attacks on the Smart Grid". IEEE Trans. Smart Grid, vol.2 ,no 4, Dec 2011

[6] R. Bobba, K. Rogers, Q. Wang, H. Khurana, K. Nahrstedt, and T. Overbye, "Detecting false data injection attacks on dc state estimation," in Proc. 1st Workshop Secure Control Syst. (CPSWEEK 2010).

Authors are with Computer Science and Electrical Engineering Department, West Virginia University, Morgantown, WV 26505 USA (e-mails: detiwari@mix.wvu.edu, jignesh.solanki@mail.wvu.edu, Sarika.Khushalani-Solanki@mail.wvu.edu

.

# Effect of Stealth Data Attack on AC Optimal Power Flow

B. Khaki, *Student Member, IEEE,* J. Solanki, *Member, IEEE,* S. K. Solanki, *Senior Member, IEEE*

***Abstract*--as the main characteristic of smart grid is the communication between different parts of the grid in order to provide a real-time monitoring and control system, this type of grids is considered a cyber-physical system which its cyber layer is vulnerable to malicious data attacks. The data corruption can affect the performance of the physical system and make it unstable or compel it to operate under the conditions with is not optimal from the economic point of view. In the cases of data attacks, especially stealth attacks, the manipulated data remains unobservable to the operator and may affect the optimal operation of the power grid. In this paper, malicious data attack effect on AC optimal power flow and its consequences on operator's decisions are investigated through the formulation of the system and simulation results.**

***Index Terms*-- Data Attack, Smart Grid, Power Flow.**

## I. Introduction

SMART grid is an idea introduced as a controllable power grids so that the costs of producing electricity decreases as much as possible. To satisfy this goal, electricity resources and loads are communicated with control centers where in addition to monitoring the system, real-time decisions made by the controllers and operators.

According to the communication backbone of the smart grid, it is considered a cyber-physical system which its cyber layer is vulnerable to malicious data attacks. Corrupted data attacks, particularly unobservable attacks, may affect the controllers and operators performance, as they manage the systems according to the manipulated measurements. Therefore, many researchers have investigated the effect of these attacks on power flow and energy market studies. [1,2] studies the effect of data attack on power market, considering linearized power flow model. [3] considers the nonlinear model in studying the effect of data attack on energy markets and illustrates the nonlinearity alleviate the effect of attack designed based on the linear model. Then in [4], the authors propose partitioned state space of the system into price regions, and they investigated the effect of meter data and topology data to find the worst data attack by defining relative price perturbation criteria.

[5, 6] demonstrate that Bad Data Detection (BDD) is not capable to detect stealth attacks in estate estimators. [7] considers the linear optimal power flow model to explore the stealth attacks which are able to deceive the operator and satisfy the adversary's goal. [8] introduces a method of designing an unobservable data attack based on AC power flow model.

In this paper, considering [7], the effect of stealth attack, based on the nonlinear optimal power flow, on the operator and closed loop control is examined.

B. Khaki, J. Solanki, S. K. Solanki are with Computer Science and Electrical Engineering Department, West Virginia University, Morgantown, WV 26505 USA (e-mails: bekhaki@mix.wvu.edu, jignesh.solanki@mail.wvu.edu, Sarika.Khushalani-solanki@mail.wvu.edu).

## II. Key Equations

### A. OPF Equation

$$\min_{P_g} \quad c(P_g)$$
$$s.t. \quad h(P_g, P_d) = 1^T P_g + 1^T P_d = 0$$
$$f(P_g, P_d) = F_g P_g + F_d P_d + F_0 \leq 0$$

$$with$$
$$F_g = \begin{bmatrix} G_g \\ -G_g \\ I \\ -I \end{bmatrix}, F_g = \begin{bmatrix} F_d \\ -F_d \\ 0 \\ 0 \end{bmatrix}, F_0 = \begin{bmatrix} -\overline{P^f} \\ -\overline{P^f} \\ -\overline{P^g} \\ 0 \end{bmatrix}$$

### B. Attack Model

Z , in the following equation, is the measurement vector..

$$Z = h(x) + W$$

A is the attack vector injected into the system.

$$Z_a = h(x) + W + A(Z_0)$$

## III. References

[1] L. Xie, Y.Mo, and B. Sinopoli, "Integrity data attacks in power market operations," IEEE Trans. Smart Grid, vol. 2, no. 4, pp. 659–666, 2011.

[2] L. Jia, R. J. Thomas, and L. Tong, "Impacts of malicious data on real time price of electricity market operations," in *Proc. HICSS*, 2012, pp. 1907–1914.

[3] J. Liyan, R. J. Thomas, and L. Tong, "On the nonlinearity effects on malicious data attack on power system," PESociety General Meeting 2012, pp. 1-6, July 2012.

[4] L. Jia, J. Kim, R. J. Thomas, and L. Tong, "Impact of Data Quality on Real-Time Locational Marginal Price, " IEEE Trans on Power Systems, issue: 99, Nov. 2013.

[5] Y. Liu, M. K. Reiter, and P. Ning, "False data injection attacks against state estimation in electric power grids," 16th ACM Conf. on Computer and Communications Security, New York, NY, USA, 2009.

[6] H. Sandberg, A. Teixeira, and K. H. Johansson, "On security indices for state estimators in power networks," First Workshop on Secure Control Systems, Stockholm, Sweden, April 2010.

[7] A. Teixeira, H. Sandberg, G. Dan, and K. H. Johansson, "Optimal power flow: Closing the loop over corrupted data, " American Control Conference (ACC) 2012, pp. 3534 - 3540, July 2012.

[8] K.R. Davis, K. L. Morrow, R. Bobba, and E. Heine, "Power flow cyber attacks and perturbation-based defense, " IEEE International Conference on Smart Grid Communications (SmartGridComm) 2012, pp. 342 - 347, Nov. 2012.

# Cyber-Security Vulnerability Assessment of Smart Grids

Reza Kazemi, *Student Member, IEEE*
Lane Dept. of Electrical Engineering and Computer Science,
West Virginia University, Morgantown, WV

Jignesh. M. Solanki, *Member IEEE*
Sarika K. Solanki, *Senior Member IEEE*
Lane Dept. of Electrical Engineering and Computer Science,
West Virginia University, Morgantown, WV

***Abstract*— The development and expansion of new smart electrical grids brings increased capacity, reliability and efficiency through the merging of new communication and computer technologies with the existing electricity network. This integration, however, creates a new host of vulnerabilities stemming from cyber intrusion and injection of corrupted data in an attempt to subject the electric grid to physical and financial losses. Analysis of these new threats calls for a modeling framework that is able to model the effects of these cyber threats on the physical components of the power system by taking into account the interactions between the cyber and physical components of the smart grids.**

***Index Terms*—Smart Grid, Cyber-security, Cyber Intrusion.**

## I. INTRODUCTION

A smart grid is defined as the integration of real-time monitoring, advanced sensing, and communications, utilizing analytics and control, enabling the dynamic flow of both energy and information to accommodate existing and new forms of supply, delivery, and use in a secure and reliable electric power system, from generation source to end-user [1]. Wide integration of communication networks and intelligent devices in the smart grids makes it more vulnerable to cyber threats compared to old power systems. For smart grid attackers, a general goal is to maximize the effect of their attacks with lower cost and risk, which usually means their attacks, will aim at triggering cascading failures by just taking down a few components whose failure can lead to blackouts in power grids [2]. In general these intrusions can lead to loss of load, loss of information, economic loss or equipment damage according to scale and intention of the intrusion. Intruders can also affect critical activities required for operation and control of the power system like state estimation and contingency analysis by manipulating the data readings from smart meters in the grid [3]-[6], or conduct a topology attack by transferring false information about in service transmission lines to the control center [7]

## II. MODELING THE CYBER INTRUSION IMPACT ON THE SMART GRIDS

There has been some research work to evaluate the effect of the cyber intrusions on the electrical smart grids in recent years [1], [8]. One of the major issues in simulation of these effects is coming up with a method to take the interactions of cyber and physical parts of the smart grids in to account in a way that enables us to accurately predict the potential impacts of a cyber attack plot on the stability of the network as well as safety of the components. In order to reach this goal for simulating such interactions and dependencies within cyber physical power systems can be considered as a graph with every electrical component like transformers, generators, loads, plug-in hybrids and circuit breakers considered as a node. Cyber parts of the smart grid such as switches and control centers, sensors and breaker actuator controls are also assumed as a node. The dependencies between the nodes are represented by edges.

## REFERENCES

[1] D. Kundur, F. Xianyong S. Mashayekh, S. Liu, T. Zourntos, and K.L. Butler-Purry. "Towards modelling the impact of cyber attacks on a smart grid." International Journal of Security and Networks 6, no. 1, 2011, pp. 2-13.

[2] J. Yan , Y. Zhu , H. He and Y. Sun "Revealing temporal features of attacks against smart grid", 2013 IEEE PES Innovative Smart Grid Technologies (ISGT**).**

[3] A. Giani, E. Bitar, Garcia, M. M., McQueen, P. Khargonekar, and K. Poolla, "Smart Grid Data Integrity Attacks: Characterizations and Countermeasure," IEEE SmartGridComm, 2011.

[4] S. Zonouz, C. M. Davis, K. R. Davis, R. Berthier, R. B. Bobba, and W. H. Sanders, "SOCCA: A Security-Oriented Cyber-Physical Contingency Analysis in Power Infrastructures." ," IEEE Trans. Smart Grid, vol. 3, no. 4, pp. 1790–1799, 2014.

[5] M**.** Esmalifalak, G Shi, Z Han, L Song. "Bad Data Injection Attack and Defense in Electricity Market Using Game Theory Study." IEEE Trans. Smart Grid, vol. 4, no. 1, pp.160 -169, 2013.

[6] L. Xie , Y. Mo and B. Sinopoli "Integrity data attacks in power market operations", IEEE Trans. Smart Grid, vol. 2, no. 4, pp.659 -666 2011.

[7] J. Kim and L. Tong, "On Topology Attack of a Smart Grid," 2013 IEEE PES Innovative Smart Grid Technologies (ISGT), 2013.

[8] W. Eberle and L. Holder, "Insider threat detection using graph-based approaches," in Proc. Cybersecurity Applications and Technology Conference for Homeland Security, 2009, pp. 237–241.

# NISTIR 7628 Visualization Model

Matthew Harvey, *Student Member, IEEE*, Dan Long, *Student Member, IEEE*, Karl Reinhard, *Student Member, IEEE*
Trustworthy Cyber Infrastructure For the Power Grid (TCIPG)
Department of Electrical Engineering, University of Illinois Urbana-Champagin

***Abstract*-- NISTIR 7628 is a report that lists out guidelines on what should be done to secure the Smart Grid from cyber-attacks. This document stands 600 pages and can be difficult to understand and conceptualize due to the density of information. This poster lays out new ways to visualize the NISTIR 7628 in a number of different models that are currently being created. Research is currently being done to see how we can use this new model to data mine all sorts of information that is currently in NISITR 7628. Some goals of this research is to compare actual utility firewall systems with such suggested in the guidelines to see how they match up, as well as coming up with what resources are most vulnerable and how many resources need to be spared to secure certain aspects of the power grid.**

## I. Introduction

In August of 2010, the National Institute of Standards and Technology Computer Security Division, NIST, released NISTIR 7628 Guidelines for Smart Grid Cyber Security. This document was written in response to this new set of problems that has arisen and is accompanied by the "NIST Framework and Roadmap for Smart Grid Interoperability Standards", which came out in 2008. The report is written as a 600 page, three volume document that is meant to serve as an "analytical framework" and with the hope that individual organizations will be able to reference it. The document is not only very long, but it tends to repeat itself a good amount. The NISTIR 7628 document does attempt to combat this with a series of diagrams, many of which work to illustrate the entire power infrastructure. One focus of many of these illustrations is to show and explain the relationships between different parts of the infrastructure. These are two dimensional "maps" of the grid that are still hard to understand and require a good amount of page flipping.

The document focuses mainly on the cyber-security aspects of this new digital grid. That means most physical threats are left out. The framework built from NISTIR 7628 focuses intensely on the IT and telecommunication aspects of the infrastructure. It discusses, with security being the paramount point, the ways to integrate these systems that previously may have not been involved, or least have not been as important, into the new grid.

One question raised is, how can one take the information already represented within the NISITR 7628, and make a more concise tool that industry and researchers could use to better understand the guidelines, and research the connections more in depth? The information provided is very thorough and useful, but the problem is its inaccessibility. This document that many professionals try to reference is not well understood. The goal of the NISTIR 7628 Visualization is to provide visual aid to the document that will make the information can be accessed much more easily and therefore can be more helpful in making our next-generation grid more secure.

[1] NISTIR 7628: Guidelines to Smart Grid Cyber Security, NISTIR 7628, 2013.

## II. Modeling NISTIR 7628

Within the NIST document, a number of visual representation and diagrams are used to illustrate the complexity of the power grid infrastructure by drawing security connections between different aspects of the power grid. NIST divides the power grid into seven different domains including, Markets, Operations, Service Provider, Bulk Generation, Transmission, Distribution and Customers. The visualizations included in the NIST document have been combined together into a computer model to allow for a great functionality and easy grasp of the information being represented in the diagrams. Please refer to the NISTIR 7628 to view the current visualizations provided.

### *A. 3D Model*

Two models have been developed, the first an HTML web page, second a 3D MATLAB model. These have both reflected the diagrams already in the NIST document. Currently, a newer model is being developed to incorporate more information form the NISTIR 7628 as well as a well labeled 3D model that allows any user to easily gather information about security requirements and different actors, or components of the power grid infrastructure. The two platforms that are being explored for this updated model use JAVA and HTML5. Both allow for better visual aspects and better functionality.

### *B. Goals*

The tool has proven to have potential after feedback received from industry, academia, and government partners. We are seeking effective methods to label actors, logical interfaces, and interfaces compatible with interactive perspective changes, seeking ways to easily zoom-in and pan-out, and seeking ways to increase information content available to user; user selects and controls the information displayed.

# Effects of Micro-Structured Surface Geometries on Condensation Heat Transfer

Andrés Martínez, Caleb Chiroy, and Amy R. Betz
Department of Mechanical and Nuclear Engineering
Kansas State University
Manhattan, Kansas, USA
Email: marmot91@ksu.edu

***Abstract*—The purpose of this research is to experimentally study how micro-structured geometries affect the heat transfer coefficient on a surface under filmwise condensation conditions. Filmwise condensation is a major concern when designing steam condensers for thermoelectric power plants. These plants currently account for 40% of freshwater withdrawal and 3% of freshwater usage in the United States. Filmwise condensation averages five times lower heat transfer coefficients than those present in dropwise condensation. Currently, filmwise condensation is the dominant condensation regime in thermoelectric power plants due to their prolonged usage. The film thickness is directly proportional to the condenser's overall thermal resistance. This investigation focuses on optimizing surface geometries with sinusoidal patterns to reduce film thickness and maximize filmwise heat transfer. The experimental setup allows us to control the cooling load, pressure, and steam quality in order to measure the steam-side surface temperature under steady state conditions. The test apparatus allows control of the cooling load and steam properties while being able to interchange the surface structures. The heat transfer coefficient is determined by measuring surface temperature. By comparing the heat transfer coefficients, we can find the optimal surface geometries by varying fin height, fin pitch, and surface curvature. A four axis micro milling machine with precision of one micron was used to machine the desired surface patterns. Aluminum was chosen based on its machinability, cost, and thermal properties. Type T thermocouples, hygrometers, and pressure transducers were used for data acquisition. A vacuum pump creates low pressure conditions and temperature steam that mimics condenser conditions. The steam-surface temperature is measured once the system achieves steady state conditions.**

# Optimal Strategy for Minimizing Load Shedding in Microgrids subsequent to Fault-Triggered Islanding

Shanshan Ma, *Student Member, IEEE*, and Wei Sun, *Member, IEEE*

*Abstract*–Microgrid (MG) is defined as part of distribution system, which consists of load, storage sources and distributed generations (DGs) or renewable energy sources. With the large penetration of DGs, MG can operate in two modes, grid-connected mode or islanded mode. In the grid-connected mode, the outputs of DGs are set at a certain level, and the main grid compensates any insufficient power requirement of load. In the islanded mode, MG is disconnected from the main grid and makes full use of DGs and storage resources to sustain automatically and independently.

A smooth transition from grid-connected to islanded mode is desirable but still a challenge for MG operation. Islanding could be caused by disturbances such as an intentional switch incident or a sudden fault happens in the main grid. In the case of intentional switching, the power sharing of each DG and storage resource is scheduled ahead with smooth transition. However, a fault in the main grid with subsequent to unintentional islanding may result MG in voltage and frequency instability. Without appropriate control strategies, the severe voltage and frequency variation can lead DGs to operate abnormally or be damaged. Consequently, MG can't operate automatically after islanding occurs.

While many control strategies have been proposed to solve the transient stability issue, most of them focus on voltage and frequency control of DGs rather than directly minimizing the power imbalance. As renewable energy sources must be interfaced with MG through inverters, advanced inverter control strategies are required to maintain stable frequency and voltage. Therefore, directly minimizing power imbalance may help to avoid the complex control strategy, but requires system to shed some load.

Network reconfiguration is able to minimize the load shedding and keep system stable. Considering the possible imbalance between DGs and load in MG after the islanding, network reconfiguration can directly transfer power from one DG to another load by changing the state of the sectionalizing and tie switches. In this way, MG can make full use of existing power and minimize power imbalance between generation and load. Furthermore, network reconfiguration considers the system level constraints, which helps to avoid any voltage or current violation. However, reconfiguration may not completely avoid load shedding. The generation re-dispatch will be applied to achieve an automatic and seamless transition from grid-connected to islanded mode.

In this paper, it is assumed that power imbalance exist in the islanding mode. A novel optimization strategy that combines network reconfiguration with generation re-dispatch is proposed to minimize the load shedding, as shown in Fig. 1. When MG detects the signal of islanding, the optimization process will provide a strategy to reconfigure network and re-dispatch generations in real time. The inputs of the optimization process are network model of MG, monitored data from system and islanding detection. The outputs are the strategies of generation re-dispatch and network reconfiguration. The constraints include DG capacity limits, transient stability constraints, and the statistic model of renewable energy source outputs. A novel solution methodology is proposed to solve this stochastic optimization problem. The modified CERTS Microgrid test system is used to demonstrate the advantage of developed strategy.

Based on the proposed strategy, MG is able to run automatically in islanded mode subsequent to fault-triggered incidents or unscheduled outage of main grid. The developed strategy can also be integrated to future distributed energy management systems and achieve a resilient microgrid.

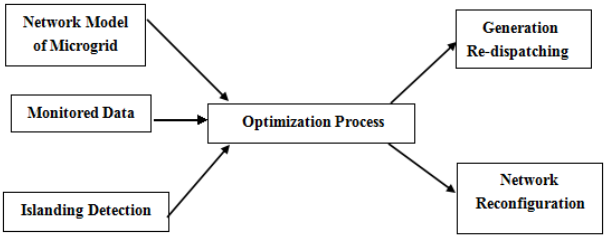


Fig. 1: The structure of developed optimal strategy.

*Index Terms*—Generation re-dispatch, islanding, load shedding, Microgrid, reconfiguration.

S. Ma and W. Sun are with the Department of Electrical Engineering, South Dakota State University, Brookings, SD 57006 USA (e-mail: shanshan.ma@sdstate.edu, wei.sun@sdstate.edu).

# A Hybrid Dynamic Optimization Approach for Stability Constrained Optimal Power Flow

Guangchao Geng[1], Venkataramana Ajjarapu[2], and Quanyuan Jiang[1]

College of Electrical Engineering[1]
Zhejiang University
Hangzhou, China
Email: ggc@zju.edu.cn, jqy@zju.edu.cn

Department of Electrical and Computer Engineering[2]
Iowa State University
Ames, IA, United States
Email: vajjarap@iastate.edu

***Abstract* — Stability constrained optimal power flow (SOPF) is an effective and economic tool to enhance stability performance by adjusting initial steady-state operating conditions, with the consideration of rotor angle and short-term voltage performance criteria. SOPF belongs to the category of dynamic optimization problems which are computational expensive. In order to reduce its computational complexity, a hybrid dynamic optimization approach is proposed for efficient and robust solving SOPF problems. Based on direct multiple shooting method, this approach combines the algorithmic advantages from existing direct sequential and simultaneous approaches. Coarse-grained parallelism among multiple shooting intervals is explored. A modular-based implementation architecture is designed to take advantage of the loose coupling between time-domain simulation and optimization. Case studies on various test systems indicate the proposed approach is able to reduce computation time compared with other direct approaches for dynamic optimization. Also, the investigated parallelization are effective to achieve acceleration on a symmetric multiprocessing platform.**

## I. Key Equations

$$\min_{x,u} \boldsymbol{\Phi}(u) \quad s.t \begin{cases} \boldsymbol{F}(\dot{x},x,u)=0 \\ \underline{\boldsymbol{\Psi}} \le \boldsymbol{\Psi}(x) \le \overline{\boldsymbol{\Psi}} \\ \boldsymbol{H}(u)=0 \\ \underline{\boldsymbol{\Gamma}} \le \boldsymbol{\Gamma}(u) \le \overline{\boldsymbol{\Gamma}} \end{cases} \qquad \min_{s,u} \boldsymbol{\Phi}(u) \quad s.t \begin{cases} s_i = \boldsymbol{S}_i(s_{i-1},u) \\ \underline{\boldsymbol{\Psi}} \le \boldsymbol{\Psi}(s_i) \le \overline{\boldsymbol{\Psi}} \\ \boldsymbol{H}(u)=0 \\ \underline{\boldsymbol{\Gamma}} \le \boldsymbol{\Gamma}(u) \le \overline{\boldsymbol{\Gamma}} \end{cases} \quad i \in [1...N_S]$$

## II. Key Figures

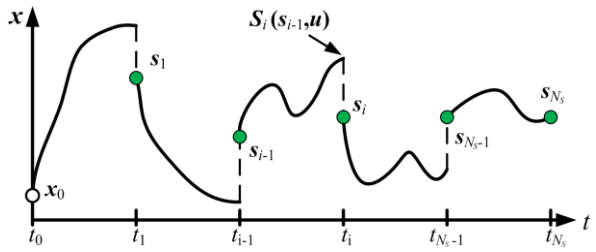


Fig. 1. Algorithm principle demonstration for direct multiple shooting method

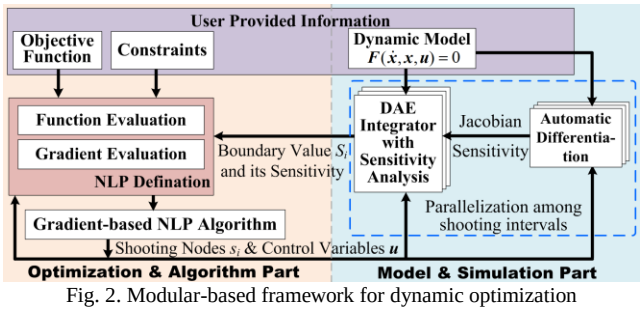


Fig. 2. Modular-based framework for dynamic optimization

## III. Key Results

TABLE I
Comparison of Convergence and Objective Values

| Test System | SEQ Iter | SEQ Obj ($/hr) | DMS Iter | DMS Obj ($/hr) | SIM Iter | SIM Obj ($/hr) |
|---|---|---|---|---|---|---|
| **CASE9** | 79 | 3,994.859 | 11 | 4,014.751 | 10 | 4,018.629 |
| **CASE39** | 26 | 26,230.732 | 22 | 26,230.738 | 18 | 26,230.759 |
| **CASE57** | 21 | 40,525.660 | 20 | 40,525.665 | 12 | 40,525.667 |
| **CASE118** | 60 | 119,757.520 | 62 | 119,756.949 | 53 | 119,755.967 |
| **CASE162** | FAIL-C | | 34 | 12,756.558 | 20 | 12,765.106 |
| **CASE300** | FAIL-C | | 113 | 670,651.911 | FAIL-M | |

TABLE II
Comparison of Computational Performance

| Test System | SEQ CPU (sec) | SEQ Mem (MB) | DMS CPU (sec) | DMS Mem (MB) | SIM CPU (sec) | SIM Mem (MB) |
|---|---|---|---|---|---|---|
| **CASE9** | 0.284 | 322 | 0.456 | 333 | 0.154 | 363 |
| **CASE39** | 0.389 | 333 | 0.728 | 340 | 1.381 | 360 |
| **CASE57** | 0.296 | 335 | 0.552 | 338 | 0.583 | 382 |
| **CASE118** | 2.881 | 380 | 9.953 | 886 | 101.244 | 6,051 |
| **CASE162** | FAIL-C | 343 | 3.914 | 448 | 8.304 | 1,253 |
| **CASE300** | FAIL-C | 453 | 23.416 | 887 | FAIL-M | >7,680 |

Note: The symbol 'FAIL-C' denotes failure to converge, 'FAIL-M' denotes out of memory.

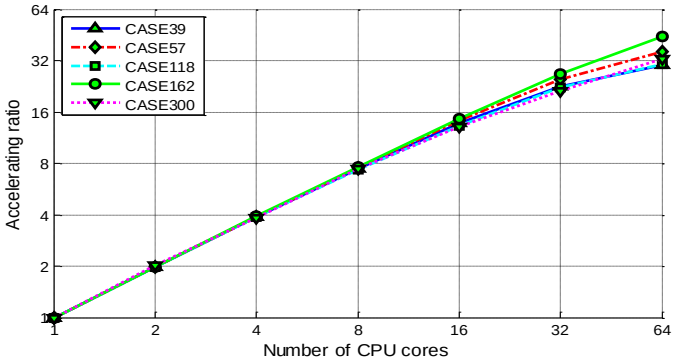


Fig. 3. Accelerating ratio curves for the proposed approach.

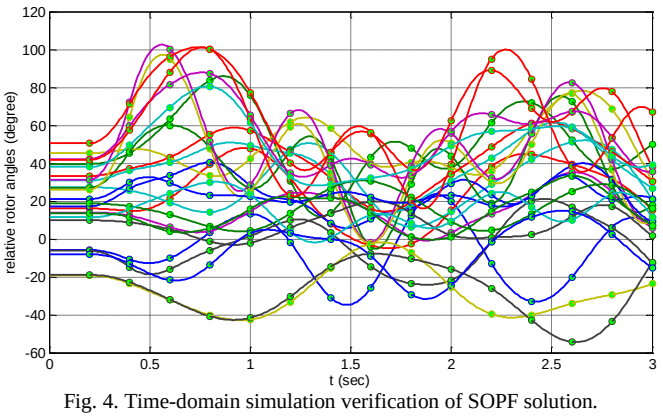


Fig. 4. Time-domain simulation verification of SOPF solution.

# Reactive Power Planning Considering High Penetration Wind Energy

Xin Fang, Fangxing Li
Department of EECS
The University of Tennessee
Knoxville, TN, USA
Emails: xfang2@utk.edu, fli6@utk.edu

Yan Xu
Power & Energy Systems Group
Oak Ridge National Laboratory
Oak Ridge, TN, USA
Email: xuy3@ornl.gov

***Abstract*— This paper addresses the optimal placement of reactive power (Var) sources under the paradigm of high penetration wind energy. The reactive power planning (RPP) investment in this particular condition involves a high level uncertainty due to the wind power characteristic. The correlation between wind speeds of different wind farms should also be considered when there are multiple wind farms. To properly model the wind generation uncertainty, a multi-scenario framework optimal power flow that considers the voltage stability constraints is developed. The objective of RPP is to minimize the total cost (Var cost and the expected generation cost). So the RPP under this condition is to optimize the Var location and size, meanwhile minimizing the fuel cost and therefore find the global optimal RPP results. The proposed approach is based on two sets of variables (TSV) combined with multi-scenario model. A Benders decomposition technique is used to solve this model with an upper problem (Master problem) for Var allocation optimization and a lower problem (subproblem) for generation cost minimization. Impact of the potential reactive power support from DFIG is also analyzed. Case studies are provided to verify the proposed method.**

***Index Terms*- Voltage stability constrained optimal power flow (VSCOPF), reactive power planning (RPP), wind power, Weibull distribution, Benders decomposition**

## I. INTRODUCTION

Wind power is known as an intermittent energy resource that often has a negative correlation with load peaks [1]. The increasing penetration of wind energy presents significant challenges to the operation and planning of the bulk power transmission systems. At the same time, conventional synchronous-machine-based power generation, currently the main source of reactive power of the system, is being exhausted as a result of increasing wind penetration. Therefore, reactive power (Var) is needed to accormadate the wide operation ranges of the wind generation and maintain appropriate voltage profiles because voltage collapse is often associated with reactive power deficiencies.

The target of reactive power planning (RPP) or Var planning is to optimize the reactive resources (both by location and size). This optimization problem is a mixed integer nonlinear programming problem. Determination of the buses that should be considered as potential candidates for Var resources and their size is complex and often be treated as a heuristical problem. The problem is further complicated with the integration of wind energy, due to the uncertainty of wind power plant output. In this paper, a systematic method for providing optimized quantity and location for Vars is proposed.

This paper will present a Benders decomposition based multi-scenario, two sets of variables (TSV) optimization model to solve RPP problem with high penetration wind energy. The wind power is modeled as a multi-level generation resource. The correlation among different wind farms is modeled and the reactive power support from DFIG are considered and analyzed. The objective of the optimization problem in this paper is the total cost of Var compensation and the generation cost (fuel cost) after integrating wind energy.

## II. WIND POWER MODEL

The wind speed in a single wind farm can be easily generated utilizing Monte Carlo simulation. When there are multiple wind farms, the correlation should be considered. To solve this problem, at first the correlated normally distributed series are generated, and then transform these normally distributed series into Weibull distributed wind speed series.

For instance, in the case of a normal distribution variable $x$, the cumulative probability $F_x$ of CDF is obtained from (4) and (5).

$$F_x = \frac{1}{2}(1+erf(\frac{x-u}{\sqrt{2}\sigma})) \tag{1}$$

$$erf(x) = \frac{2}{\sqrt{\pi}}\int_0^x e^{-t^2}dt \tag{2}$$

So the transformation from normal distribution to Weibull distribution can be shown as:

$$w = \lambda[-\ln(1-\frac{1}{2}(1+erf(\frac{x}{\sqrt{2}})))]^{\frac{1}{k}} \tag{3}$$

Fig. 1 shows the transformation of Normal distribution ($u$ =0, $\sigma$ =1) to Weibull distribution ($\lambda$ =7, $k$ =2.2).

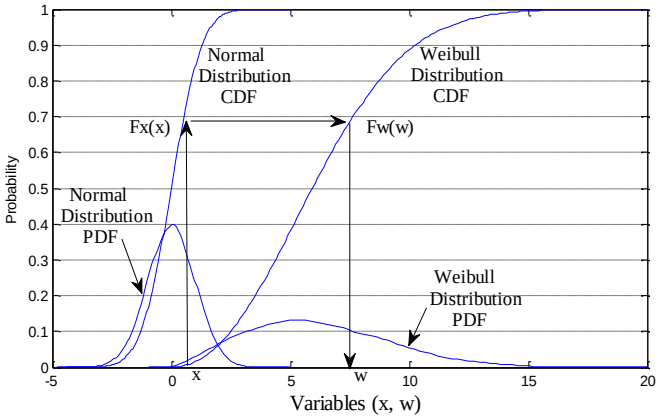


Fig. 1. Transformation of Normal distribution to Weibull Distribution

## III. Problem Formulation and Decomposition

The purpose of the RPP in this paper is to maintain the system voltage stability under high penetration wind energy. Here the load margin is employed as the voltage stability margin. Therefore, the objective is to minimize the reactive compensation cost under the specific operating point and the fuel cost under the normal operating point. Two sets of variables (TSV) are specified for these two operating points.

$$\text{Min:} \quad \sum_{k\in N^Q}\left(c_1 + c_2 \cdot Q_{ck}^*\right)\cdot u_k + \sum_{t\in W^N} p_t \sum_{i\in N^G} f(P_{Gi,t}) \tag{4}$$

From the objective function in (4), the optimization model can be decomposed into two levels. The upper-level (the master problem) is to optimize Var compensation with the voltage stability constraints. The lower-level (the subproblem) is the ACOPF with given Var compensation allocation and gets the minimum expected generation cost considering all different wind scenarios

## IV. Case Studies and Results

The proposed voltage stability constrained optimal power flow (VSCOPF) model is studied on IEEE 14 bus and IEEE 118 bus system.

### *A. IEEE 14-Bus system*

Two wind farms with total capacity of 77MW are connected to bus 2, the capacity penetration is 30%. One wind farm is 30MW, and the other one is 47MW, in which all the wind turbines are DFIG which have three reactive power control strategies: unity power factor, D curve reactive power capability and power factor 0.98. In the simulation, the system load margin $\delta$ is 50%. Fig. 2 is the wind active power output bar figure. In all cases, fixed cost $c_1$ is 33.47$/hr and varying cost $c_2$ is 1.23$/(MVar*hr).

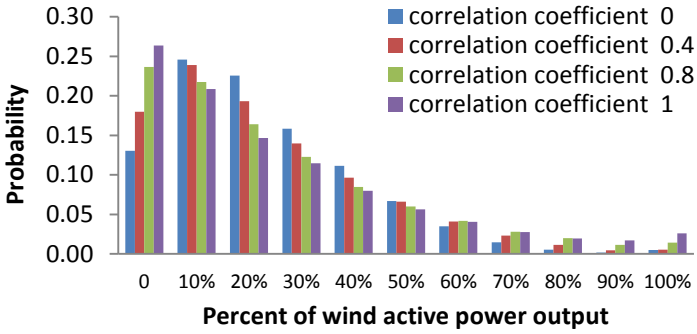


Fig. 3 Wind power output bar figure for different wind speed correlation

Fig. 3 shows that the correlation coefficient changes the wind active power output distribution significantly. TABLE I is the Var allocation results for different correlation and reactive power control strategies.

TABLE I. Var allocation under different wind speed correlation

| Correlation Coefficient | Bus 5 | Bus 9 | Fuel cost ($) | VAR cost($) | Total cost($) |
|---|---|---|---|---|---|
| 0 | 16.4 | 30 | 11464.4 | 129.6 | 11594 |
| 0.4 | 16.4 | 30 | 11496.8 | 129.6 | 11626.4 |
| 0.8 | 16.4 | 30 | 11525.9 | 129.6 | 11655.5 |
| 1 | 16.4 | 30 | 11535.2 | 129.6 | 11664.8 |

## V. Reference

[1] "U.S. Renewable Electricity: How Does Wind Generation Impact Competitive Power Market," CRS Report for Congress, Nov. 2012 [Online]. Available at : www.fas.org/sgp/crs/misc/R42818.pdf, accessed in Dec. 2012.

# Interval Power Flow Using Linear Relaxation and Optimality-based Bounds Tightening (OBBT) Methods

Tao Ding*, *Student Member, IEEE*, Rui Bo, *Senior Member, IEEE*, Fangxing Li, *Senior Member, IEEE*

**Abstract**

With increasingly large scale of intermittent and non-dispatchable resources being integrated into power systems, the power flow problem presents greater uncertainty. In order to obtain the upper and lower bounds of power flow solutions, Cartesian coordinates-based power flow is utilized to formulate the interval power flow problem as a quadratically constrained quadratic programming (QCQP) model. This non-convex QCQP model can be relaxed to linear programming problem by introducing convex and concave enclosures of the original feasible region. To improve interval solution that includes the true interval solution, optimality-based bounds tightening (OBBT) method is employed to find a better outer hull of the feasible region.

In interval power flow analysis, power injections are volatile and can be represented using intervals, which can be formulated as a standard QCQP problem without the loss of generality:

$$(\mathbf{QCQP}) \qquad \max_{\boldsymbol{x}\in\mathcal{R}^{2n}} / \min \quad \boldsymbol{x}^T\boldsymbol{Q}_0\boldsymbol{x}+\boldsymbol{c}_0^T\boldsymbol{x} \tag{1}$$

$$s.t. \quad \underline{d_j} \le \boldsymbol{x}^T\boldsymbol{Q}_j\boldsymbol{x}+\boldsymbol{c}_j^T\boldsymbol{x} \le \overline{d_j} \qquad j=1,\ldots,m \tag{2}$$

$$l_i \le x_i \le u_i \qquad i=1,\ldots,2n \tag{3}$$

where $m$ denotes the number of quadratic constraints, $Q_j$ ($j$=1,…,$m$) are indefinite $2n\times 2n$ matrices, $\boldsymbol{c}_j$ ($j$=0,…,$m$) are $n$-dimensional vectors, the set $\Omega=\bigcup_{i=1}^{2n}[l_i, u_i]$ is assumed to be nonempty and bounded.

Let dummy variable $\boldsymbol{Z}=\boldsymbol{x}\boldsymbol{x}^T\in\mathcal{R}^{2n\times 2n}$ and substitute $\boldsymbol{Z}$ for $\boldsymbol{x}\boldsymbol{x}^T$ in QCQP model, the objective and constraints become bilinear. Furthermore, the convex envelopes and concave envelopes as defined in (6)-(9) are introduced to obtain the tractable linear relaxation (LR) model of the non-convex problem QCQP, formulated as follows:

$$(\mathbf{QCQP\text{-}LR}) \qquad \max_{\boldsymbol{x}\in\mathcal{R}^{2n},\boldsymbol{z}\in\mathcal{R}^{2n\times 2n}} / \min \quad \boldsymbol{c}_0^T\boldsymbol{x}+\boldsymbol{Q}_0\bullet\boldsymbol{Z} \tag{4}$$

$$s.t. \quad \underline{d_j} \le \boldsymbol{c}_j^T\boldsymbol{x}+\boldsymbol{Q}_j\bullet\boldsymbol{Z} \le \overline{d_j} \tag{5}$$

$$z_{ij}-l_ix_j-l_jx_i+l_il_j\ge 0 \tag{6}$$

$$z_{ij}-u_ix_j-u_jx_i+u_iu_j\ge 0 \tag{7}$$

$$z_{ij}-l_ix_j-u_jx_i+l_iu_j\le 0 \tag{8}$$

$$z_{ij}-u_ix_j-l_jx_i+u_il_j\le 0 \tag{9}$$

$$l_i \le x_i \le u_i \tag{10}$$

Tao Ding (e-mail: dingt12@mails.tsinghua.edu.cn) is with the Department of Electrical Engineering, Tsinghua University, Beijing, China. T. Ding is also a visiting scholar with the Department of Electrical Engineering and Computer Science, The University of Tennessee, Knoxville, TN 37996 USA.

Rui Bo is with the Midwest Independent Transmission System Operator (Midwest ISO), St.Paul, USA. (e-mail: rui.bo@ieee.org).

Fangxing Li is with the Department of Electrical Engineering and Computer Science, The University of Tennessee, Knoxville, TN 37996 USA. (e-mail: fli6@utk.edu)

where $\forall A, B\in\mathcal{R}^{2n\times 2n}$, $A\bullet B=\sum_{i=1}^{2n}\sum_{j=1}^{2n}a_{ij}b_{ij}$.

For minimization problem of the original QCQP, the QCQP-LR is a relaxed linear programming model and therefore provides a lower bound of the original QCQP. Similarly, it provides an upper bound for the maximization problem of the original QCQP. It can be observed that the relaxed IPF-LR model is dependent on the hyper-rectangular variable domain. At the beginning, the initial domain is usually so large that leads to a conservational interval solution, so it is desirable to schedule a more rigorous hyper-rectangle domain to achieve an optimal interval solution. For this reason, the OBBT method is employed in Fig.1 to solve the IPF-QCQP model, which will tighten the relaxed model IPF-LR based on linear optimality by cycling through each participating variable until the volume fails to improve.

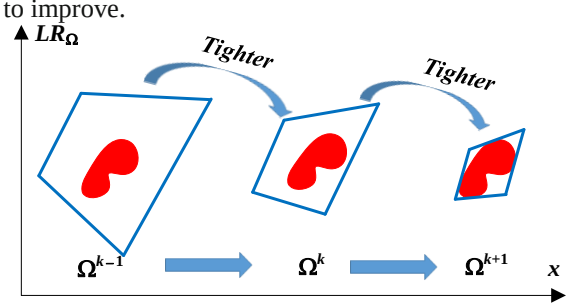


Fig.1 Gradually tightened convex hull using OBBT-based method

The proposed method was verified on the IEEE 57-bus system, with a ±20% variation on load and generator powers. The results were compared with those of Monte Carlo (MC) simulation with 5000 sample size. Fig.2 depicts the interval lower and upper bounds for voltage magnitudes. The comparison between QCQP and MC simulation illustrates the effectiveness of the proposed method, and the maximum error of voltage magnitude is no more than 3% and average error is about 1%.

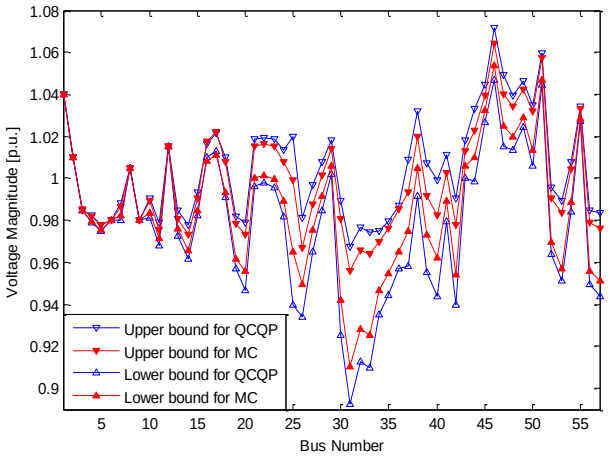


Fig.2 Bounds of voltage magnitudes under 20% variation

# Exploration of Multifrontal Method with GPU in Power Flow Computation

Xue Li, Fangxing Li, Joshua M. Clark
The Department of Electrical Engineering and Computer Science, the University of Tennessee, Knoxville, TN 37996, USA,
Email: {xli44, fli6, jclark74}@utk.edu

*Abstract*— **Solving sparse linear equations is the key part of power system analysis. The Newton-Raphson and its variations require repeated solution of sparse linear equations; therefore improvement in efficiency of solving sparse linear equations will accelerate the overall power system analysis. This work integrates multifrontal method and graphic processing unit (GPU) linear algebra library to solve sparse linear equations in power system analysis. Multifrontal method converts factorization of sparse matrix to a series of dense matrix operations, which are the most computational intensive part of multifrontal method. Our work develops these dense kernel computations in GPU. Example systems from MATPOWER and random matrices are tested. Results show that performance improvement is highly related to the quantity and size of dense kernels appeared in the factorization of multifrontal method. Overall performance, quantity and size of dense kernels from both cases are reported.**

## I. KEY EQUATIONS

$$\begin{matrix}\Delta P(\delta,V)=0\\ \Delta Q(\delta,V)=0\end{matrix} \rightarrow \begin{bmatrix}\Delta P\\ \Delta Q\end{bmatrix} = \begin{bmatrix}\frac{\partial \Delta P}{\partial \delta} & \frac{\partial \Delta P}{\partial V}\\ \frac{\partial \Delta Q}{\partial \delta} & \frac{\partial \Delta Q}{\partial V}\end{bmatrix}\begin{bmatrix}\Delta \delta\\ \Delta V\end{bmatrix}$$

## II. KEY FIGURES

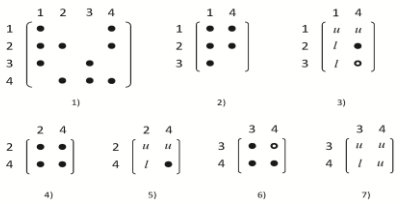

Fig. 1. Example of Multifrontal Method

## III. KEY RESULTS

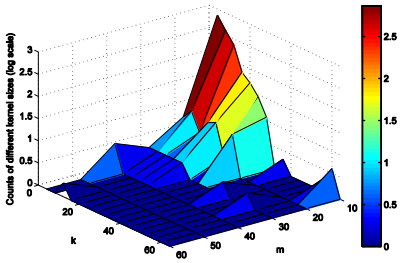


Fig. 2. Sizes of dense computation kernels of case3012wp

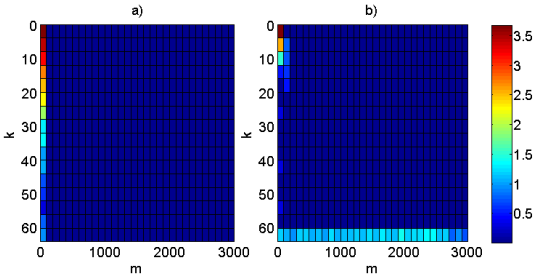


Fig. 3. a) Sizes of dense computation kernels of studied MATPOWER cases; b) Sizes of dense computation kernels of random generated sparse matrices with the same dimension and sparsity as MATPOWER cases accordingly

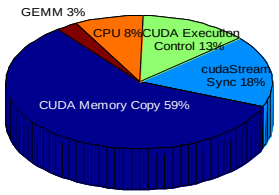


Fig. 4. Dense kernel run-time break down

TABLE I PERFORMANCE SUMMARY FOR MATPOWER CASES

| | case2383wp | case2736sp | case2737sop | case2746wp | case3012wp | case3120sp | case3375wp |
|---|---|---|---|---|---|---|---|
| **Size** | 4438 | 5237 | 5280 | 5127 | 5725 | 5991 | 6357 |
| **Sparsity** | 0.9986 | 0.9988 | 0.9988 | 0.9988 | 0.9989 | 0.9990 | 0.9990 |
| **Multifrontal w/BLAS(s)** | 0.0564 | 0.0676 | 0.0682 | 0.0715 | 0.0774 | 0.0757 | 0.0722 |
| **Multifrontal w/CUBLAS(s)** | 0.0591 | 0.0701 | 0.0712 | 0.0673 | 0.0756 | 0.0802 | 0.0773 |
| **Improvement** | -4.77% | -3.69% | -4.43% | 5.82% | 2.31% | -5.90% | -7.07% |

# Multi-objective Robust Optimization Model for Microgrids Considering Tie-line Power Constraints and Wind Uncertainty

Linquan Bai, Fangxing Li, Tao Ding, Hongbin Sun

**Extended Abstract:**

As an important clean energy source, wind power develops very fast in recent years, including microgrids. The wind power prediction techniques have been significantly studied. However, it is very difficult to accurately predict the wind power due to the intermittent nature of wind, which brings negative effects on the utilization of wind power.

When the microgrids operate at grid-connected mode, the tie-line power is always scheduled within a certain range to ensure the grid's security and stability in case of a contingency event.

The objectives of the energy management in microgrids may include maximizing the lifetime of energy storage (ES) and minimizing the utilization of power produced by the thermal units from the grid.

To address the above challenges, this paper proposes a multi-objective robust optimization model for microgrids with the consideration of tie-line constraints and wind uncertainty. The proposed method can effectively identify the optimal scheduling of ES and thermal power from the grid under the worst wind power forecast scenarios.

The objective function is given by:

$$f = \max_{P_w^{\min} \le \forall P_w^{(s)} \le P_w^{\max}} \begin{cases} \min\limits_{P_g} & \sum C_1\left(P_g\right) \\ \max\limits_{E} & \sum C_2\left(E\right) \end{cases} \quad (1)$$

where $P_g$ is the power produced by thermal units from the grid; $E$ is the energy in the ES; $P_w^{max}$ and $P_w^{min}$ denote the upper and lower bound of wind power output with the consideration of the wind power forecast errors; and $P_w^{(s)}$ is the wind power in a specific scenario.

In order to solve the multi-objective problem, the Pareto frontier is employed by transforming the multi-objective into a single one via the dualistic factor contrast method.

The constraints of the model can be expressed as (2)-(7).

(i) Tie-line power constraint:

$$P_{line}^{\min}(t) \le \sum_{i=1}^{N_g} P_{g,i}(t) + \sum_{k=1}^{N_w} P_{w,k}^{f}(t) + \sum_{j=1}^{N_e} P_{E,j}(t) - \sum_{r=1}^{N_d} P_{d,r}(t) \le P_{line}^{\max}(t) \quad (2)$$

where $P_{g,i}(t)$ is the power supplied by the $i$th thermal unit to the microgrid; $P_{w,k}^{f}(t)$ is the forecasted wind power; $P_{E,j}(t)$ is the ES output; and $P_{d,r}(t)$ is the load in the microgrid.

It should be noted that (2) is different from the energy balance constraints of traditional economic dispatch model, since the microgrid could exchange energy with the grid within a scheduled range $\left[P_{line}^{\min}, P_{line}^{\max}\right]$.

(ii) Ramping constraint:

$$DR_i \le P_{g,i}(t) - P_{g,i}(t-1) \le UR_i \quad (3)$$

where $UR_i$ and $DR_i$ are the upper and lower ramping power, respectively, for a thermal unit.

(iii) Transmission line constraint:

$$\left|P_{l-ij}(t)\right| \le P_{l-ij}^{\max} \quad (4)$$

where $P_{l-ij}(t)$ is the power flow on the transmission line and $P_{l-ij}^{\max}$ indicates the capacity for each transmission line.

(iv) Energy storage constraints:

In this work, the power output of ES is positive when it discharges and negative when it is charged.

$$-E_e \cdot \beta_C \le E(t) - E(t-1)(1-\sigma) \le E_e \cdot \beta_D \quad (5)$$

$$SOC_{\min} \le E(t)/E_e \le SOC_{\max} \quad (6)$$

where $\beta_C$ is the maximum charge rate, $\beta_D$ is the maximum discharge rate, $\sigma$ is the self-discharge rate of ES; $E_e$ is the rated capacity of ES; $SOC_{max}$ is the upper limit of SOC; and $SOC_{min}$ is the lower limit.

The equations with superscript ($s$) indicate all possible scenarios within the given wind power output range.

$$\begin{cases} P_{line}^{\min}(t) \le \sum\limits_{i=1}^{N_g} P_{g,i}^{(s)}(t) + \sum\limits_{k=1}^{N_w} P_{w,k}^{(s)}(t) + \sum\limits_{j=1}^{N_e} P_{E,j}^{(s)}(t) - \sum\limits_{r=1}^{N_d} P_{d,r}(t) \le P_{line}^{\max}(t) \\ DR_i \le P_{g,i}^{(s)}(t) - P_{g,i}(t-1) \le UR_i \\ \left|P_{l-ij}^{(s)}(t)\right| \le P_{l-ij}^{\max} \\ SOC_{\min} \le E^{(s)}(t)/E_e \le SOC_{\max} \\ -E_e \cdot \beta_C \le E^{(s)}(t) - E(t-1)(1-\sigma) \le E_e \cdot \beta_D \end{cases} \quad (7)$$

where the second and the fifth sub-equations in (7) are the ramping constraints to deal with the uncertain wind power next time period.

To solve the above optimization problem, robust optimization method is very suitable to be introduced to find the optimal solutions of scheduling ES and thermal power in the worst scenario.

L. Bai and F. Li are with the EECS Department, The University of Tennessee at Knoxville (UTK), TN, USA.

T. Ding is with the Department of Electrical Engineering, Tsinghua University, Beijing, China and the EECS Department at UTK, TN, USA.

H. Sun is with the Department of Electrical Engineering, Tsinghua University, Beijing, China.

Contact: F. Li, fli6@utk.edu.

# Impact of Load Models on the Statistics of Voltages in Stochastic Power Systems

Goodarz Ghanavati, Paul D. H. Hines and Taras I. Lakoba
College of Engineering and
Mathematical Sciences
University of Vermont
Burlington, VT

***Abstract*—This paper presents a study of the impact of different load models on the statistics of bus voltage magnitudes in stochastic power systems. Prior research shows that the stastistics of voltage magnitudes such as variance and autocorrelation rise as a power system approaches a critical transition such as voltage collapse or oscillatory instability. The increase in these statistics is due to critical slowing down which occurs in nonlinear stochastic dynamical systems. In this paper, we examine how these statistics vary with changes in load models. The results indicate that load characteristics can impact bus voltage statisitcs significantly. Therefore, if these statistics are to be used for power system stability monitoring, it is important to consider the uncertainty introduced by changes in load characteristics.**

## I. Introduction

Power systems are vulnerable to large scale failures such August 2003 blackout in the U.S. and Canada [1]. Integration of renewable energy sources into power systems results in increased stochasticity, which may increase the system's vulnerability. Also, power systems are increasingly operated near their stability limits. Therefore, it is important to enhance situational awereness to reduce the risk of blackouts.

Stochastic nonlinear dynamical systems research shows that there are early-warning signs (EWS) that indicate the approach of critical transitions [2]. Increase in variance and autocorrelation of state variables are two generic EWS. The increase in these statistics is sign of a phenomena known as critical slowing down (CSD), which is the slower recovery of dynamical systems from prerturbations as they approach critical transitions. These EWS are suggested in [2] as measures for determining the distance of a dynamical system to critical transitions.

Earlier research [3] has shown that CSD occurs in power systems as they approach voltage or oscillatory instability. Therefore, CSD signs may be useful indicators of stability in power systems. Also, the authors have previously shown that CSD signs are more clearly observable in voltage magnitudes than in other state variables [3]. In this paper, we examine how these statisitics change with load characteristics.

## II. Simulation and results

We model the system with a set of stochastic differential-algebraic equations:

$$\dot{\underline{x}} = f\left(\underline{x}, \underline{y}\right) \quad (1)$$

$$0 = g\left(\underline{x}, \underline{y}, \underline{\eta}\right) \quad (2)$$

where $f, g$ represent the set of differential and algebraic equations of the system, $\underline{x}, \underline{y}$ represent the vectors of differential and algebraic variables, $\underline{\eta}$ is the vector of gaussian random variables added to the load $\eta \sim \mathcal{N}\left(0, 0.01\right)$.

We studied the impact of load characteristics on the statistics of bus voltage magnitudes in a small three-bus system [4]. In this system, by increasing the load, the system moves toward the Hopf bifurcation. Fig. 1 shows the variance and autocorrelation of the load bus voltage magnitude versus the load level for three ZIP loads with different parameters. The variance and autocorrelation of the voltage magnitude increase as the system approaches instability. In the poster, we will discuss how varying the proportions of Z, I, P affects the variance and autocorrelation of voltages.

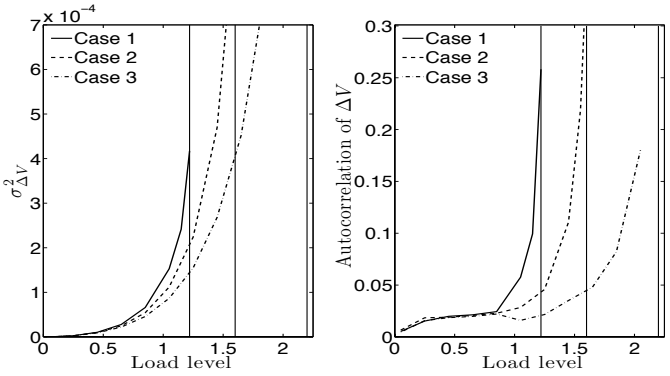


Figure 1. Variance and autocorrelation of the load bus voltage magnitude versus load level, the ratio of the load power to its nominal value. The parameters of ZIP load for cases 1,2,3 are respectively [100%P], [50%P, 50%I], [25%P, 50%I, 25%Z]. Vertical lines show the bifurcation points for three cases.

## References

[1] S. Abraham and J. Efford, "Final report on the August 14, 2003 blackout in the United states and Canada: causes and recommendations," US–Canada Power Syst. Outage Task Force, Tech. Rep., 2004.

[2] M. Scheffer, J. Bascompte, W. A. Brock, V. Brovkin, S. R. Carpenter, V. Dakos, H. Held, E. H. Van Nes, M. Rietkerk, and G. Sugihara, "Early–warning signals for critical transitions," *Nature*, vol. 461, no. 7260, pp. 53–59, Sep. 2009.

[3] G. Ghanavati, P. D. Hines, T. I. Lakoba, and E. Cotilla-Sanchez, "Understanding early indicators of critical transitions in power systems from autocorrelation functions," *arXiv preprint arXiv:1309.7306*, 2013.

[4] H. Ghasemi, "On-line monitoring and oscillatory stability margin prediction in power systems based on system identification," Ph.D. dissertation, University of Waterloo, 2006.

# Power Management of Remote Microgrids Considering Stochastic Behavior of Renewable Energy Sources

Santosh Chalise and Reinaldo Tonkoski

Electrical Engineering and Computer Science Department, South Dakota State University, Brookings, SD, USA
Email: santosh.chalise@sdstate.edu, reinaldo.tonkoski@sdstate.edu

***Abstract*—Traditionally, diesel generators are being used as a primary source of electricity generation in remote Microgrids. However, the overall fuel costs (including transportation and storage), and high maintenance, have resulted in high costs of energy. Renewable energy sources (RES) are good candidates to reduce fuel consumption, however also adds complexity in the power management system (PMS) due to the stochastic behavior of generated power output. Varying power output of RES cause a power imbalance in the system which ultimately affects the system's voltage and frequency. In addition, RES into the diesel and natural gas based microgrids reduces the loading of the generator. This power unloading forces generators to operate in the low efficiency region. The primary objective of PMS is to ensure the stable operation of microgrid system and also to optimize the energy generation with the objective to minimize the overall cost of energy. This task is of high complexity due to the presence of highly variable power generation. This research proposed an PMS framework for optimization on the day ahead as well as in the real time scale using particle swarm optimization (PSO). Hybrid control method was considered for the microgrid control. Key optimization objectives of proposed PMS are to reduce fuel consumption, maximize the use of renewable energy sources, and coordinate available resources to ensure microgrid reliability. Simulation of microgrid in different scenarios were performed and results were compared.**

***Keywords—microgrid; renewable; optimization; PSO; schedule***

## I. KEY FIGURES

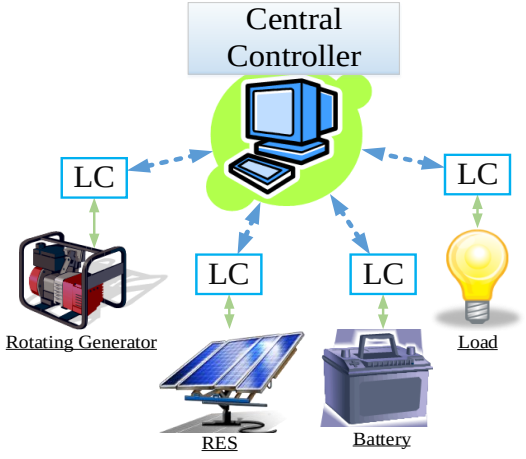


Fig 1: Hybrid control method

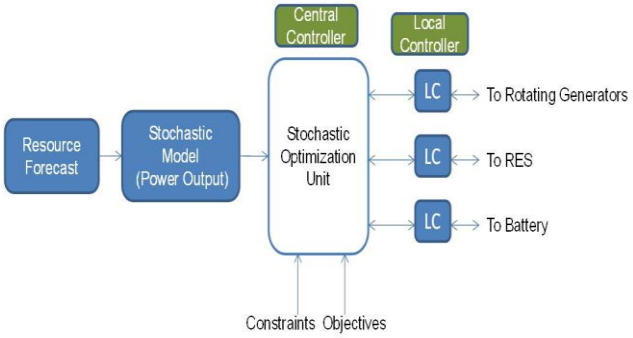


Fig. 2: Optimization framework

Fig 2: Microgrid optimization framework

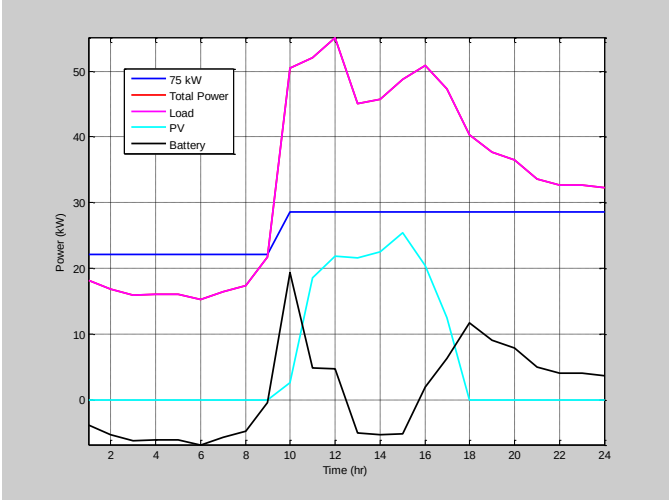


Fig. 3: Scheduled output of Generator and Battery

Table 1: Fuel consumption comparison

| Configuration | Fuel consumption, $ft^3/hr$ |
|---|---|
| Single Generator | 10050 |
| Single Generator with Battery | 9700 |

# FLUE GAS DESULFURIZATION WASTEWATER TREATMENT USING CONSTRUCTED WETLANDS

**Jose M. Paredez[1]**, Natalie Mladenov[1], Madhubhashini B. Galkaduwa[2], Ganga M. Hettiarachchi[2], Stacy Hutchinson[3]
*[1]Department of Civil Engineering, [2]Department of Agronomy,*
*[3]Department of Biological and Agriculture Engineering,*
*Kansas State University*
*Manhattan, KS, USA*

***Abstract*--BACKGROUND AND PURPOSE**: Coal-fired power plants emit harmful pollutants such as sulfur dioxide, nitrogen oxides, and carbon dioxides. To combat these harmful emissions the Clean Air Act was established in 1970. To comply with these federal regulations, coal-fired power plants implemented Flue Gas Desulfurization (FGD) to reduce sulfur dioxide emissions. Although FGD systems reduce atmospheric emissions they create wastewater containing harmful pollutants such as selenium, arsenic, and mercury. Constructed wetlands are increasingly being employed for the removal of these toxic trace elements from FGD wastewater. This study investigates constructed wetland's native microbes' dependency on organic carbon and the competitive interactions between selenium and arsenic in column experiments that simulate FGD wastewater treatment by constructed wetlands. Laboratory column outflow experiments using soils with natural FGD wastewater are underway. **ANTICIPATED RESULTS:** It is anticipated native microbes will be capable of treatment but require a carbon source and the competitive interactions between selenium and arsenic will rapidly fill sorption sites that may lead to a shorter treatment cell life. **CONCLUSION:** FGD technology has great potential for reducing harmful air pollutants from being emitted. Now the challenge remains to design treatment systems for the sequestration of toxic trace elements that are released in the FGD wastewater stream. Therefore our evaluation of the sustainability and most effective process parameters of constructed wetland systems is important for power providers.

# Optimal Power Flow Including Magnetic Amplifier by Using Sequential Quadratic Programming

Xiaohu Zhang[1], Kevin Tomsovic[1] and Aleks Dimitrovski[2]
[1]Dept. of Electrical Engineering and Computer Science, University of Tennessee, Knoxville, Tennessee, USA
[2]Oak Ridge National Laboratory, Oak Ridge, Tennessee, USA
Email: xzhang46@utk.edu

***Abstract*—Magnetic Amplifier (MA), a series reactor with continuous reactance regulation, is recently proposed to control the power flow. The cost of a MA is far less than a comparative FACTS device because it uses a simple and low power AC/DC power electronics to control its output reactance. Therefore, multiple devices can be installed in one system to maximize the utilization of the existing transmission system. Optimal Power Flow (OPF) is the fundamental approach for efficient power dispatch. To incorporate MA, standard OPF should be modified because the transmission line reactance will be considered as the optimization variable. This increases the nonlinearity of the OPF problem. In this study, the Sequential Quadratic Programming (SQP) [1] is adopted to solve the nonlinear and nonconvex problem. Numerical simulation results based on IEEE 9 bus, IEEE 30 bus are given to show the effectiveness of the method.**

## I. Key Equations

The modified OPF can be formulated as:
To minimize

$$f(w) \tag{1}$$

subject to

$$g(w) = 0 \tag{2}$$

$$h(w) \leq 0 \tag{3}$$

$w$ is the optimization vector which includes the transmission line reactance $x$:

$$w = [\theta \ V \ P_g \ Q_g \ x]^T \tag{4}$$

- $f(w)$ is the objective function, the total generation cost is selected.
- $g(w)$ is the real and reactive power balance equation at each bus.
- $h(w)$ is the limits on line flows, voltage magnitude, real and reactive power output for each generator and the reactance output for the MA.

The Lagrangian is given by:

$$\mathcal{L}(w, \lambda, \mu) = f(w) + \lambda^T g(w) + \mu^T h(w) \tag{5}$$

The QP subproblem at iteration k is formulated as:
To minimize

$$\nabla f(w^k)^T \Delta w + \frac{1}{2} \Delta w^T W^k \Delta w \tag{6}$$

subject to

$$g(w^k) + \nabla g(w^k)^T \Delta w = 0 \tag{7}$$

$$h(w^k) + \nabla h(w^k)^T \Delta w \leq 0 \tag{8}$$

$W^k$ is the Hessian of the Lagrangian at iteration k:

$$W^k = \nabla^2 \mathcal{L}(w^k, \lambda^k, \mu^k) \tag{9}$$

The solution of the subproblem is $[\Delta w^k \ \lambda^{k+1} \ \mu^{k+1}]$. The vector gives the search direction and the new value of the multiplier for next iteration. This process will continue until the solution converges.

## II. Key Results

The simulation test is based on IEEE 9 bus, and IEEE 30 bus system. Assume every non-transformer lines are installed with MA, the following table shows the comparison of generation cost.

TABLE I
Generation Cost

| | Cost $\$/h$ without MA | Cost $\$/h$ with MA |
|---|---|---|
| 9 bus | 12881 | 12717 |
| 30 bus | 964.4966 | 949.3825 |

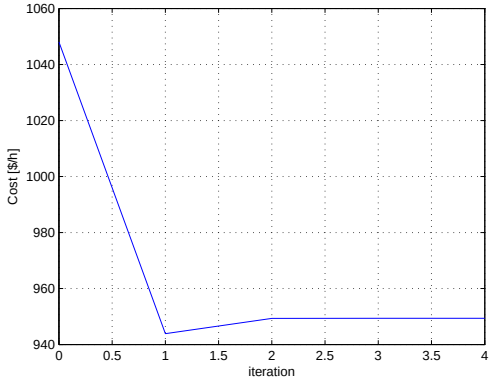


Fig. 1. Iteration Process for IEEE 30 bus system

## References

[1] J. Nocedal and S. Wright, Numerical Optimization. Springer, 2006 (2nd edition)

# NMSU Power Generating Capacity: Vision and Roadmap for 2050

Craig Bear, Shawn Benoit, Luis Caldera, Alejandro Castro Jr., Andrew Garcia,
and Marcus Wolschlager, *Student Members, IEEE*
Satish J. Ranade, Nadipuram Prasad

***Abstract*--Energy sustainability has become a key consideration in planning for future infrastructure during the past few decades. As campus loads are projected to increase well into the future, there is an abundant need for upgrading current infrastructure as well as researching and implementing novel energy harvesting technologies for the purpose of increasing campus sustainability. This poster presents a visionary roadmap of how such sustainability-minded programs can be implemented by the year 2050.**

## I. Introduction

New Mexico State University's power generating capacity must increase to meet the energy demands of campus facilities by the year 2050. In its current configuration, NMSU's co-generation plant can only supply around 40% of the present campus load. The remainder of the demand is provided by the El Paso Electric Company, primarily from the Tortugas substation. With the student population on the rise and the price of electrical energy increasing due to political climates, inflation, and growing scarcity of resources, NMSU faces a classic challenge seen in the utility industry: current power generation is being utilized at its economic maximum and is being rapidly outpaced by growing demand. This poster explores potential solutions that would help NMSU keep up with growing demands.

At a minimum, if present power generating capacity is maintained, all campus facilities must employ alternate means to generate power in order to contribute towards meeting increased growth in campus energy requirements. New building construction must integrate energy harvesting capabilities to harness energy from air exhaust systems, utilize available space on rooftops for solar energy, and explore other innovative ideas in energy storage and generation toward developing sustainable environments. The goal is to create environments that are self-sufficient in their energy requirements. The integration of such novel energy harvesting technologies will transform NMSU's campus into a true microgrid configuration.

Simple modifications to current infrastructure are also explored in this poster. Currently, NMSU's co-generating station is comprised of an AC generator driven by a natural gas fired turbine through a gearbox operating at 1800 RPM. A potential solution that could improve sustainability would be to replace the AC generator with a direct shaft connected DC generator. Such a DC generation could generate sufficient amounts of power to create an energy surplus, which could be sold back to El Paso Electric. This would provide long-term benefits to the University by increasing generation capacity, lowering tuition, and enabling the University to use the profits to make campus improvements. The bottom line is that if NMSU can become sustainable, it could become a localized self-sufficient microgrid and eventually produce even more power than that required by the campus.


Fig 1: Concept for harvesting energy from building air exhaust systems

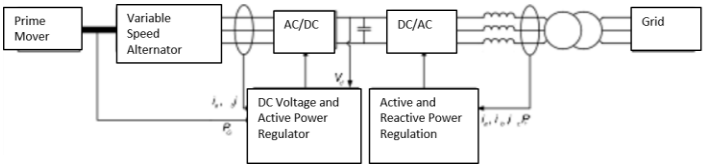


Fig 2: Proposed configuration of a variable speed alternator without a gearbox and a synchronous generator

While predominantly a visionary outlook on campus sustainability, the roadmap presented in this poster may serve as a model for other campuses seeking to implement similar changes. Microgrid and energy sustainability projects are actively being researched by students at NMSU under the direction of Dr. Satish Ranade and Dr. Nadipuram Prasad.

# Power System Events Identification using Feature Selection and Extraction Techniques

Prem Alluri, *Student Member, IEEE,* Sarika Khushalani Solanki, *Senior Member, IEEE,*
Jignesh Solanki, *Member, IEEE*

Lane Department of Computer Science and Electrical Engineering
West Virginia University (WVU)
Morgantown, WV, USA
e-mail: skhushalanisolanki@mail.wvu.edu

***Abstract*— An Electric Power Grid is a vast interconnected network which delivers electricity from suppliers to consumers. Large number of dynamic events occur in the grid on daily basis with some having negligible effect whereas others leading to Catastrophic Failures. Recent trends in wide area measurement systems (WAMS) have brought techniques that can be used to identify and prevent these events in turning into catastrophic failures. This paper presents a novel technique to identify dynamic events in the grid by considering only minimal set of system parameters (measurements). Symbolic Aggregate Approximation (SAX) is used to discretize the time series non-linear measurements and the obtained symbolic data is clustered into predominant groups. Feature extraction and selection techniques are used on each of the clustered groups to identify minimal sets of measurements that are capable to identify specific power system events. The proposed methodology recognizes Power System events in a minimal time with accuracy around 89%.**

## I. Symbolic Aggregate Approximation

SAX is a process of symbolic representation of time series data with an approximate distance function with the lower bound of the Euclidean distance [1]. It uses PAA in which each sequence of time-series data is divided into s segments of equal length (Sliding Window segments) and the average value of each segment is used as a coordinate of an s-dimensional feature vector. Figure 1, shows an example of time series to symbolic string conversion

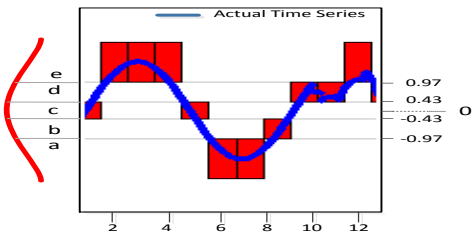


Figure 1. Time series discretization using SAX. The SAXified output of the above time series is a symbolic string 'c e e e c a a b d d e'

After transforming time series using PAA, discretization step is performed to produce symbols of equal probability. The division point on the numeric axis is decided to equalize the cumulative probability in the division section according to the number of digitization (break point size β). In Figure 1, sliding window length is 11 and the break point size β is 5 i.e (a,b,c,d,e).

## II. Methodology of Implementation

The Proposed approach has two steps a) Offline training mode and b) Online classification mode. In the offline mode, training data set is built using all the instances (events) generated and this data set is grouped into coherent clusters based on the information it gives out. In the Online classification mode, each newly arrived test instances are compared with the clusters built in the offline mode and the nearest observed cluster gives out the information of the event occurred. Once the classification of the new instances is made, these classified ones are then added to their respective cluster in the training data set.

## III. Key Results

The proposed methodology is performed on IEEE 24 bus Reliability test system with 11 generator units.

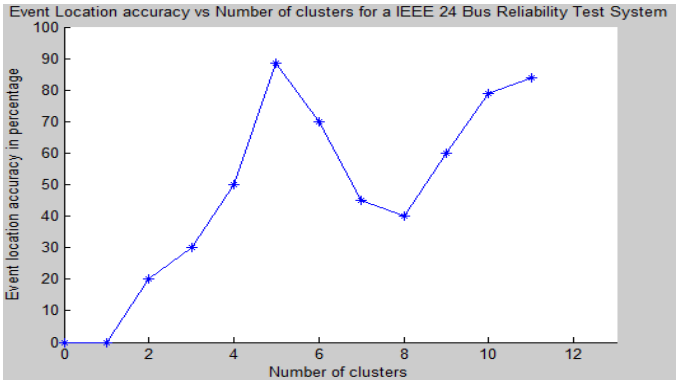


Figure 2. Event Location accuracy with resepct to the number of clusters.

## References

[1] J. Lin, E. Keogh, S. Lonardi, J.P. Lankford and D.M. Nystrom, "Visually Mining and Monitoring Massive Time Series," *proceedings of the tenth ACM SIGKDD International Conference on Knowledge Discovery and Data Mining. Seattle, WA, Aug 22-25, 2004.*

# Locating Sub-Cycle Faults in Distribution Network Applying Half-Cycle DFT Method

Po-Chen Chen, Vuk Malbasa, and Mladen Kezunovic
Power System Control and Protection Laboratory, Department of Electrical and Computer Engineering,
Texas A&M University, TX 77843
Email: pchen01@neo.tamu.edu, vmalbasa@tamu.edu, kezunov@ee.tamu.edu

***Abstract*— It is necessary to accurately detect and locate sub-cycle faults in order to prevent unexpected outages. However, conventional fault location methods cannot locate these faults as typically data windows longer than the fault's signature are used for phasor extraction. This paper presents an overall analysis of how the single-phase-ground sub-cycle fault in the distribution network can be located using voltage sag. The half-cycle Discrete Fourier transform is used for phasor extraction in the time-domain simulations. Our results reveal that the proposed approach is capable of accurately locating sub-cycle faults whose duration is between 0.5 and 1.0 cycles. The results also suggest that the placement of meters may significantly affect the capability of the proposed approach to locate sub-cycle faults.**

## I. KEY FIGURES

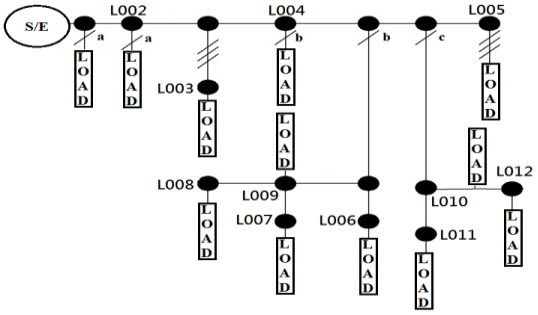


Figure 1. Saskpower network, Canada.

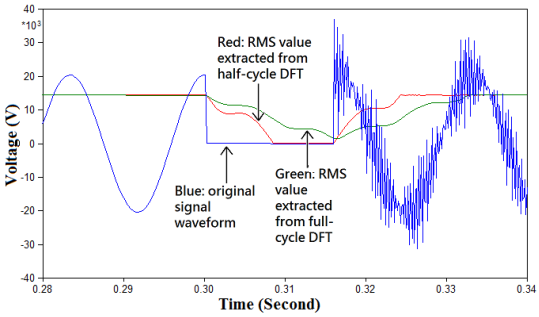


Figure 2. Comparison between data extracted from full-cycle and half-cycle DFT.

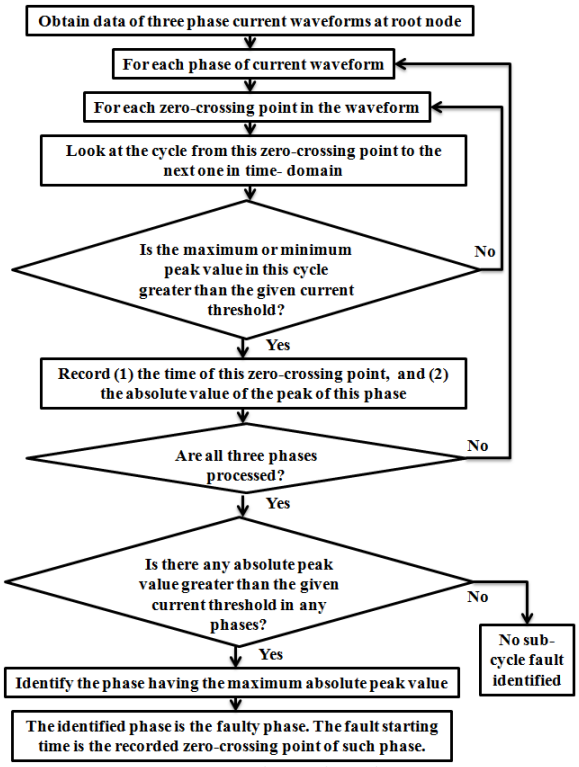


Figure 3. The procedure of identifying fault starting time and faulty phase.

## II. KEY RESULTS

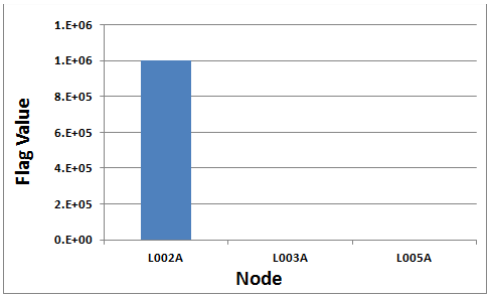


Figure 4. Results of cases, meters at all nodes: fault at L002A.

# A Lyapunov Function Based Remedial Action Screening Tool Using Real-Time Data

Mohammed Benidris, *Student Member, IEEE* and Joydeep Mitra, *Senior Member, IEEE*

***Abstract*—This work introduces a fast transient stability screening tool to classify a designated set of contingencies into stable and unstable subsets using direct methods. The proposed method is based on the conservativeness of the transient stability direct methods. The classification processes of the contingencies are performed along the solution trajectory towards the Controlling Unstable Equilibrium Point, controlling UEP. The proposed screening tool is intended to reliably capture the unstable contingencies and efficiently reduce the number of contingencies that need further analyses. If a numerical problem is encountered during the computation, the proposed scheme applies homotopy-based approaches to find the desired solution. If the numerical problem can not be solved using homotopy-based methods, the contingency is sent to a time-domain simulator for further analysis. The method is applied to the Western System Coordinating Council (WSCC) test system and results are presented.**

***Keywords*—*Transient stability, screening, Lyapunov function, homotopy.***

## I. Introduction

As a result of market forces, increased renewable generation, and recent advances in power flow control technologies, power systems are increasingly being operated closer to their stability limits. On-line transient stability assessment, TSA, has become one of the important features for systems that operate in such stressed environment. Attempts to reach on-line transient stability assessment have been facing high computation burden and low calculation speed. Most of the current strategies drop off the non-severe contingencies using screening tools and perform detailed simulations on the severe contingencies. The most important factors of any screening tool are the absolute capture of the unstable events and the efficiency of capturing the stable events.

The existing on-line transient stability analysis tools based on transient stability direct methods have introduced several system dependent thresholds for classifications. These thresholds are used to classify a set of contingencies to stable, unstable or undecided subsets. The undecided contingencies are the contingencies that have numerical convergence problems such as failure to calculate the controlling unstable equilibrium point, controlling UEP. In order for these thresholds not to fail in classifying the contingencies, off-line transient stability analyses are required. Also, for the unstable or undecided contingencies, detailed time-domain simulations are performed. Therefore, we can see that these methods need off-line transient stability assessments and may excessively use time-domain simulations.

The authors are with the Department of Electrical and Computer Engineering, Michigan State University, East Lansing, MI, 48823 USA e-mail: (benidris@msu.edu andmitraj@msu.edu).

## II. Focus of this Work

In this work, we propose a fast screening tool to classify a designated set of contingencies into stable and unstable subsets using transient stability direct methods. The proposed method utilizes the advantages of the conservativeness of the direct methods to initially classify the designated set of contingencies into stable, "potentially" unstable and undecided subsets. The potentially unstable subset is further divided into stable, potentially unstable and undecided subsets along the solution trajectory towards the controlling UEP. The undecided subset which has numerical problem is checked again using homotopy-based approaches.

The effective scheme utilized in this work is to check the stability of different points by transient stability direct methods to screen out a large number of stable contingencies, and then apply time-domain simulation to check those potentially unstable contingencies. The excessive use of time-domain simulations is considerably reduced by applying homotopy-based approaches in the case iterative methods fail to find a solution.

Depending on the speed of the computation and the extent of conservation, this procedure checks stability by sequentially checking energy margin at exit point, minimum gradient point and controlling UEP. If numerical problems, such as convergence issues, are encountered during the computation, the studied contingency is sent to time-domain simulation for stability check. However, before sending the contingency for the time domain simulator, if the numerical problem is related to the calculation of the post-fault stable equilibrium point, SEP, the minimum gradient point or the controlling UEP, we use homotopy-based approaches to find the controlling UEP. On the other hand, if the numerical problem is related to the exit point or the homotopy-based approaches fail to find the desired solution, the contingency is sent to the time-domain simulator for further analysis. The homotopy-based approaches are utilized in this work to increase the efficiency of the screening tool and to reduce the number of contingencies that need further analyses using time-domain simulations. The strategy of using direct method to filter out a large number of contingencies first and conducting further analysis on a much smaller number of contingencies makes the on-line transient stability screening feasible.

# Development of an FPGA based controller for islanding and anti-islanding of microgrid

Kumaraguru Prabakar, *Student Member, IEEE,* Yan Xu, *Member, IEEE,* and Fangxing Li, *Senior Member, IEEE*

***Abstract*—Microgrids are typically systems with distributed energy resources and loads. They have the capability to connect or disconnect from the grid through a switch. This differentiates the microgrids from a typical distribution system. The microgrid switch is usually located at the point of common coupling to enable the microgrid connect and disconnect itself from the main grid. The microgrid switch controller should have the capability to identify the black out and disconnect from the grid. Moreover, it should also connect back to the grid once the grid comes back. One such controller is developed using an FPGA based device. The logic of the controller is explained in this article.**

***Keywords*—Microgrid, Microgrid controller, FPGA.**

## I. Introduction

MICROGRIDS are systems which have distributed energy resources (DERs) and loads with the capability to connect or disconnect from the main grid [1]. In order to connect or disconnect from the grid, the microgrid controller should be able to identify the status and health of the grid and either connect or disconnect from the grid.

## II. Microgrid model used for testing

The microgrid model used for testing is shown in Figure 1. The microgrid model has four buses and it is connected to the main grid through bus number 1. The microgrid switch is located before bus number 3. The microgrid controller will decide when to open or close the switch to enable islanded or anti-islanded mode respectively.

## III. Islanding and anti-islanding requirements

The controller should check the operating characteristics on both sides of the switch. Parameters such as $3-\phi$ rms voltage, frequency and phase. If these parameters are not within a specific limit, the controller will island the system. Otherwise, if these parameters are within the limit under an islanded mode, the controller will anti-island the microgrid. This is shown as a flow chart in Figure 2.

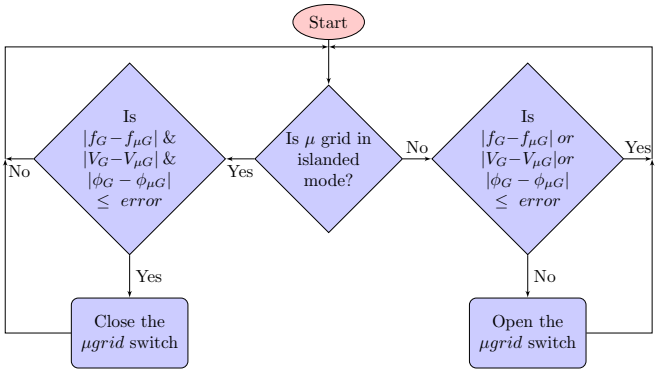


Fig. 2: Flowchart for operation of microgrid switch controller

## IV. Conclusion

This work discusses the development of FPGA based controller to island the microgrid from the main grid when the parameters shown above do not lie within the limits. Also, the controller will have the capability to resynchronize back to the grid, when the system parameters lie within the operating limits prescribed by the utility.

## References

[1] N. Hatziargyriou, H. Asano, R. Iravani, and C. Marnay, "Microgrids," *Power and Energy Magazine, IEEE*, vol. 5, no. 4, pp. 78–94, 2007.

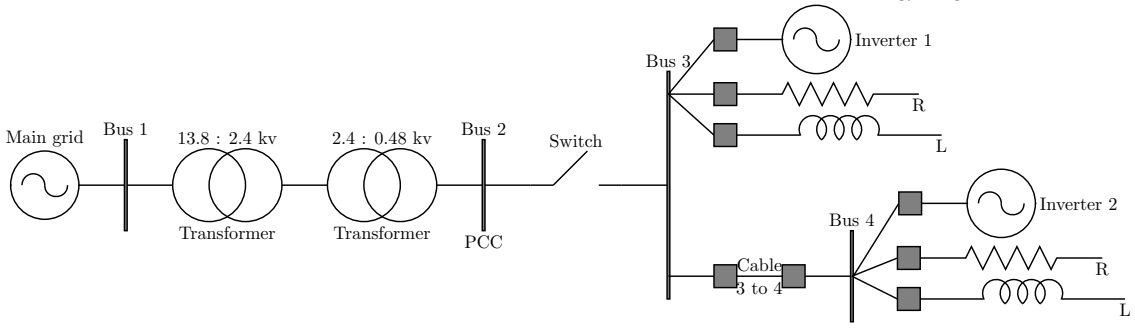


Fig. 1: Microgrid model used for switch controller test

# Development of Graphical User Interface for Reactive Power Planning and VAR Benefit Assessment for Power Systems with High Penetration of Renewable Energy

Riyasat Azim, *Student Member, IEEE*, Xin Fang, *Student Member, IEEE*, Weihong Huang, *Student Member, IEEE*, Fangxing 'Fran' Li, *Senior Member, IEEE*, Yan Xu, *Member, IEEE*

***Abstract*—The ever increasing renewable energy penetration in modern power systems tends to pose complex operational and planning challenges for the system operators. Reactive power planning and benefit sensitivity analysis of reactive power sources have become essential part of modern power system operation and planning. This Poster presents the functionalities of a graphical user interface under development which intends to provide a useful platform for voltage stability constrained reactive power planning and VAR benefit sensitivity analysis suitable for budget constrained reactive power planning. The graphical user interface integrates the capabilities of powerful optimization and power system analysis tools in order to provide a common platform for static VAR optimization, dynamic VAR optimization and VAR sources benefit sensitivity analysis with visualization and analysis capabilities.**

# Synchrophasor monitoring of line outages in WECC with an angle across an area

Atena Darvishi Ian Dobson
Electrical and Computer Engineering Department
Iowa State University, Ames IA USA
darvishi@iastate.edu, dobson@iastate.edu

***Abstract*—The area angle is a scalar measure of power system area stress that responds to line outages within the area and is a combination of synchrophasor measurements of voltage angles around the border of the area. Both idealized and practical examples are given to show that the variation of the area angle for single line outages can be approximately related to changes in the overall susceptance of the area and the line outage severity.**

## I. Introduction

The angle across an area of a power system is a weighted combination of synchrophasor measurements of voltage phasor angles around the border of the area [**?**]. The weights are calculated from a DC load flow model of the area in such a way that the area angle satisfies circuit laws. We previously showed how area angle responded to single line outages inside the area in some simple Japanese test cases [**?**]. Here we want to show and explain how the area angle responds to single line outages in an area of the WECC system. The changes in area angle can usually distinguish the single line outage severity, and can be related to changes in the overall susceptance of the area. We give some simple idealized examples to explain how the area angle works and then show results for an area of WECC.

## II. Results for angles across an area of WECC

We illustrate the use of area angles to monitor single, non-islanding line outages inside two areas of the WECC system. The WECC area shown in Figure **??** covers roughly Washington and Oregon. The northern (and western) border is near the borders of Canada-Washington, Washington-Montana and Oregon-Idaho, and the south border is near the Oregon-California border. North-south transfers through this area are of considerable economic importance. The area angle is

$$\begin{aligned}\theta_{\text{area2}} = {} & 0.223\,\theta_1 + 0.006\,\theta_2 \\ & + 0.008\,\theta_3 + 0.01\,\theta_4 + 0.02\,\theta_5 + 0.18\,\theta_6 + 0.59\,\theta_7 \\ & - 0.39\,\theta_8 - 0.41\,\theta_9 - 0.004\,\theta_{10} - 0.03\,\theta_{11} - 0.18\,\theta_{12}\end{aligned}$$

We are interested in monitoring the north-south area stress with the area angle when there are single non-islanding line outages, and relating changes in the area angle to the area susceptance and the outage severity. We take out each line in the system in turn and calculate the monitored area angle $\theta^{(i)}_{\text{area}}$ and the area susceptance $b^{(i)}_{\text{area}}$ in each case. We consider the maximum power coming to the area as a measure of the severity of the outage.

Both the area angle and the area susceptance track the severity of the outage for each line outage in Figure **??**. The similar patterns of changes in the area angles and the severity of the outage confirm the relationship between area angle and the severity of the outage.

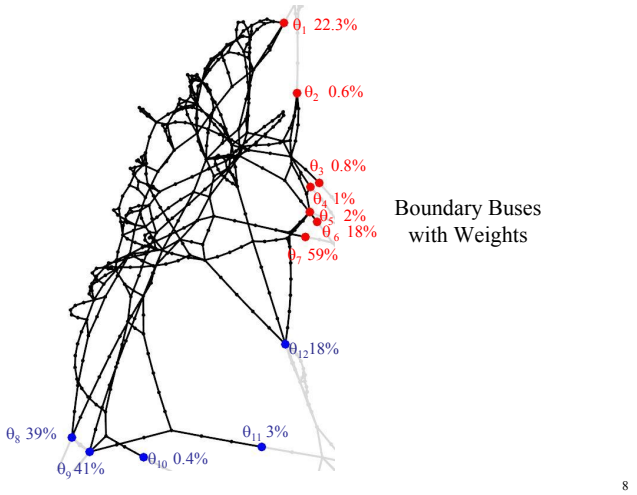


Fig. 1. An area of WECC system with area lines in black, north border buses in red and south border buses in blue. Layout detail is not geographic.

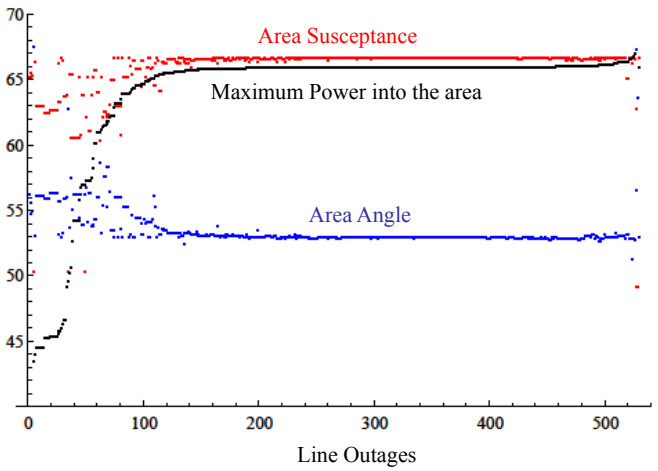


Fig. 2. Area angle $\theta^{(i)}_{\text{area}}$, area susceptance $b^{(i)}_{\text{area}}$, and max power into the area for each line outage in WECC area . Base case (the point at extreme right) is $\theta_{\text{area}} = 52.9^{\text{o}}$, $b_{\text{area}} = 66.7$ pu, max power = 66.0 pu.

## References

[1] I. Dobson, Voltages across an area of a network, *IEEE Transactions on Power Systems*, vol. 27, no. 2, May 2012, pp. 993-1002.

[2] A. Darvishi, I. Dobson, A. Oi, C. Nakazawa, Area angles monitor area stress by responding to line outages, NAPS North American Power Symposium, Manhattan KS USA, September 2013.

# Optimization Active Power Curtailment (APC) with Load Tap changing (OLTC) Regulators to Control Voltage fluctuating in Renewable supply

Hameed R. Atia
Electrical and Computer Engineering
South Dakota State University
Brookings, SD
Hameed.atia@sdstate.edu

***Abstract*—Abstract: The electric power grid has been growing constantly by high penetration of distributed generators (DGs) such as photovoltaic, wind turbines, and microturbines. Voltage Fluctuating is one of many challenges faced. This paper presents a novel method to optimize active power curtailment (APC) with Load Tap changing (OLTC) regulators to control voltage fluctuating in Microgrid. With significant level of solar or wind energy penetration, overvoltage can occur and the voltage at the load end may be greater than the voltage at the substation. On Load Tap changing (OLTC) regulators maybe not detect the overvoltage at the end of the feeder, optimized active power curtailment (APC) will control of voltage. Coordination of OLTC and APC with DG operation mode can control voltage rise and improve voltage profile, and ultimately minimize power loss.**

**Index Terms - Power curtailment, on load tap changing, distributed generators, voltage drop, objective function, constrain.**

***Index Terms*— Power curtailment, on load tap changing, distributed generators, voltage drop, and objective function, constrain. Linear programing.**

## I. INTRODUCTION

RENEWABLE energy is regularly growth worldwide because of energy [1]. At this day, distributed generation is seen mainly as a means of producing electrical energy. Conventionally, distribution systems have been designed to take power from the transmission system and to distribute it to customers [2]. Real power (P) impact to the voltage angle (θ) and reactive power (Q) impact to the voltage magnitude. Therefore the flowing of real power and reactive power has been from the higher to the lower voltage levels with angle (θ). This is shown in Figure1. However, with high penetration of renewable electrical energy the power flows may convert reversed and the distribution system is no longer a supplying loads. Distribution system operator has an responsibility to supply its customers at a voltage within specified limits (typically around _5% of nominal). This requirement often determines the design and capital cost of the distribution circuits and so, over the years, techniques have been developed to make the maximum use of distribution circuits to supply customers within the required voltages.

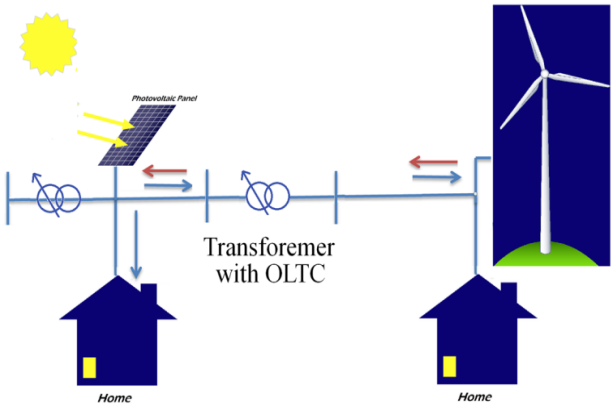


**Fig. 1. Typical Microgrid Level**

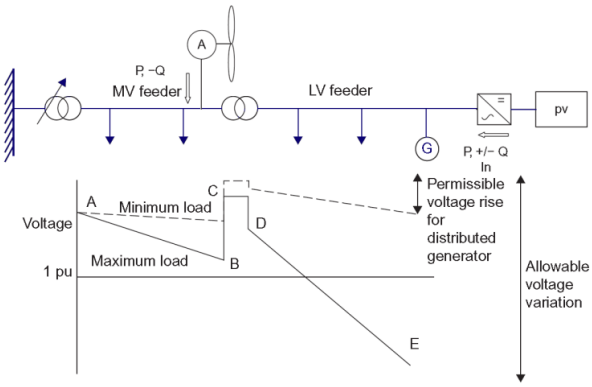


**Fig. 2. Voltage Variation down a radial Feeder**

The voltage profile of a radial distribution feeder is shown in Figure 2 with the key volt drops identified:

# A Wavelet-Based Method for High Resolution Multi-Step PV Generation Forecasting

Ahlmahz Negash, Ali Hooshmand, Ratnesh Sharma

***Abstract*-- Forecasts play a vital role in integrating renewable energy while maintaining power system stability and maximizing economic benefits of various energy resources. The issue with PV generation forecasting is that it relies on forecasts of solar irradiation which, due to the complex, nonlinear relationship between meteorological variables such as humidity, pressure, temperature, and cloud transients, can be quite difficult to model. Two important decisions in the forecasting process are selection of the forecasted variable (model output) and selection of explanatory variables (model inputs). This paper proposes a new method to forecast PV generation using wavelet based input selection and an output variable that directly represents clouds transients. We model this cloud effect by first determining a clear sky model (CSM) and forecasting the difference between the CSM and actual measurements of GHI. Potential model inputs are first decomposed using wavelet multi resolution analysis and final input selection is based on the correlation between the inputs and output at various timescales. Separate neural network structures are designed to separately forecast sunny and cloudy days. Using the high resolution forecast of GHI (20 min increments), the next day's PV generation is determined. The wavelet-based input selection step improves average PV power forecast accuracy by up to 15% on cloudy days and 25% on sunny days.**

***Index Terms*—High Resolution Forecasting, NARX Model, Multi-Step Prediction, Photovoltaics, Solar Irradiance**

## I. Results (Cloudy)

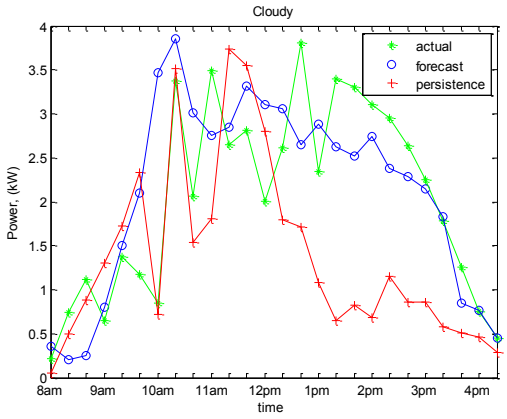


## II. Results (Sunny)

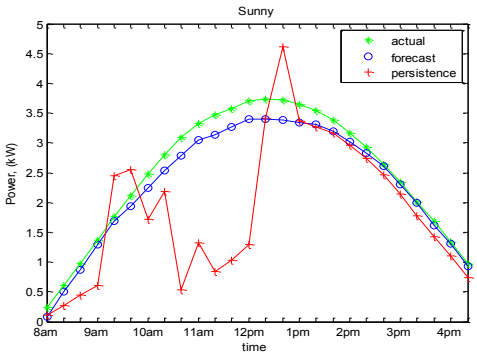


## III. Proposed Methodology

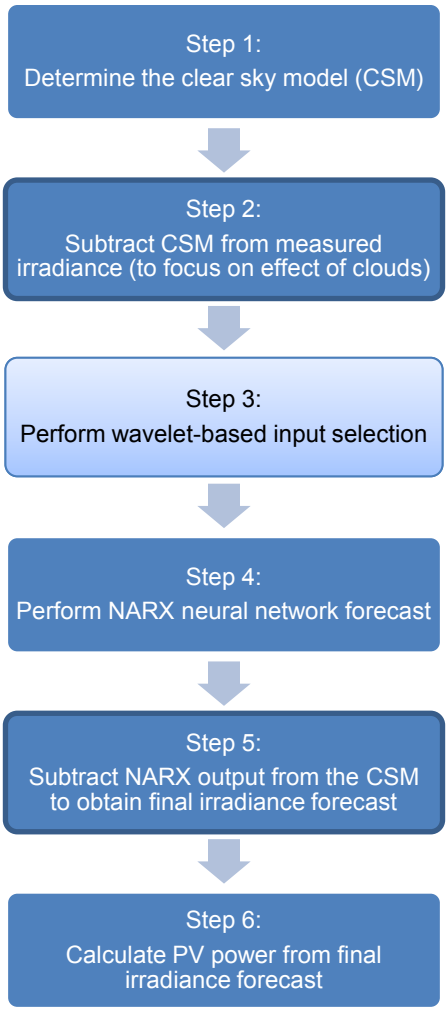


This work was supported in part by the National Science Foundation Graduate Research Fellowship Program (GRFP) and the Engineering Innovation Fellows Program (EIFP).

# Emission-based Optimal Dispatch Framework with DR and Volatile Wind Power

Hantao Cui, Fangxing Li
The Department of Electrical Engineering and Computer Science, University of Tennessee, Knoxville, TN 37996, USA
Email: {hcui7, fli6}@utk.edu

***Abstract*—The increasing penetration of wind power aims at reducing fuel consumption and the consequent emissions. On the contrary, volatility of wind power, especially the prediction error, increases the number of unintended startups or shutdowns of the prevailing thermal units thus elevates the emission level. This paper presents a framework for ISO and LSE to handle emission-based security-constrained optimal dispatch that accommodates demand response (DR) and volatility of wind power (WP) output. Expected results for the established model would demonstrate the effectiveness of minimizing emissions.**

## I. Framework Description

In the proposed framework, for day-ahead market, ISO commits the units according to emissions bids from generators, predicted WP output and informed load level by load side entity (LSE). ISO also checks network security of each commitment result to rule out violations. LSE, as an aggregator of demand side, performs voluntary DR programs internally and reviews load interrupting requests outside from ISO. LSE can be viewed as the sole demand side participant, on behalf of all loads, in the market operated by ISO.

Two types of incentive-based DR programs are included: voluntary and mandatory. Voluntary programs are managed by LSE with the forecasted electricity price. Mandatory programs are called for by ISO during network security check and verified by LSE. Volatility of WP is also incorporated into the framework, derived from the prediction error described by Beta distribution [1].

This framework adopts the flexibility at demand side, takes into account the impact of volatile WP and aims at minimizing emissions. Through nodal prices, balance of demand side and generation is achieved. It also clarifies the duties and steps for ISO and LSE, which is amenable for day-ahead optimal dispatch. Scheme of the framework is shown in Fig. 1.

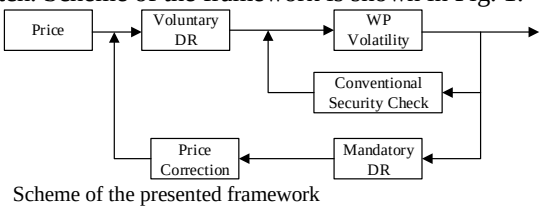


Fig. 1. Scheme of the presented framework

## II. Modeling Formulation

An input-based model is used to capture the emission characteristics of units. With a non-parametric Nadaraya-Watson kernel estimator of $SO_x$ and $NO_x$ emissions level[2], an estimate function that specifies the pollution level of pollutant $p$ as a function of generator $g$'s burned fuel $f$ is given as (1) , where $\phi_{g,p}$ and $f_g^n$ are the observed actual emission level and the actual fuel consumed, respectively. $K(\cdot)$ is the kernel of smoothing function and $h$ the bandwidth by which weight is exercised on neighboring observations.

$$\phi_{g,p}(f)=\frac{\sum_{n\in N}K\left(\frac{f-f_g^n}{h}\right)\phi_{g,p}^n}{\sum_{n\in N}K\left(\frac{f-f_g^n}{h}\right)} \tag{1}$$

Voluntary DR are modeled with fixed price elasticity and determined at early stage of the iterative scheduling process. Elasticity is given as

$$\varepsilon_k=\frac{\partial D_k / D_k}{\partial PR_k / PR_k} \tag{2}$$

Mandatory DR supplied by generators with high marginal emissions rate would be demanded curtailment by ISO, rather those located within high LMP zones. However, ISO faces the dilemma that each location differs in the sensitivity of price and emission. To identify the nodes where curtailment of DR is both economically and environmentally beneficial, emissions price (in \$/ton $SO_x$ and $NO_x$) is defined to convert emissions reduction to value in dollar. Overall value of DR at bus j composes of LMP reduction and emissions reduction value, is given as

$$\beta_j = f(\lambda_j)+\mathrm{g}(\kappa_j) \tag{3}$$

where $\lambda_j$ and $\kappa_j$ are the LMP and marginal emissions rate at bus *j*, respectively[3].

Finally, with Bender's decomposition, UC with SC for ISO is decomposed into two iterative problems. Master problem solves unit commitment and eliminates Bender's cut from sub problem, while sub problem checks network security and generates Bender's cuts. The whole framework is modeled as mixed-integer programming problem and solved by CPLEX.

## III. Expedted Results

To illustrate the validity and effectiveness of the presented framework and model, case study will be performed on ISO New England 39-bus system with 10 generators. Volatility of wind power will be identified with fixed Beta distribution parameters, followed with Monte-Carlo sampling and Cholesky decomposition. Voluntary DR resources will also follow a fixed elasticity.

Design of cases will focus on the configuration of Mandatory DR resources, i.e. locations, maximum curtailment power and duration. Successful solving the iterative model will show the validity of the model. A more promising result would be that under certain circumstances DR will be dispatched for emissions reduction purpose at the cost of higher LMP, although it could be used to reduce the latter. Meanwhile, time consumption to solve the model needs concern as an evaluation of its practical use.

# Energy Resource Scheduling in Real Time Considering a Real Portuguese Generation and Demand Scenario

Pedro Faria, Marco Silva, Zita Vale
GECAD - Knowledge Engineering and Decision Support Research Center
IPP - Polytechnic Institute of Porto
Porto, Portugal
pnfar@isep.ipp.pt, marsi@isep.ipp.pt, zav@isep.ipp.pt

***Abstract*— The development power systems and the introduction of distributed generation and Electric Vehicles (EVs), both connected to distribution networks, bring several huge challenges in the operation and planning tasks. This new paradigm requires improved energy resources management approaches in order to accomplish not only the generation, but also the consumption management through demand response programs, energy storage units, EVs and other players in a liberalized electricity markets environment. The work here presented includes a methodology to be used by Virtual Power Players (VPPs), concerning the energy resource scheduling in smart grids, considering day-ahead, hour-ahead and real-time energy resources scheduling. The case study considers a 33-bus distribution network with huge penetration of distributed energy resources. The wind generation profile is based on a real Portuguese wind farm. The obtained results concerns four scenarios taking into account 0, 1, 2 and 5 periods (hours, minutes, or other) ahead of the scheduling period, in the hour-ahead and real-time scheduling.**

***Index Terms*— Demand response, distributed generation, wind generation, remuneration tariffs.**

## I. KEY EQUATIONS

$$In = \sum_{t=1}^{T} \left[ \begin{array}{l} \sum_{L=1}^{N_L} MP_{Load(L,t)} \times P_{Load(L,t)} + MP_{Sell(t)} \times P_{Sell(t)} + \\ \sum_{ST=1}^{N_{ST}} MP_{Ch(ST,t)} \times P_{Ch(ST,t)} + \sum_{V=1}^{N_V} MP_{Ch(V,t)} \times P_{Ch(V,t)} \end{array} \right] \quad (1)$$

$$C = \sum_{t=1}^{T} \left[ \begin{array}{l} \sum_{DG=1}^{N_{DG}} c_{DG(DG,t)} \times P_{DG(DG,t)} + \sum_{SP=1}^{N_{SP}} c_{SP(SP,t)} \times P_{SP(SP,t)} + \\ \sum_{ST=1}^{N_{ST}} c_{Dch(ST,t)} \times P_{Dch(ST,t)} + \sum_{V=1}^{N_V} c_{Dch(V,t)} \times P_{Dch(V,t)} + \\ \sum_{L=1}^{N_L} c_{Cut(L,t)} \times P_{Cut(L,t)} + \sum_{L=1}^{N_L} c_{Red(L,t)} \times P_{Red(L,t)} + \\ \sum_{L=1}^{N_L} c_{NSD(L,t)} \times P_{NSD(L,t)} + \sum_{DG=1}^{N_{DG}} c_{GCP(DG,t)} \times P_{GCP(DG,t)} \end{array} \right] \quad (2)$$

This work is supported by FEDER Funds through COMPETE program and by National Funds through FCT under the projects FCOMP-01-0124-FEDER: PEst-OE/EEI/UI0760/2011, PTDC/SEN-ENR/122174/2010 and SFRH/BD/80183/2011 (P. Faria PhD), and by the GID-MicroRede, project nº 34086, co-funded by COMPETE under FEDER via QREN Programme.

## II. KEY FIGURE

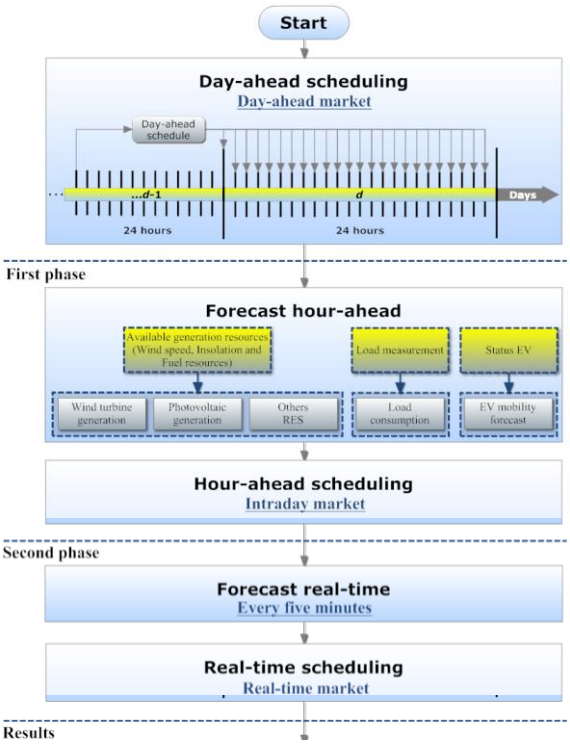


Figure 1. ERM proposed methodology.

## III. KEY RESULTS

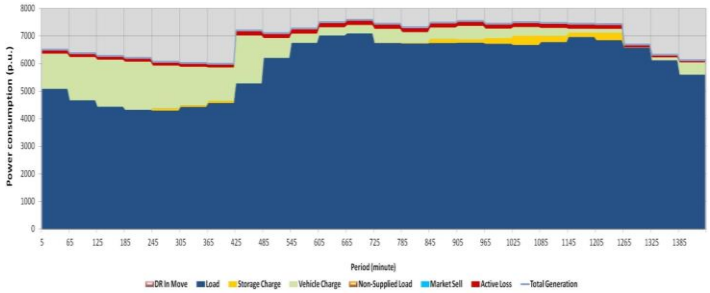


Figure 2. Day-ahead load demand forecast and EVs charge scheduling.

# Renewable Energy Forecasting using Hybrid Artificial Neural Network Technique.

Chiranjeevi Bharadwaj Kotharu[1*], *Student Member, IEEE*, Dipesh Patel[1**], *Student Member, IEEE*, Ziyad M. Salameh[1**], *Life Fellow, IEEE*

***Abstract*— Renewable energy forecasting presented a huge demand for better and accurate prediction models in the electric utilities market. Being able to predict future energy generation not only helps energy traders but also helps utility, schedulers and operators of electricity. This poster presents the application of an iterative hybrid Artificial Neural Network (ANN) method known as Genetic Algorithm based Back-Propagation (GA-BP) neural network on energy forecasting. For analyzing this model the data was taken from a hybrid renewable energy data monitoring system at Renewable Energy Laboratory (REL) of University of Massachusetts Lowell. The results were validated against the available data and other methods of forecasting. The proposed method was implemented in Matlab & Simulink. The proposed method shows a significant improvement in efficiency with a mean relative error of 20% which is better when compared to those other prediction models with Mean relative error of up to 30%**

***Index Terms*— Hybrid Artificial Neural Networks, Short-Term Forecasting, Power Forecasting, reliability, Utility.**

## I. Proposed Architecture

The advent of Artificial Neural Networks into forecasting has improved the performance of prediction models to a great extent. The GA-BP methodology is well known for its accuracy and performance. The entire system is coded in Matlab and a Simulink model was created for it.

$$n = \sqrt{n_i + n_o} + a \tag{1}$$

The latest 24-hr data of wind speed, irradiance, wind power and solar power generated by the RES are used as inputs for network to predict the following 1-hr data. The input nodes of the network are 144 i.e. (24X6=144) equals the 24-hr data count. The output readings count for 6 as for 1-hr. The hidden layer nodes are judged according to the equation 1.

Where $n$ is the number of hidden layer nodes, $n_i$ and $n_o$ are the number of input and output nodes respectively and $1 \leq a \geq 10$. The fitness evaluation is formulated in order to obtain minimum value of the root mean square error (RMS). The objective function is the reciprocal of the RMS value as shown in equations 2, 3 and 4.

$$E_a = (T_a - O_a)^2 \tag{2}$$

$$E = \sqrt{\frac{\sum_{a}^{n} E_n}{n}}; \tag{3}$$

$$F_n = \frac{1}{E} \tag{4}$$

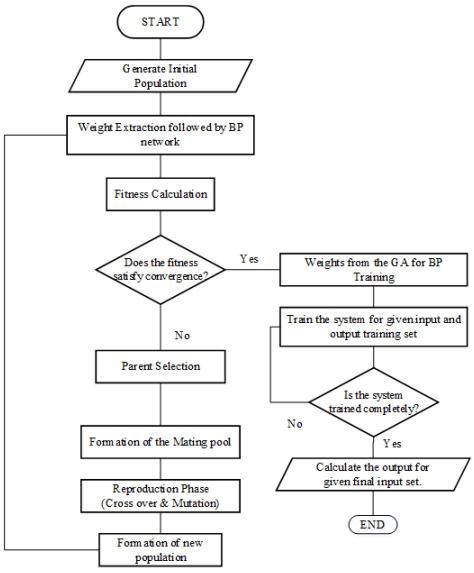


Fig.1 Algorithm for GA-BP used for power forecasting.

$$W_k = \begin{cases} + \dfrac{x_{kd+2}10^{d-2} + x_{kd+3}10^{d-3} + .....x_{(k+1)d}}{10^{d-2}}, if\ 5 \leq x_{kd+1} \leq 9 \\ - \dfrac{x_{kd+2}10^{d-2} + x_{kd+3}10^{d-3} + .....x_{(k+1)d}}{10^{d-2}}, if\ 0 \leq x_{kd+1} < 5 \end{cases} \tag{5}$$

Where $x_{1,}x_{2\ldots,}$ $x_d$ represent chromosomes and $x_{kd+1,}$ $x_{kd+2,\ldots\ldots,}x_{(k+1)d}$ represent the $k$th gene in chromosome. While the actual weight is $W_k$, $T_a$ is the actual output, $O_a$ is the calculated output, $E$ is the error and $F_n$ is the objective function.

## I. Key Result

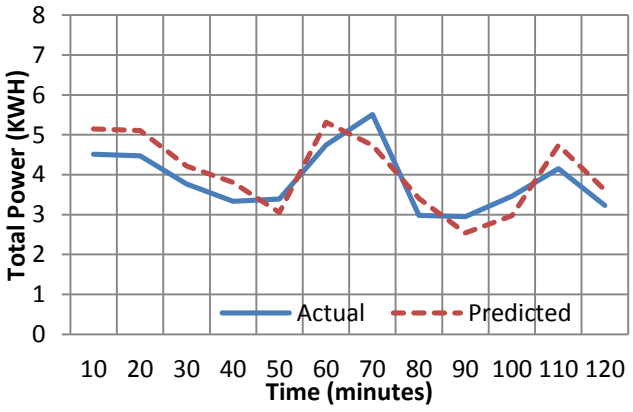


Fig.2 Predicted Vs Actual measured total power generated by the hybrid RE.

# Harmonic Analysis in Distribution System with Electric Vehicles and Wind Generators

Ritam Misra
Department of Electrical and Computer Engineering
Michigan Technological University
Houghton, USA
rmisra@mtu.edu

Sumit Paudyal, Member IEEE
Department of Electrical and Computer Engineering
Michigan Technological University
Houghton, USA
sumitp@mtu.edu

***Abstract*— Harmonic distortion on voltages and currents increases with the increased penetration of Electric Vehicle (EV) loads in distribution systems. Wind Generators (WGs), which are source of harmonic currents, have some common harmonic profiles with EVs. Thus, WGs can be utilized in careful ways to subside the effect of EVs on harmonic distortion. This paper studies the impact of EVs on harmonic distortions and integration of WGs to reduce it. A decoupled harmonic three-phase unbalanced distribution system model is developed, where EVs and WGs are represented by harmonic current loads and sources, respectively. The developed model is first used to solve harmonic power flow on IEEE 34-bus distribution system with 100% penetration of EVs are modeled in OPENDSS, and its effect on current/voltage total harmonic distortions (THDs) is studied. Next, carefully sized WGs are selected at different locations in the 34-bus distribution system to demonstrate reduction in the current/voltage THDs.**

***Index Terms*--Total harmonic distortion, Electric Vehicles, Wind energy, Distributed generation, Load management.**

## I. KEY EQUATIONS

The L wye-connected constant power loads on a per-phase basis has been designed as:

$$\left|I_{p,L}^{h}\right|\left(\angle V_{p,L}^{h}-\angle I_{p,L}^{h}\right)=\left|I_{0}{}_{p,L}^{h}\right|\angle\theta_{p,L}^{h}(1)$$

To represent the line current balance in each case after the integration of wind and PEV the following equation is used:

$$I_{w}{}_{p,n}^{h}+\sum_{\alpha}I_{p,l,r}^{h}=\sum_{\beta}I_{p,l,s}^{h}+\sum_{L}I_{p,l}^{h_1}+I_{ev}{}_{p,n}^{h_2} \qquad (2)$$

The total harmonic distortion of voltage ($THD_v$) and current ($THD_i$) are defined as

$$THD_{v}=\left[\left(\sum_{h=2}^{13}|V_{n}^{h}|^{2}\right)^{1/2}\Big/|V_{n}^{1}|\right]\times 100\%(3)$$

$$THD_{i}=\left[\left(\sum_{h=2}^{13}|I_{n}^{h}|^{2}\right)^{1/2}\Big/|I_{n}^{1}|\right]\times 100 \qquad (4)$$

## II. KEY FIGURE

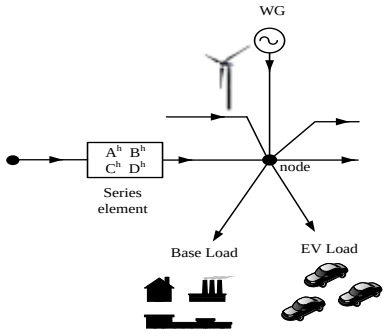


Fig. 1 Integration of EVs and WGs in the system

## III. KEY RESULTS

Table I. THD of Line Currents

| Case Studies | Monitors | Line Current THD of phase a | Line Current THD of phase b | Line Current THD of phase c |
|---|---|---|---|---|
| Case A | M1 | 40.5245 | 33.8273 | 33.5022 |
| | M2 | 10.201 | 9.0188 | 7.4814 |
| | M3 | 6.7618 | 7.9453 | 7.6573 |
| | M4 | 9.8209 | 5.237 | 9.261 |
| Case B | M1 | 4.8969 | 6.1360 | 5.1628 |
| | M2 | 35.3252 | 46.5441 | 37.8092 |
| | M3 | 17.0135 | 32.1931 | 37.6465 |
| | M4 | 8.8201 | 6.0144 | 7.7061 |
| Case C | M1 | 6.2027 | 7.5608 | 7.3108 |
| | M2 | 5.2343 | 6.4292 | 6.5506 |
| | M3 | 7.9585 | 7.8224 | 6.9416 |
| | M4 | 6.3561 | 5.067 | 6.3421 |

# Optimization of a Solar-Diesel-Battery Hybrid Energy System for Remote Regions

Mu Chai, Zichun Tang and Moonyoung Lee
Department of Engineering Science, University of Toronto, Toronto, ON, M5S 3G4 Canada
Email: mchai@ieee.org, zichun.tang@mail.utoronto.ca, moonyoung.lee@utoronto.ca

***Abstract*** **– The cost of Photovoltaic (PV) panels has gone down rapidly in the last ten years. Although rooftop installations in Canadian urban areas have yet to reach grid parity without government incentives, PVs among other renewables are increasingly being considered to meet the load demands of Canadians in remote northern areas due to their high cost of electricity. While many qualitative studies have been done, this paper aims to both quantify and optimize the cost of a Solar-Diesel-Battery Hybrid Energy System to power a remote research centre. In order to achieve high model accuracy, the on-site actual annual irradiance will be used in conjunction with an approved PV model to simulate PV generations. Through the use of accurate PV modelling and Mixed Integer Linear Programing (MILP), the optimal number of batteries, number of solar panels as well as the types of panel out of 20 off-the-shelf models will be determined. Only actual data and manufacturers' fact sheets are used in this model, while certain underlying assumptions are made.**

## I. Key Equations and Graphs

Objective function: The following function represents the cost function that the optimization algorithm desires to minimize:

$$TotalCost = (Cost\ of\ Diesel\ Unit\ \left[\frac{\$}{kw}\right] \times P_{Disel}) + (Cost\ of\ Battery\ \left[\frac{\$}{bat}\right] \times Number\ of\ Battery) + (Cost\ of\ Panel\ \left[\frac{\$}{panel}\right] \times Number\ of\ panel)$$

Or, simply:

$$Min\ C^T X = Min \begin{bmatrix} C_{Diesel} \\ C_{Battery} \\ C_{Panel} \end{bmatrix}^T \begin{bmatrix} P_{Disel} \\ N_{Battery} \\ N_{Panel} \end{bmatrix}$$

$$Where\ C_{Diesel} = [0.59\ 0.59 \dots 0.59] \in \mathbb{R}^{1x(24*365)},$$

$$C_{Battery} \in \mathbb{Z}, C_{Panels} \in \mathbb{Z}^{1\times 20}$$

$$P_{Diesel} \in \mathbb{R}^{(24*365)x\,1}, N_{Battery} \in \mathbb{Z}, N_{Panel} \in \mathbb{Z}^{20\times 1}$$

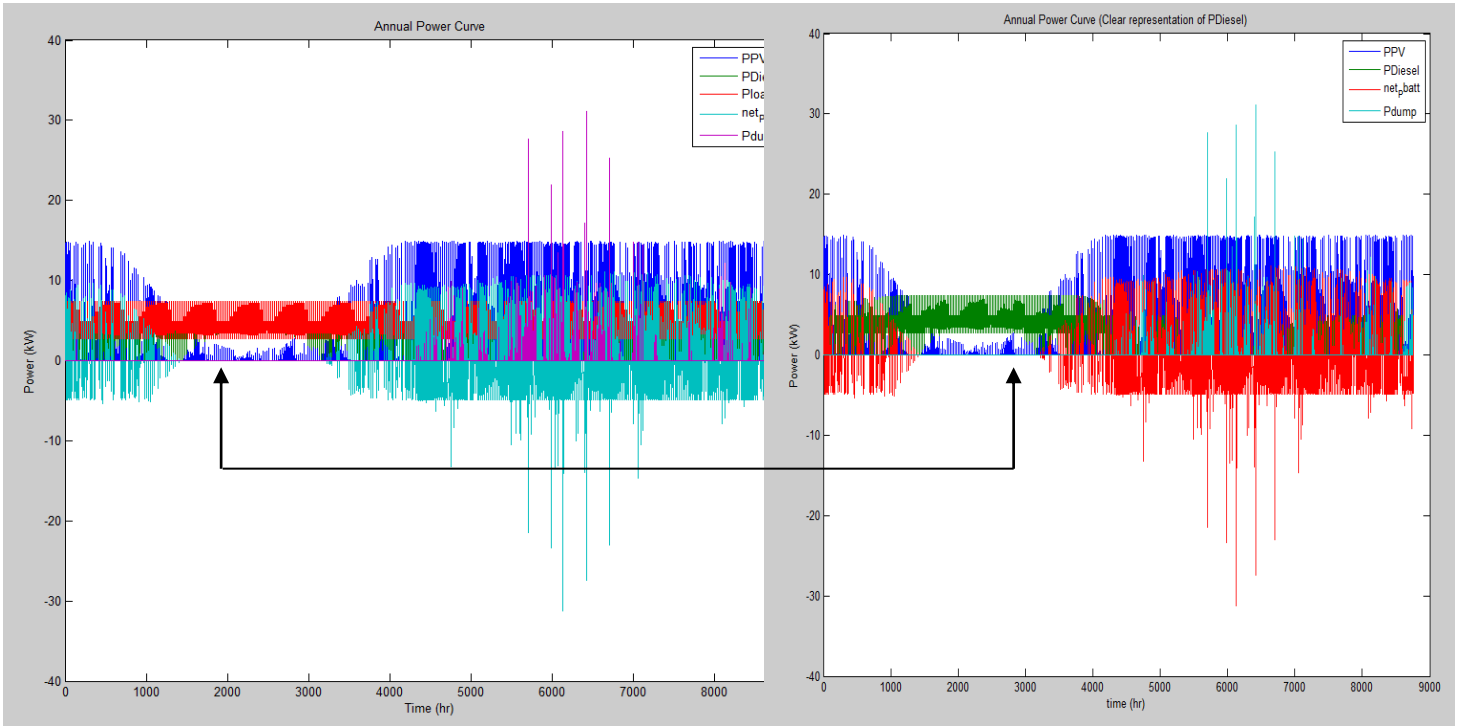


*Figure 1 Annual Power Curve*

*Figure 2 Annual Power Curve (Clearly shows $P_{Diesel}$)*

# Integration of Photovoltaic with Hydro only System in an Isolated Network

Pratiksha Tiwari, Reinaldo Tonkoski and David. Galipeau
Department of Electrical and Computer Science
South Dakota State University
Brookings, SD, USA
pratiksha.tiwari@sdstste.edu

***Abstract*—** In an isolated remote areas of developing countries, micro hydro is one of the main energy sources. Availability of water decreases significantly in winter season which directly effects the hydro power generation. Combining solar photovoltaics with micro hydro can be an effective solution for isolated areas where grid extension is not feasible. Photovoltaics (PV) can supply power during day and hydropower supply power during night and cloudy days. Increase in photovoltaic power reduces hydro generation. However, injecting photovoltaic power can cause disturbance in system frequency due to its intermittent nature. Previous work has shown the simulation of hydro and photovoltaic with battery backup system can meet the power demand. But, the ability of hydro to handle frequency deviations due to photovoltaic variability has not addressed. Frequency response of the system with photovoltaic and governor controlled hydro was investigated, but was not validated in a real system. The goal of this research is to analyze the frequency transients in an isolated network with solar photovoltaics and hydropower as power sources. Hydro model was developed in Matlab/Simulink with synchronous machine, excitation system and its governor system and photovoltaic power was injected as a current source to the system. The change in frequency due to variations in photovoltaics power output and load curve was analyzed. Simulation was done for different irradiance data obtained experimentally in the microgrid lab. Simulation results show that, hydro can handle the frequency transients due to photovoltaic power fluctuation and load variation if existing hydro has the sufficient inertia. Further to validate the system, real time simulation of developed model will be done in the real time digital simulator. An inverter based hydro emulator will be developed to have the same characteristics of the hydro system and a real photovoltaics system will be implemented. Control signals from real time digital simulator will drive hydro emulator. A power hardware in the loop simulation with real photovoltaics and inverter based hydro system emulator will be used to investigate the frequency response of hybrid photovoltaics and hydro system.

Fig. 1 shows a block diagram of the PV/hydro system which includes PV panels with a grid tied micro- inverter, a hydro system and loads connected to a common 400 VAC bus. Fig. 2 shows the daily load profile, PV generation, hydro generation and frequency response of the PV/hydro system for a sunny day. The frequency of the system was within ±2.5% of the nominal frequency of 50 HZ up to 160 seconds. After that the load decreased from 95 to 10 kW (89%) in 20 seconds which increased the frequency above 2.5% but returned back to the steady state. This indicates that the system was stable but may need additional inertia to maintain frequency within ±2.5% of nominal frequency.

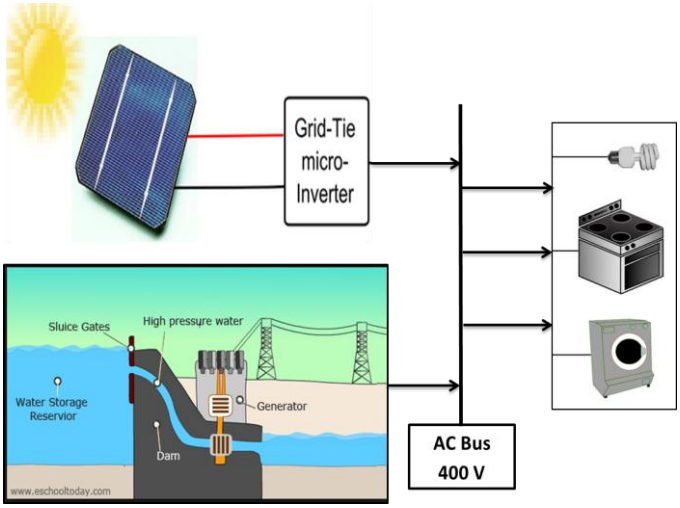


Fig. 1 Block diagram for PV/hydro system

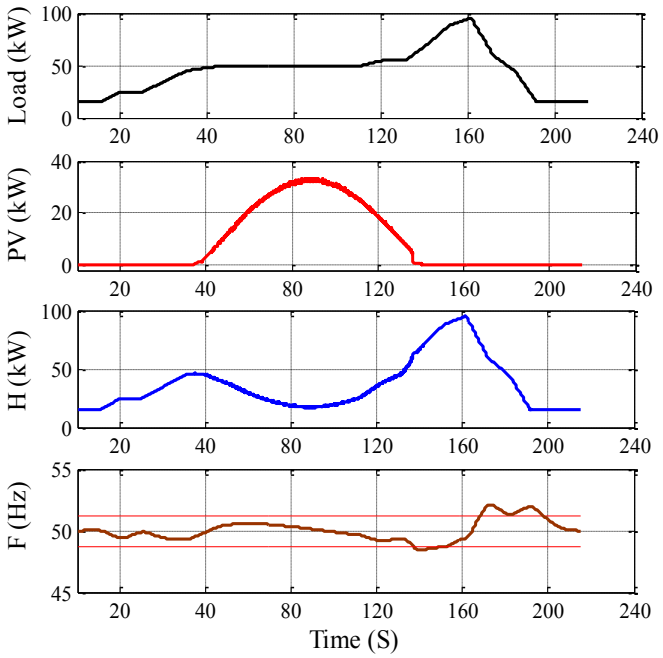


Fig. 2 Frequency response of PV/hydro system with daily load profile

# Locational Dependence of PV Hosting Capacity

Kyle Coogan, Matthew J. Reno, and Santiago Grijalva
Georgia Institute of Technology
Atlanta, Georgia USA

Robert J. Broderick
Sandia National Laboratories
Albuquerque, NM, USA

***Abstract* — With rising adoption of solar energy, it is increasingly important for utilities to easily assess potential interconnections of photovoltaic (PV) systems. In this analysis, we show the maximum feeder voltage due to various PV interconnections and provide visualizations of the PV impact to the distribution system. We investigate the locational dependence of PV hosting capacity by examining the impact of PV system size on these voltages with regard to PV distance and resistance to the substation. We look at the effect of increasing system size on feeder violations. The magnitude of feeder load is also considered as an independent variable with repeated analyses to determine the effect on the PV impact analysis. A technique is presented to determine and visualize the maximum capacity for possible PV installations for distribution feeders. Ultimately, these methods will serve as a basis for continuing to formulate a technique for identifying key criteria and circuit parameters to establish the likelihood of feeder impact due to high penetrations of PV.**

## I. Methodology

A real, 12.47 kV feeder with mostly industrial customers was used for this analysis. To examine the impact of central PV installations on the feeder, an extensive process is used to step through all considered locations, storing data from the power flow solutions for each scenario. The set of scenarios include a significant range of system sizes and locations. Due to the fact that Ckt7 is an industrial feeder, the focus of the analysis is on single, large-scale, central PV plants. The PV systems were sized ranging from 0 to 10 MW in 100 kW increments, and all three-phase buses were considered.

The unbalanced three-phase power flow is solved using the distribution system software OpenDSS with GridPV to perform analysis in MATLAB. The solutions from the power flow simulations for each PV study case are analyzed to determine any violations or limitations in the distribution system that would not allow the particular interconnection.

## II. Results

Maximum feeder bus voltage was analyzed for each PV size and location by finding the maximum bus voltage on the feeder (in pu). The combination of these 200 locations for each of these 101 system sizes (including base case 0 MW) yields the distribution shown in Figure 1. For example, consider the case of a 10 MW PV system. For this system size, approximately 25% of the 200 potential three-phase buses will result in a max bus voltage above 1.05 pu given a load of 50% of peak.

The same data used for Figure 1 was analyzed using the distance of the PV interconnection to the substation as an independent variable. Each data point in Figure 2 represents a power flow solution with the maximum feeder bus voltage plotted as a function of this distance and colored to indicate the PV system size. Figure 2 validates the difference in slopes between percentile ranges in Figure 1. Interconnections toward the end of the feeder exhibit a wider range of maximum voltages, and therefore a larger response to differences in system size. We looked at the maximum system size allowed at each of the buses before any voltage or thermal violations occurred, shown in Figure 3, varying both marker size and color to correspond to maximum system size.

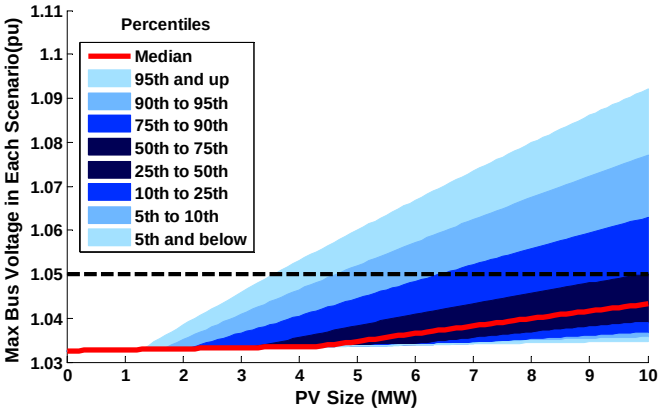


Figure 1. Effect of PV size on max bus voltage under 50% load.

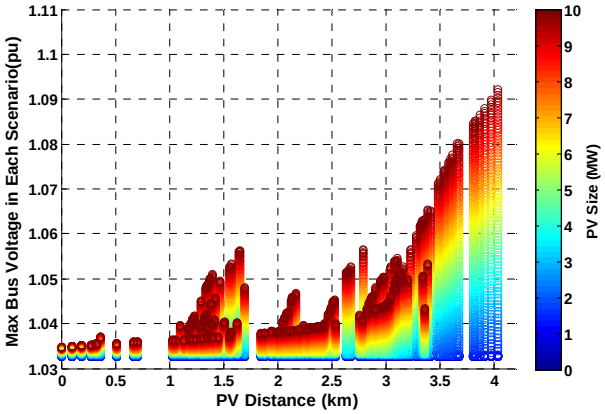


Figure 2. PV size and distance effect on max bus voltage under 50% load.

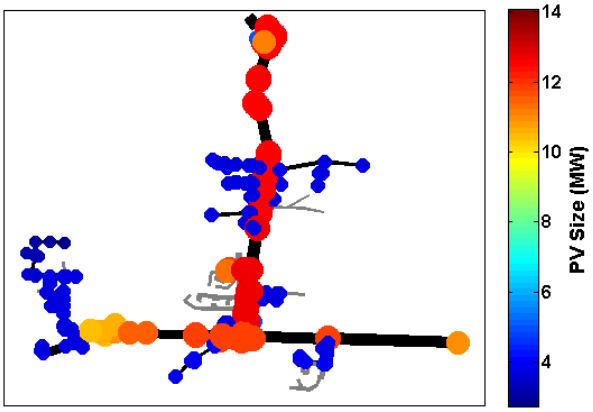


Figure 3. Maximum allowed PV size at a single bus under 50% load.

Sandia National Laboratories is a multi-program laboratory managed and operated by Sandia Corporation, a wholly owned subsidiary of Lockheed Martin Corporation, for the U.S. Department of Energy's National Nuclear Security Administration under contract DE-AC04-94AL85000.

# An Analytical Method for Constructing a Probabilistic Model of a Wind Farm

Samer Sulaeman, *Student Member, IEEE*, Sirisha Tanneeru, Mohammed Benidris, *Student Member, IEEE* and Joydeep Mitra, *Senior Member, IEEE*
Department of Electrical and Computer Engineering
Michigan State University
East Lansing, Michigan 48824, USA
(samersul@msu.edu, sirisha.tanneeru@xcelenergy.com, benidris@msu.edu and mitraj@msu.edu)

***Abstract*—Wind energy penetration levels have increased in recent years all over the world. Despite the advantages of wind power, wind power introduces complexity to the planning and operation of power system due to output fluctuations. In addition, maintaining the efficiency, reliability and operation of the main power grid in present of intermittent resources has become a vital challenge. For power systems, the intermittent nature and uncertainty of wind turbine generators (WTG) output power introduce complexity of applying traditional reliability methods to evaluate system reliability for planning and operation. In contrast to conventional generators, the operational characteristics of WTG add complexity to the reliability assessment methods applied on conventional generators. Since the output power of WTG depends mainly on wind speed regime in a particular wind farm geographical location, and mechanical availability of WTG, wind power output will exhibit variation due to the intermittent nature of wind speed which adds complexity of applying traditional techniques used for adequacy assessment of power system. Therefore, it is important to investigate the expected output power of wind turbines due to wind speed and mechanical availability. In addition, a model represents wind power should consider the intermittent nature of power output, and should also be applicable to meet with adequacy assessment techniques used for conventional generation with inclusion of variability and intermittency nature of wind power. This poster introduces a new method to model the output power of wind farms in reliability evaluation. The proposed model is presented in terms of capacity outage probability table (COPT) considering the mechanical failure of WTG and the correlation between the outputs of turbines on the same farm. Normal convolution methods are not applicable because the correlation between the turbines. Based on the proposed model, the COPT of wind farm has been constructed and applied on the IEEE RTS-79 to calculate the well known reliability indices. Furthermore, a comparison of the reliability indices with and without considering the mechanical failures of WTG is shown. The results indicate the importance of inclusion WTG mechanical availability in estimating reliability of wind power. The results were validated using Monte Carlo simulation.**

***Keywords*—Wind power, reliability of wind turbine, adequacy assessment.***

## I. Modeling Approach

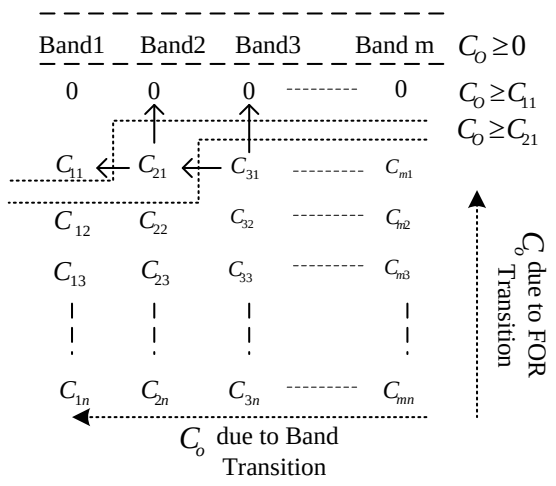


Fig. 1. Wind power transition between bands

TABLE I. Reliability indices

| Unit Commitment | LOLP | EDNS MW/yr | LOEE MWh/yr | LOLE Hr/yr |
|---|---|---|---|---|
| Using Discrete Convolution | | | | |
| Base Case | 0.00107 | 0.13521 | 1181.16 | 9.3681 |
| Wind power only | 0.00073 | 0.08903 | 777.726 | 6.3910 |
| Including wind (FOR) | 0.00081 | 0.09842 | 859.823 | 7.0347 |
| Using Monte Carlo State Sampling | | | | |
| Base Case | 0.00117 | 0.13840 | 1209.05 | 10.2211 |
| Wind power only | 0.00076 | 0.08592 | 750.60 | 6.6394 |
| Including wind (FOR) | 0.00083 | 0.10900 | 952.22 | 7.2509 |

# Dynamic Compensation of Electronic Transformer Phase Delay

Can Huang and Fangxing Li
EECS Department, University of Tennessee, Knoxville
Knoxville, TN 37996, USA
Email: chuang16@utk.edu

Jun Mei
School of Electrical Engineering, Southeast University
Nanjing, 210096, China

***Abstract*— Accuracy and timeliness of sampled values is a crucial issue in smart substations. To improve the phase accuracy of electronic transformers, a dynamic phase compensation method for electronic transformers is proposed. It calibrates the phase errors by the real-time measured delays, instead of the fixed estimated values in traditional compensation methods. In order to minimize the additional errors generated in the calibration process, a Coordinate Rotation Digital Computer (CORDIC) algorithm is applied in rotating plane coordinates and calculating square root. Then, the iterative architecture of CORDIC is optimized as pipelined and implemented in FPGA. The total delay caused by the algorithm is 111.32 ns under 100MHz system clock. Finally, experimental results verify the validity of the proposed method.**

## I. Dynamic Compensation of Phase Delay

In general, the phase delay of electronic transformers is modeled as two components: a rated phase delay $2\pi f \cdot t_d$ (f means sampling frequency and $t_d$ is the rated time delay) and an uncertain phase error $\varphi_e$. In this poster, $\varphi_e$ is real-time measured and compensated in Merging Unit (MU) using CORDIC algorithm.

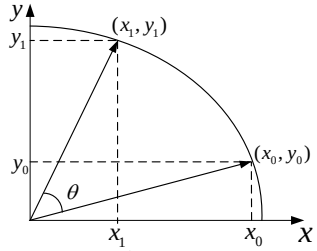


Figure 1. Circle rotation diagram of the CORDIC algorithm.

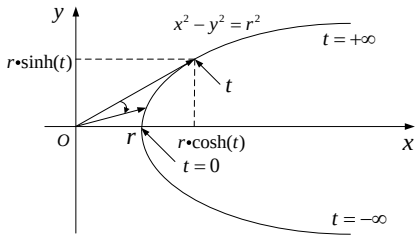


Figure 2. Hyperbolic vector diagram of the CORDIC algorithm.

$$\begin{bmatrix} x_1 \\ y_1 \end{bmatrix} = \cos\theta \begin{bmatrix} 1 & -\tan\theta \\ \tan\theta & 1 \end{bmatrix} \begin{bmatrix} x_0 \\ y_0 \end{bmatrix} \quad (1)$$

$$\begin{bmatrix} x_n \\ y_n \end{bmatrix} = \left(\prod_{i=1}^{n} \cos\theta_i\right) \begin{bmatrix} 1 & -S_n 2^{-n} \\ S_n 2^{-n} & 1 \end{bmatrix} \cdots \begin{bmatrix} 1 & -S_1 2^{-1} \\ S_1 2^{-1} & 1 \end{bmatrix} \begin{bmatrix} x_0 \\ y_0 \end{bmatrix} \quad (2)$$

## II. Experimental Results

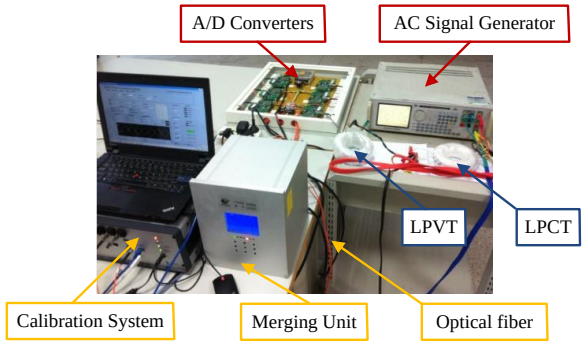


Figure 3. Test bed of calibration system.

Table1 Experimental results of traditional compensation method

| Rate/% | Ratio/% | Delay/us | Phase difference/degree |
|---|---|---|---|
| 99.9948 | 0.0462 | -7.4 | 7’58” |
| 99.9950 | 0.0464 | -4.8 | 5’10” |
| 99.9946 | 0.0468 | -5.2 | 5”39” |
| 99.9951 | 0.0470 | -4.6 | 4”57” |
| 99.9945 | 0.0480 | -5.4 | 5”49” |

Table2 Experimental results of dynamic compensation method

| Rate/% | Ratio/% | Delay/us | Phase difference/degree |
|---|---|---|---|
| 99.9947 | 0.0457 | -6.5 | 1’15” |
| 99.9946 | 0.0467 | -4.2 | 0’13” |
| 99.9949 | 0.0477 | -5.1 | 0’37” |
| 99.9950 | 0.0454 | -7.7 | 1’16” |
| 99.9950 | 0.0455 | -6.2 | 0’55” |

## III. Acknowledgements

The authors would like to thank NARI Group Corporation (NARI) for providing the technical support for this project.

# A Multi-Agent Design for Power Distribution Systems Automation

M. Jawad Ghorbani, Muhammad A. Choudhry, and Ali Feliachi,

***Abstract*—A new Multi Agent System (MAS) design for fault location, isolation and restoration in power distribution systems is presented. When there is a fault in the Power Distribution System (PDS), MAS quickly isolates the fault and restores the service to the fault-free zones. Hierarchical coordination strategy is introduced to manage the agents which integrate the advantages of both centralized and decentralized coordination strategies. Proposed MAS is composed of Zone Agents (ZA), Feeder Agents (FA) and Substation Agents (SA). In this framework, ZAs locate and isolate the fault based on the locally available information and assist the FA for reconfiguration and restoration. FA can solve the restoration problem using the existing algorithms for the 0-1 Knapsack problem. A novel Q-learning mechanism is also introduced to support the FAs in decision making for restoration. The design is illustrated by the use of case studies of fault location, isolation and restoration on West Virginia Super Circuit (WVSC). The results from the case studies indicate the performance of proposed MAS design.**

***Index Terms*—Fault location and isolation, multi agent system, Power Distribution, Q-learning, restoration, self-healing.**

## I. Introduction

A self-healing PDS, when subject to a contingency (fault), is able to automatically perform remedial actions to restore the system to the best possible state. The objective of self-healing PDS is to minimize the duration of outages as well as the customers interruptions, in favor of overall PDS reliability.

Basically, PDS is in the normal state while system parameters are within normal operating range. System enters the abnormal state when an outage happens. In this paper various aspects of a self-healing PDS are discussed, including:

*1) Fault Location:* when a fault occurs in the PDS, the self-healing system is triggered by an automatic re-closer trip in real-time operation, and starts to detect the fault location and identifies the fault type by monitoring data along the feeder.

*2) Isolation:* the first corrective action after locating the fault is to open the relevant switches (in arbitrary order) in order to isolate the fault from the rest of the system.

*3) Reconfiguration & Restoration:* finding a reconfiguration strategy which determines the switching sequence necessary to reconfigure the system in order to allow the broadest possible power access.

In this paper, authors compare the possible MAS frameworks considering the reliability and communications requirements and proposed a hierarchically decentralized MAS architecture composed of upper and lower level agents. In the bottom-up order, agents are classified as Zone Agents (ZA), Feeder Agents (FA) and Substation Agents (SA). In the proposed framework, ZAs are responsible for locating the fault and isolating it. While reconfiguration and restoration are handled by FAs.

In that framework, ZAs have access to the voltage and current phasor data of themselves and their immediate neighbors to a defined neighborhood through communication. Using these data and by real-time monitoring of indices introduced in this paper, ZAs can decide whether the fault is in their neighborhood or not. Following fault location and isolation by ZAs and informing the corresponding FA about the fault information, FA first restores the upstream zones of faulted area and starts negotiating with alternative FAs, that have tie switches to faulty feeder. FAs evaluate the possible reconfiguration and choose the best reconfiguration using deterministic optimization problem solving techniques to supply as many loads as possible.

Although agents in MAS can solve the optimization techniques to find the near optimal configuration, it is also necessary that they learn new behaviors online, such that the performance of the agents and MAS gradually improves. Therefore, a learning methodology ($Q$-Learning) is used to teach agents to use their experiences and prevent them from doing the time consuming optimization process each time a fault happens. The $Q$-Learning technique introduced in this paper is modified for power distribution systems and uses defined $Q$-Matrices as the repositories for all the information learned through previous restoration experiences.

The main contributions of this work can be summarized as follows.

- MAS architecture: A hierarchical distributed MAS that perform the FLIR using less communicated messages than the existing methods.
- Fault Location and Isolation Algorithm: Proposed FLI algorithm is fully distributed and ZAs along the feeder can locate and isolate the faulty section by communicating with their immediate neighbors.
- Restoration Learning algorithm: A reinforcement learning algorithm is developed in conjunction with restoration mathematical programming to take the advantage of restoration experiences and use the learning knowledge for future restorations.

The performance and feasibility of proposed framework is demonstrated on West Virginia Super Circuit (WVSC) which is composed of 5 distribution feeders.

# An Online Algorithm for Health Diagnosis and Prognosis of Circuit Breaker

Saugata S. Biswas, *Student Member, IEEE* and Anurag K. Srivastava, *Senior Member, IEEE,*
Smart Grid Demonstration & Research Investigation Lab (SGDRIL),
Washington State University, Pullman, WA, USA

***Abstract* — With ongoing efforts to make the power grid smarter, utilities are upgrading the substations with enhanced automation. One of the important aspects of substation automation is online monitoring and prediction of the health of the substation assets. Circuit breaker is one of the most vital components in a substation for tripping action during the occurrence of a fault. It is of high importance to ensure that the circuit breaker is in healthy condition, and can operate as per expectation whenever required. There is requirement of keeping a continuous watch on the health of all the components within circuit breaker itself including trip coil and detect and predict the possibility and cause of potential health problem. This research work involves the development of an online algorithm that runs in a substation and continuously monitors and predicts the health condition of a circuit breaker and suggests proper control actions if and when necessary. Arrangement has also been made such that the algorithm results can be remotely accessed for engineering access. Results obtained by online implementation of the proposed algorithm using actual circuit breaker data shows successful operation.**

## I. Introduction

High voltage or medium voltage circuit breakers are extremely vital components in substations. As one of the important functions of these circuit breakers involve disconnecting faulty part of power system circuits during the faults. Reliability of their operation should be guaranteed at all times. The component inside a circuit breaker that is responsible for actuating a tripping action is the trip coil assembly. Thus, there is need to ensure that this trip coil arrangement is in proper health condition at all times, and has not deteriorated due to repeated operations. One way of ensuring this is by doing regular periodic maintenance of circuit breakers. However, the biggest disadvantage of this approach is that, most of the times, utility personnel are sent to these unmanned substations for maintenance, when actually there is no need for maintenance at that time. This would result in loss of time, effort and money. On the other hand, sometimes an actual deterioration of trip coil condition may even remain undetected and unnoticed unless this deterioration leads to a catastrophic failure leading to a non-trip condition of the trip coil and hence the circuit breaker power contacts. An alternative approach is to design an algorithm to run online in an IED (intelligent electronic device) stationed at the remote substation that would take in data from substation for tripping of circuit breaker to analyze the health condition of the trip coil automatically. Also, analyzed information can be used to inform the engineer about the real time health condition of the monitored trip coil. This kind of online algorithm could lead to the saving of time, effort, and money, at the same time ensuring that an actual deterioration of trip coil health would not go unnoticed or unattended. This poster discuss about the development of an online algorithm for carrying out diagnostic and prognostic analysis of a circuit breaker trip coil in real time. This algorithm cannot only detect a health problem, but can also categorize them as either mechanical or electrical problem depending on the root cause. Further, it can suggest maintenance actions based on analyzed results by the algorithm.

## II. Key Figure

Figure 1 shows the trip coil current profile, which is used by the proposed algorithm to analyze the health condition of a trip coil. Individual sections in this profile (as marked in the figure) are analyzed by the algorithm to analyze diagnostic and prognostic information regarding the circuit breaker health.

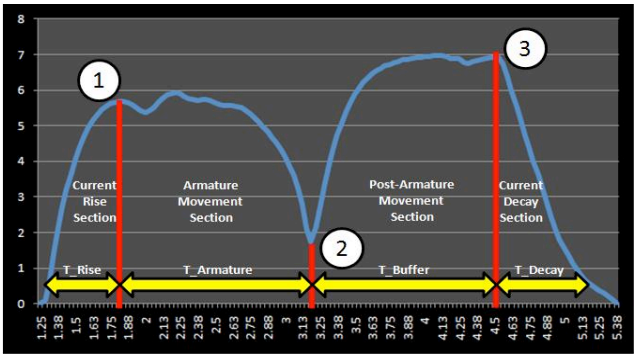


Fig. 1. Trip Coil current profile showing various sections that are analyzed

## III. Acknowledgement

We would like to thank Schweitzer Engineering Lab (SEL) for sponsoring this research project.

# IMPROVEMENT OF TRANSIENT STABILITY OF PV-HYDRO SYSTEM USING VIRTUAL SYNCHRONOUS MACHINES

Ujjwol Tamrakar, David W.Galipeau and Reinaldo Tonkoski
Department of Electrical Engineering
South Dakota State University
Brookings, SD, USA
ujjwol.tamrakar@sdstate.edu

The integration of hydro can improve the reliability of photovoltaic (PV) systems without the need of the expensive and toxic storage. Hydro plants have limited inertia and damping property while PV systems do not. Increased PV penetration in these PV–Hydro integrated systems can have significant impact on microgrid dynamic performance and transient stability, especially in the isolated mode of operation due to insufficient inertia and damping from conventional synchronous generators of the microgrid. A solution to improve the transient stability of such integrated PV-Hydro systems is to add virtual inertia and damping to the system through Virtual Synchronous Machines (VSM).

When there is a change in the load ($\Delta P_L$), the system frequency drops or rises. The governor system responds to this change in frequency; however the response time of the governor will be slow. If the change in load is significantly large, inertia and damping of the hydro unit might not be sufficient and the integrated PV-Hydro system may lose stability. A VSM can inject or absorb the active power during the transient period when there is a mismatch between generation and load. Depending upon the change in system frequency (Δf), the active power to be injected or absorbed by the VSM is calculated based on:

$$P_{VSM} = P_0 + K_i \frac{d(\Delta f)}{dt} + K_p (\Delta f) \quad (1)$$

where, $P_0$ is the VSM's steady state active power, $K_i$ is the gain for transient power supported by VSM due to virtual inertia and $K_p$ is the gain for transient power supported by VSM due to virtual damping

If the VSM is designed to supply the transient active power only, equation (1) can be further simplified as:

$$P_{VSM} = K_i \frac{d(\Delta f)}{dt} + K_p (\Delta f) \quad (2)$$

$K_i$ is the inertia emulating characteristics and can be represented by $K_i = \frac{2HP_{g0}}{f_0}$ ; where H represents the amount of inertia, $P_{g0}$ represents the nominal output power of the generator and $f_0$ is the nominal system frequency. The $K_p$ emulates the effect of damper windings of a real synchronous generator.

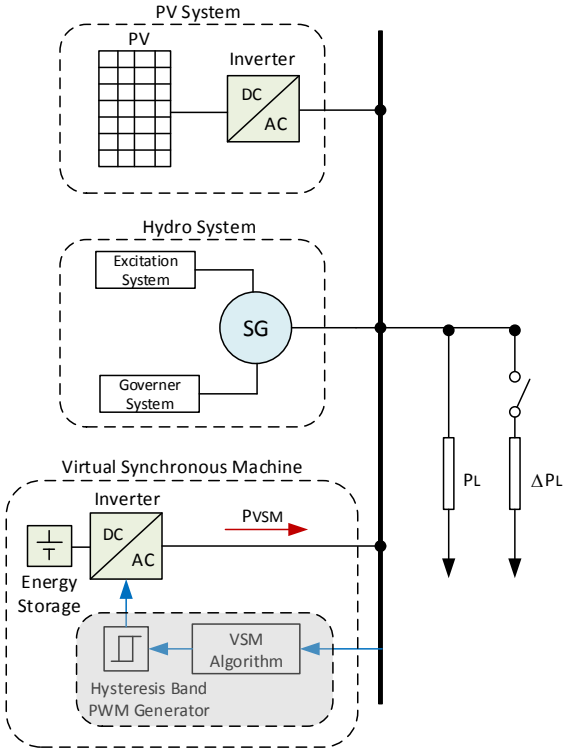


Fig. 1 Proposed PV-Hydro Integrated System with Virtual Synchronous Machine

The transient stability of the PV–Hydro system without the VSM will be analyzed first in MATLAB\Simulink model. The system will then be implemented using a Real Time Digital Simulator (OPAL-RT). A PV- Hydro system with a VSM can improve the stability of the system improving frequency regulation and outages due to cascaded trippings of relays. This allows the integration of PV systems and other intermittent renewable sources with high penetration in a microgrid system.

# An Out-Of-Step Detection of Multi-machine Power System using PMU Data

Yawei Wei, Sumit Paudyal, and Bruce A.Mork
Department of Electrical and Computer Engineering, Michigan Technological University, Houghton,Michigan,USA
Email: yawweiw@mtu.edu,sumitp@mtu.edu, bamork@mtu.edu,

***Abstract*— This research proposes an algorithm for out-of-step detection of multi-machine power system by using PMU devices and which is based on Zubov's method.By exploring the voltage, power angle and the rate of frequency change data from PMU during transient, the proposed method could generate required Zubov formula's parameters corresponding to the general power system swing function.The crux of this algorithm is to construct a Lyapunov function and then solve a linear partial differential equation (p.d.e), which will give a precise stability region for detection and control decision. First,using the proposed PMU data,it could give a more accurate decision. Second,it is suitable for real-time PMU data on short time detection or judgment in typically 1 second time period. What's more, the implementation is easy to achieve if the power swing equations nonlinearity is expressed as a power series function. This proposed algorithm is developed in MATLAB and tested by standard IEEE-9 and IEEE-14 bus system, both contain multi-machine in the grid configuration.By changing the fault happened locations, fault duration time and damping factors in both cases, this detection algorithm simulation result shows clear stable or unstable curve for analysis.By adjusting the data sampling rate, the presented work could detect the out-of-swing situation for both absolute stable or asymptotic stability in short time period.The results demonstrate the proposed detection algorithm has a better performance than the conventional relay protection scheme.**

## I. Key Figure

In Fig.1 and Fig.2, they depicts the result of IEEE-9 system stable and unstable situation with initial single variable of different fault clearing time. It gives an insight look on the behavior's changing under different situation, which is also visualized for system detection.

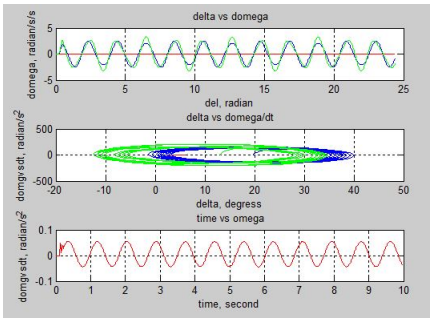


Fig. 1. 3LG fault Stable curve in IEEE-9.

## II. Key Equations

Equation (1) give the general Zubovs critical formula for stability analysis.In this equation it define the basic structure of

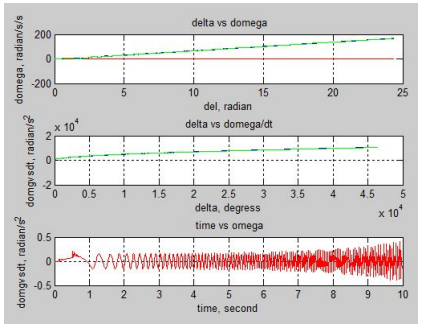


Fig. 2. 3LG fault unStable curve in IEEE-9

Zubovs function. It combines with power swing Equation(2)to give a full map for analyzing. Pesin is the electrical power and Pm is the mechanical power input. is power angle with s is the stable point and u is the unstable point.Equation(2) is normalized by adding time factor$\tau$ which yields in equation(3).

$$\sum_{i=1}^{n} \frac{\partial V}{\partial x_i} f_i(\underline{x}) = -\phi(\underline{x})(1 - V(\underline{x})) \tag{1}$$

$$M\frac{d^2\delta}{dt^2} + D(\delta)\frac{d\delta}{dt} = P - P_e\ sin\delta - P_s\ sin2\delta \tag{2}$$

$$\frac{d^2\delta}{d\tau^2} + D'(\delta)\frac{d\delta}{d\tau} = P' - sin\delta - P'_s sin2\delta \tag{3}$$

Defining $x = \delta - \delta^s$ which transfers the stable equilibrium point(S.E.P) to the initial, then equation(3) becomes

$$\frac{d^2x}{d\tau^2} + D'(x)\frac{dx}{d\tau} + R(x) = 0 \tag{4}$$

As the standard D($\tau$) could be presented as $D(\tau) = a_1\ sin^2\delta + a_2\ cos^2\delta$, the D'(x) and R(x) composed of sine and cosine terms can be expanded in a power series as

$$D'(x) = D_0 + D_1 x + D_2 X^2 + \dots \tag{5}$$

Equation(6) represents for the transformation function by defining $x_1 = x = \delta - \delta^s, x_2 = \dot{x} = \omega\delta$. Thus the equation (6) could be formulated below.

$$\dot{x_1} = x_2,\ \ \dot{x_2} = -\frac{D}{M}x_2 - \frac{1}{M}f(x_1) \tag{6}$$

# Sequential Learning Function applied to the design and tuning of a Fuzzy Controller for VSC

Ivan Riaño[1]
[1]Universidad Distrital Francisco José de Caldas, Bogotá, Colombia.

***Abstract*—This paper present the develop of a Sequential Learning Function to improve the tuning process of a fuzzy basis function expansions (FBFE) for the control of reactive power and the DC Voltage of the rectifier station of a VSC based on Differential Evolution, results are compared with a static fitness evaluation and classical control techniques.**

***Index Terms*— Differential evolution, FBFE, AC/DC Converter, Voltage Source Converter, supervised learning.**

## I. Introduction

Thanks to provides the necessary features for embedded applications in AC Grids, Voltage Source Converter (VSC) are highly used in today distributed generation systems and will play an important role in tomorrow transmission and Distribution system.

Looking for improve the response of VCS, was introduced a Sequential Learning function applied together with a differential evolution algorithm. Here is presented a short introduction and main characteristics of the tested algorithm, finally are presented a response comparison with linear control strategies, and a comparison with a static learning technique.

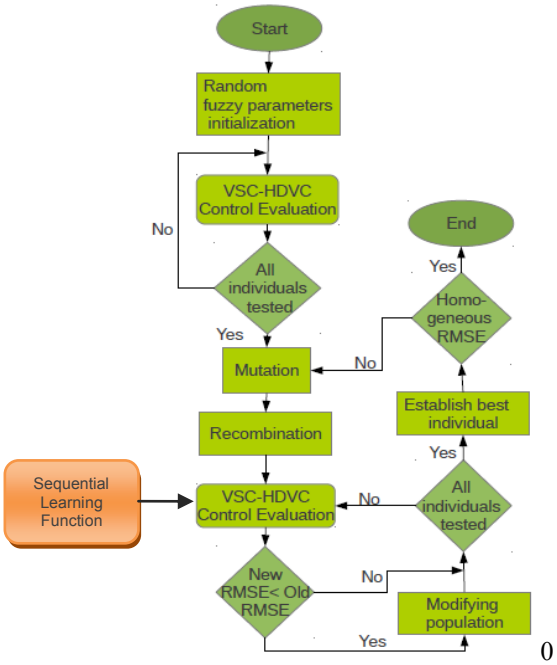


Fig. 1 Diagram flow of the differential evolution algorithm with the Sequential Learning function implemented.

.

## II. Diferential Evolution Algorithm

The fuzzy control model of the VSC was developed as an FBFE whose means and deviations were tuned using a differential evolution algorithm Fig. 1. The control variables and operation ranges were found through a switch based model of VSC System.

## III. Secuencial Learning

During the tuning process, the Fitness Function was defined following the characteristics of the VSC. First was obtained a steady state at the equilibrium point, next was performed the reactive control and finally was reduced the first peak and setting time. The best fuzzy control system was validated in the VSC model against some changes in load, and compared with a strategy of classic control linearization.

## IV. → Results

The proposed method increases the speed of the learning process Fig. 3 in comparison with static fitness functions. In the DC Voltage control Fig. 4 it can be seen that the sequential learning function present a setting time reduction of 60% and a steady-state error reduction of 50% compared with the linear control strategies proposed in precedent works.

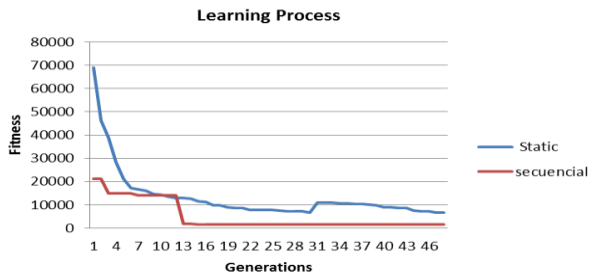


Fig.2 Learning Process

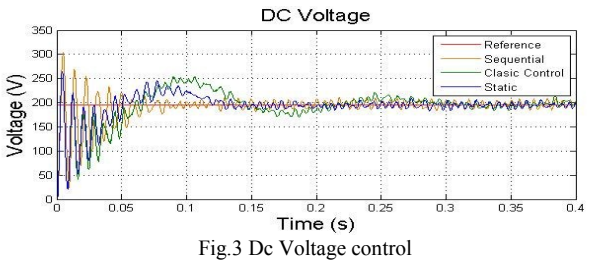


Fig.3 Dc Voltage control

# PMU-Based Wide Area PSSs to Enhance the Damping of Inter-Area Oscillations

Duaa AbuMaali, *Member, IEEE* Faisal Khan, *Member, IEEE* Hussein Taoube; Member, IEEE
Mohamad Mahjoub, *Member, IEEE* Khaled Ellithy, *Senior Member, IEEE*

***Abstract*— The operation of interconnected power systems is subject to low frequency inter-area oscillations significantly. These oscillations are undesirable as they result inefficient operation of the power systems. The stability of these oscillations is of vital concern. Adequate damping of the inter-area oscillations is a pre-requisite for secure operation of power systems. An available solution to damp out these inter-area oscillations is the addition of power system stabilizers (PSSs) to the generators excitation systems. Although conventional PSSs exist on many generators, their effect is only on the oscillations of local area and do not effectively damp out inter-area oscillations. The general problem is that the locally measured signals input to the conventional PSSs often are insufficient for damping inter-area oscillations mode. In this paper PSSs using wide-area measurements based phasor measurement units (PMUs) is proposed. The global stabilizing signals input to the proposed PSSs are detected and transmitted by the PMUs. The proposed PSS is designed to ensure satisfactory damping of the inter-area oscillations which results in maximize power transfer capacity and enhancing system stability. Two-area power system shown in Fig. 1 is used to test the effectiveness and performance of the proposed PSSs. The system state-space model with the PMUs was developed to obtain the eigenvalues associated to the inter-area and local oscillations modes. The participation factors were also determined to identify these modes. The eigenvalues results are listed in Table 1. It can be seen that the system is unstable without PSSs; the instability is caused by the inter-area mode (+0.06±j3.73). The inter-area damping was improved with the proposed PSS compared to the conventional PSS. The system model with physical PMUs loop was developed as shown in Fig. 2 and nonlinear time-domain simulations are carried out to verify the eigenvalues results and to test the effectiveness of the proposed PSS. Figure 3 shows the response of the tie-line real power with and without the designed PSS; it can be seen that the proposed PSSs based PMUs improves the damping of inter-area oscillation and enhancing the system stability. The proposed PSSs will be implemented in practice to the smart power grid of Gulf Cooperation Council (GCC).**

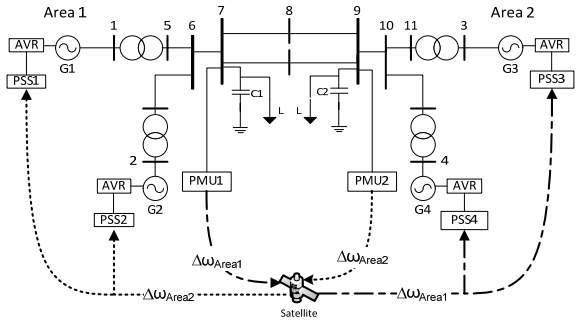


Fig. 1 Two-area power system with PMUs loop

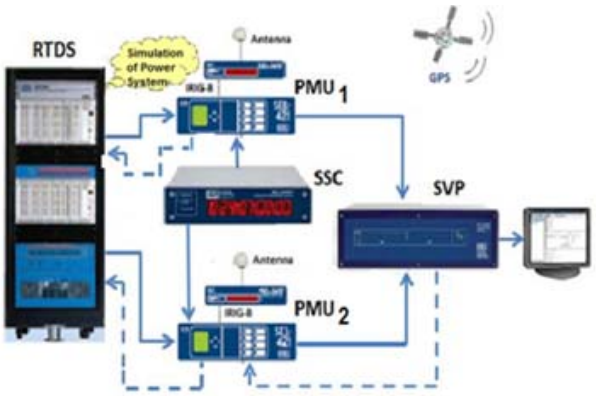


Fig. 2 Real-time system modeling using RTDS with PMUs

Table 1: Eigenvalues of inter-area and local oscillations modes

| Two-area test system | Eigenvalues | | |
|---|---|---|---|
| | **Inter-Area** | **Local 1** | **Local 2** |
| Without PSS | +0.06 ± j 3.73 | -0.14 ± j 6.5 | -0.23 ± j5.99 |
| With PSS-local signals | -0.43 ± j3.77 | -0.11± j6.51 | -1.86 ± j6.75 |
| With proposed PSS-global signals | -1.05 ± j3.74 | -0.14± j6.52 | -1.7± j 6.65 |

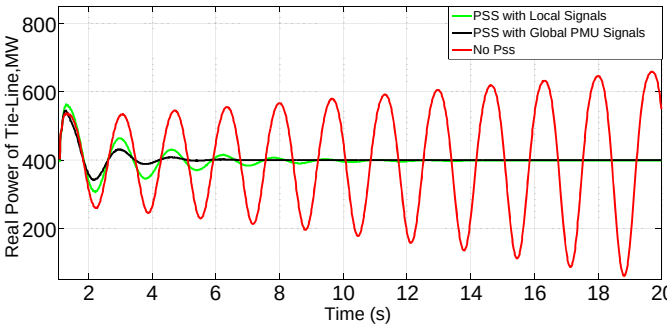


Fig. 3 Time-response of the real power of the tie-line for 3-phase fault on bus 8

## REFERENCES

[1] P. Kundur, Power Systems Stability and Control, McGraw-Hill, 1994.
[2] Yanfend Gong, Armando Guzman, Synchrophasor-Based Online Modal Analysis to Mitigate Power System Interarea Oscillation, Journal of Reliable Power, Vol. 2, no.2, pp. 4-47, 2011.
[3] Kamwa, R. Grondin, Y. Hebert, "Wide-area measurement based stabilizing control of large power systems—A decentralized/ hierarchical approach," IEEE Trans. On Power Syst., Vol. 16, no. 1, pp. 136–153, Feb. 2001.

# LMP Step Pattern Detection based on Real-Time Data

Haoyu Yuan, Fangxing Li, and Yanli Wei
Department of Electrical Engineering and Computer Science
The University of Tennessee, Knoxville
Knoxville, TN 37996
USA
{hyuan2, fli6, ywei9}@utk.edu

***Abstract*—Locational marginal pricing (LMP) methodology has been widely adopted by most independent system operators (ISOs) and regional transmission organizations (RTOs) in today's electricity markets. Previous studies show that LMP has a step change characteristic with varying load. This can be used by market participants to predict the future electricity price and potential step change of LMP. In this paper, an effective algorithm using quality threshold (QT) clustering is proposed to detect the step change pattern of the hourly LMP. A set of indices to differentiate various patterns is introduced. Furthermore, a web-based tool is built to demonstrate the price behavior of different locations based on the 5 minutes real-time LMP data from ISOs/RTOs. The user friendly design with clustering functionality ensures easy statistical study over a large amount of historical data.**

***Index Terms*—Locational marginal price (LMP), critical load level (CLL), QT clustering, step change pattern detection, market participant, price prediction.**

## I. Introduction

Most Independent System Operators (ISOs) and Regional Transmission Organizations (RTOs) in North America have adopted an economic dispatch-based model to clear day-ahead energy market. Locational marginal price (LMP) can reflect impacts of transmission congestion and losses based on network models, which contribute to the economic operation of the electricity market.

Given the known unit commitment decisions, the step change characteristic of LMP has been well studied. Critical load level (CLL) is introduced to indicate the point where the price spike occurs. When the load level is close to the CLL, there will be higher risk of having volatile price. This becomes more common especially when the system has a large amount of intermittent renewable generations. Uncertainty analysis associated with CLL has been studied from the perspective of both market participants and the operators.

Market participants, who are actively involved in the power trading business, need to investigate all the possible causes for LMP volatility. It is clear that CLL is an important signal for predicting price spikes. It is also desirable to have an easy-to-use web based tool for market participants to perform statistical analysis of the LMP over their interested time and locations.

Quality threshold (QT) clustering algorithm has been widely applied in research areas such as oncology for tumor classification [9-10]. The characteristic of not knowing cluster number in tumor classification is similar to our study in clustering LMP, which is the inspiration to this research work to adopt the QT clustering. In addition, two indices, outlier and overlap indicator (OI), are defined for efficient description of the fitness of a LMP pattern.

Despite the importance of detecting and visualizing the step pattern in real time LMP data, there is no web application in providing such information to market participants. Thus, we develop a web-based application on the JAVA EE platform to dynamically generate detected step pattern diagram to users of interest.

Historical data from ISO is studied in this work. An illustration of the step pattern detection algorithm is shown in Fig. 1

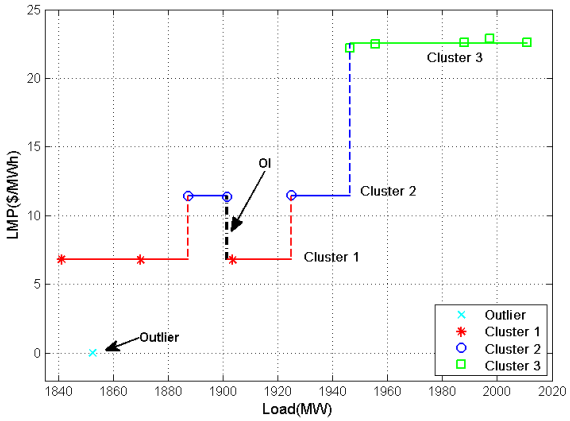


Figure 1. Illustration of Outlier and Overlap Indicator (OI).

# Customer Incentive Pricing Mechanism in the Smart Grid

Timothy Hansen, *Graduate student member, IEEE*

Colorado State University
Department of Electrical and Computer Engineering, Fort Collins, CO 80523, USA
Email: timothy.hansen@colostate.edu

*Abstract*—**As the Smart Grid introduces profound changes in the operation of the electric power industry, the need for efficient and robust resource allocation (RA) algorithms arise. This is especially difficult due to the increasingly stochastic nature of the availability of massively distributed resources. Similar challenges exist in resource allocation in the realm of computing. Based on the experiences in the computing domain, this work solves the Smart Grid RA (SGRA) problem using a heuristic framework implemented as a genetic algorithm. The SGRA problem is defined as: given a set of end-users and information about their respective assets, subject to end-user and system constraints, determine how to control assets (e.g., adjusting thermostats, rescheduling smart appliances) to maximize a given objective. To encourage increased customer participation in SGRA, a new pricing methodology known as *customer incentive pricing* (CIP) is introduced to offset the end-user inconvenience of controlling their assets. If the inconvenience of giving up control of a particular asset is not worth the incentive, the end-user can eschew participation in that time interval. This approach — enabled by a fully deregulated market structure including aggregators — offers the end-user more choices to participate in the deregulated electricity market at regular intervals.**

## I. Key Equations

Aggregator profit components (**S**, **N**, **B**) and objective function (**P**) from [1]:

$$\boldsymbol{S} = \sum_{i \in L} \left[ \gamma(i, \lambda, t_{i,resch}) \sum_{t=t_{i,resch}}^{t_{i,resch}+\delta_i-1} \frac{\lambda(t) p_i}{4} \right] \quad (1)$$

$$\boldsymbol{N} = \sum_{i \in L} \left[ \gamma(i, \lambda, t_{i,resch}) \sum_{t=t_{i,start}}^{t_{i,start}+\delta_i-1} \frac{s(t) p_i}{4} \right] \quad (2)$$

$$\boldsymbol{B} = \sum_{i \in L} \left[ \gamma(i, \lambda, t_{i,resch}) \sum_{t=t_{i,resch}}^{t_{i,resch}+\delta_i-1} \frac{s(t) p_i}{4} \right] \quad (3)$$

$$\boldsymbol{P} = \boldsymbol{N} + \boldsymbol{S} - \boldsymbol{B}. \quad (4)$$

This work was supported by the National Science Foundation under grant numbers CNS-0905399 and CCF-1302693, and the Colorado State University George T. Abell Endowment.

## II. Key Figure

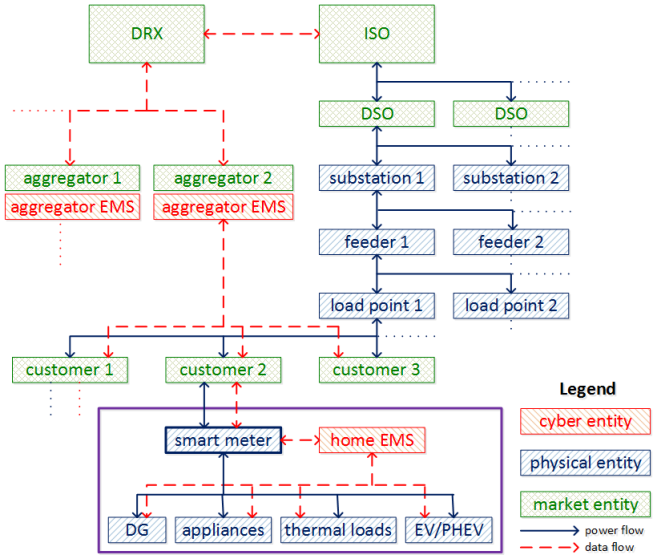


Figure 1. Cyber-physical social system (CPSS) for the SGRA (based on [1]).

## III. Key Results

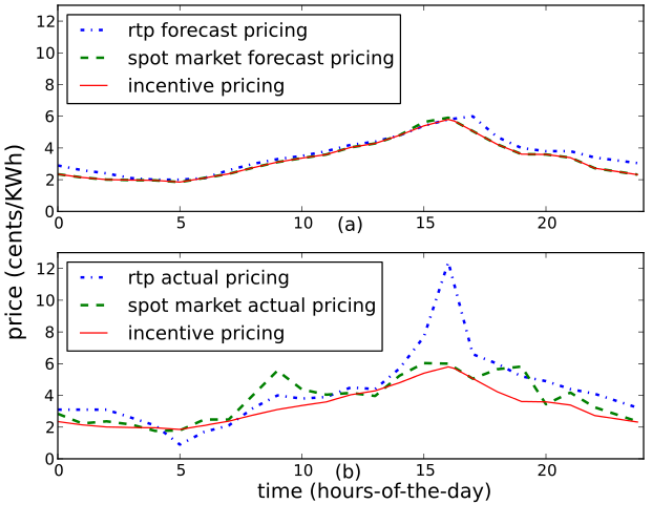


Figure 2. Comparison of real-time pricing, spot marking pricing, and customer incentive pricing [1].

## Reference

[1]. T. Hansen, et al., "Heuristic optimization for an aggregator-based resource allocation in the Smart Grid," under review, 8 pp., Dec 2013.

# Distribution Locational Marginal Price using Optimal Three-phase Current Injection Power Flow

Jie Wei, Farshid Sahriatzadeh and Anurag K. Srivastava
The School of Electrical Engineering and Computer Science, Washington State University
Pullman, WA 99164, USA

***Abstract – With ongoing*** **smart grid development, objective is to use available information to make power system more efficient, environmental friendly, reliable, economic and secure. Major part of smart grid investment is going towards distribution systems. One of the goals within smart grid is development of infrastructure to avail price signal to end users in distribution system. This price signal is currently based on estimate of nodal price in transmission system. Transmission nodal price does not reflect fair pricing signal for distribution system without consideration of distribution system constraints such as unbalanced loads and distribution lines flows. Solving optimal power flow (OPF) with applicable constraints is necessary to obtain locational marginal price (LMP) for each node that can be used in real-time pricing (RTP). Formulation and implementation of distribution LMP (DLMP) is needed for fair pricing. Although Newton-Raphson based PQ mismatch approach can be used to solve three-phase OPF in distribution system, it may lead to divergence due to large R/X ratio of distribution lines in large scale systems. In this work, three-phase current injection method (TCIM) formulation has been used to develop OPF formulation and calculate DLMP. Developed formulation is able to deal with distributed generations (DG) and suitable to implement in advanced distribution management system (DMS).**

## I. KEY EQUANTIONS

Power injection equations:

$$\left(P_k^{sp}\right)^s = P_{gk}^s - P_{lk}^s$$

$$\left(Q_k^{sp}\right)^s = Q_{gk}^s - Q_{lk}^s$$

Three-Phase Power Flow Equations:

$$\left(P_k^{calc}\right)^s = (V_{rk}^s \times I_{rk}^s) - (V_{mk}^s \times I_{mk}^s)$$

$$\left(Q_k^{calc}\right)^s = (V_{mk}^s \times I_{rk}^s) - (V_{rk}^s \times I_{mk}^s)$$

Current injection equations:

$$I_{rk}^s = \sum_{i=1}^{n} \sum_{t \in \alpha} \left(G_{ki}^{st} \cdot V_{ri}^t - B_{ki}^{st} \cdot V_{mi}^t\right)$$

$$I_{mk}^s = \sum_{i=1}^{n} \sum_{t \in \alpha} \left(G_{ki}^{st} \cdot V_{mi}^t + B_{ki}^{st} \cdot V_{ri}^t\right)$$

Three-phase current mismatches:

$$\Delta I_k^2 = \frac{\left(P_k^{sp}\right)^s - j\left(Q_k^{sp}\right)^s}{\left(E_k^{sp}\right)^s} - \sum \sum Y_{ki}^{st} E_i^t$$

## II. KEY FIGURES

System Information - IEEE 13bus

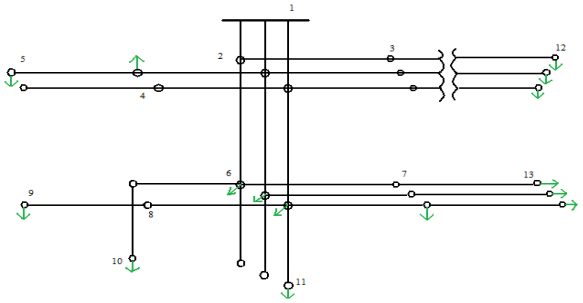


TCIM OPF Flow Chart

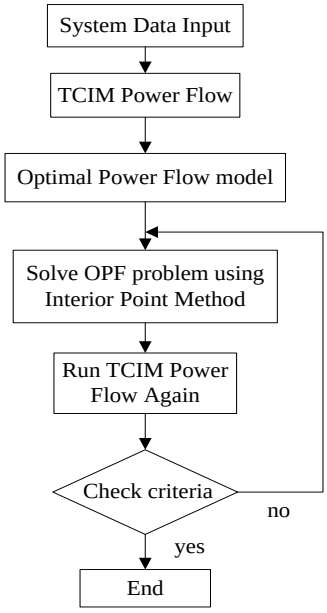


Developed algorithms uses the database of the input test system to run TCIM power flow first. The results obtained from TCIM power flow is used as initial values to establish an OPF model. Interior Point Method was used to solve the OPF problem.

# Discharge Energy Based Stage Classification of Cavity Partial Discharge in Oil-Paper Insulation

Zhenze Long [1, 2], *Student Member IEEE*, Weigen Chen [2] and David Yu [1], *Senior Member IEEE*
1. College of Engineering and Applied Science, University of Wisconsin Milwaukee, WI, USA;
2. School of Electrical Engineering, Chongqing University, Chongqing, China
Email: zlong@uwm.edu

## I. INTRODUCTION

Partial discharge is one of the main reasons for aging and disruption of the oil-paper insulation. As a result, the investigation of PDs' characteristics is important in detecting and diagnosing the internal failure of transformer oil-paper insulation.

In earlier studies, only the maximum PD magnitude and repetition rate are regarded as PD information. This simple information is not reliable to determine the developing stage for PD, which is an extremely stochastic event. Recently, fingerprint identification has been regarded as a useful tool in the recognition and classification of PDs. Phase resolved partial discharge (PRPD) pattern is the most widely used method. However, the 3-D φ-q-n pattern, whose y axis represents the apparent discharge, is not the perfect solution. Since new research indicates that when the insulation is about to break down, the apparent discharge would not change very much.

In this poster, apparent discharge in PRPD pattern is replaced by discharge energy consumption. Then twenty-nine statistical parameters are extracted from the new PRPD patterns and using Kernel principle component analysis (KPCA), eight new feature parameters are refined from the original statistical parameters. In addition, based on experimental data of cavity discharge, the discharge stages are classified into four stages which are incipient discharge, unstable discharge, consistent discharge, and disruptive discharge, according to cluster analysis.

## II. KEY FIGURES AND TABLES

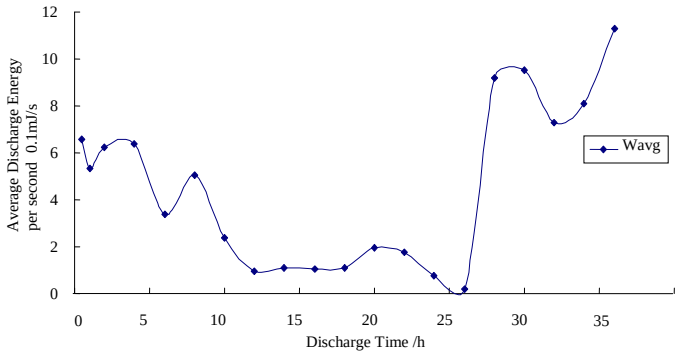


Figure 1. The variation of average discharge energy per second

$$W_{avg} = \frac{1}{2}\Delta qU \cdot \bar{n}$$

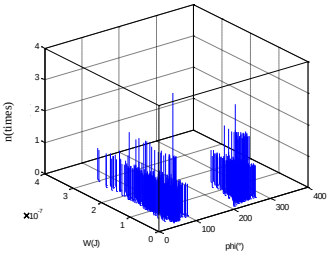


Figure 2. The images of $\varphi$-$W$-$n$ at 8h hour

Table 1. Statistical Parameters at 8th hour

| | $H_{qmax}(\varphi)$ | $H_{qn}(\varphi)$ | $H_n(\varphi)$ | $H_n(q)$ |
|---|---|---|---|---|
| *Sk-* | 0.7627 | 0.0226 | 0.2319 | N/A |
| *Sk+* | 0.8238 | 0.0367 | 0.2249 | N/A |
| *Sk* | N/A | N/A | N/A | 1.2278 |
| *Ku-* | 3.1245 | 1.8433 | 2.3611 | N/A |
| *Ku+* | 3.0018 | 1.7275 | 2.5882 | N/A |
| *Ku* | N/A | N/A | N/A | 4.8508 |
| *Pe-* | 45 | 41 | 23 | N/A |
| *Pe* | 39 | 42 | 24 | 52 |
| *Pe+* | 0.9845 | 1.0684 | 1.0167 | N/A |
| *Asy* | 0.8174 | 0.0851 | 0.3123 | N/A |
| $\alpha$ | N/A | N/A | N/A | 0.1345 |
| $\beta$ | N/A | N/A | N/A | 1.3895 |

Table 2. Contribution Rates of Principle Component

| Component | Value of λi | Contribution rate (%) | Cumulative contribution (%) |
|---|---|---|---|
| λ1 | 6.9670 | 83.3 | 83.3 |
| λ2 | 1.1147 | 13.14 | 96.44 |
| λ3 | 1.0888 | 2.31 | 98.75 |
| λ4 | 0.1795 | 0.95 | 99.70 |
| λ5 | 0.1400 | 0.19 | 99.89 |
| λ6 | 0.0416 | 0.041 | 99.931 |
| λ7 | 0.0389 | 0.053 | 99.984 |
| λ8 | 0.0007 | 0.016 | 100 |

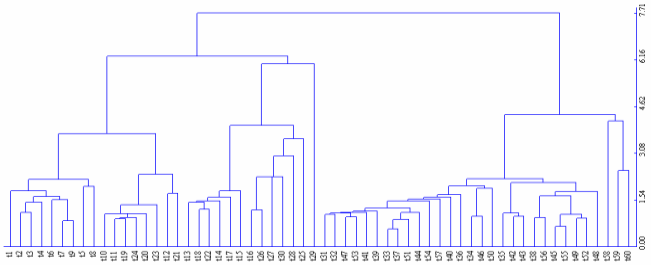

Figure 3. Cluster Analysis Result

# Impact of Voltage Reduction and Ambient Temperature on Power Consumption, Line Loss and Generation

Sushanta Paul, *Student Member, IEEE* and Dr. Ward Jewell, *Fellow, IEEE*

***Abstract*— A voltage-reduction program is one strategy applied by utilities to reduce energy consumption and peak demand. This paper presents an analysis of how consumer energy consumption, line loss, and thus total consumption and generation are affected by voltage reduction. Since bus voltage depends on line resistance, which varies with ambient temperature, the impact of temperature on power consumption, line loss and generation is discussed as well. Joint effect of voltage and ambient temperature is also analyzed by two-factor factorial design. The results are presented based on the types of loads to show how load models play an important role in the analysis. All the analyses are tested on the IEEE 13-bus system.**

***Index Terms*—Energy conservation, energy consumption, power generation, reactive power**

## I. Impact of Voltage Reduction on Load and Line Loss

TABLE I

| Load Model | Load Power Consumption | Line Loss |
|---|---|---|
| Const. Z | Constant | Decrease |
| Const. I | Decrease | Constant |
| Const. P | Decrease | Increase |
| Composite load (i) Const. P dominant | Decrease ($\Delta P_{Load}^{P}$) | Increase |
| (ii)Const. I dominant | Decrease ($\Delta P_{Load}^{C_P}, \Delta P_{Load}^{C_Z}$) $\Delta P_{Load}^{P} < P_{Load}^{C_P} < P_{Load}^{C_Z}$ | Increase (if % of const. P load > % of const. Z load) or Decrease (if % of const. P load < % of const. Z load) |
| (iii)Const.Z dominant | Decrease ($\Delta P_{Load}^{Z}$) $\Delta P_{Load}^{P} < P_{Load}^{C_P} < P_{Load}^{C_Z} < \Delta P_{Load}^{Z}$ | Decrease |

## II. Impact of Reduced Voltage on Power Generation

Variation in active power generation ($\Delta P_{Gen}$) is the summation of variations in load $\Delta P_{Load}$ and line loss ($\Delta P_{Load}$), as shown in (1).

$$\Delta P_{Gen} = \Delta P_{Load} + \Delta P_{Loss} \quad (1)$$

If, decrement and increment are considered positive, and negative respectively, then

$$\left.\begin{array}{l} \Delta P_{Load} > 0, \textit{for all types of composite load models} \\ \Delta P_{Loss} < 0, \textit{for dominant constant power load} \\ \Delta P_{Loss} > 0, \textit{for dominant constant impedance load} \\ \Delta P_{Loss} < 0, \textit{for dominant constant current load with} \text{ constant power load greater than constant impedance load} \\ \Delta P_{Loss} > 0, \textit{for dominant constant current load with} \text{ constant impedance load greater than constant power load} \\ \Delta P_{Load} \gg |\Delta P_{Loss}| \end{array}\right\} \quad (2)$$

Therefore, $\Delta P_{Load} + \Delta P_{Loss} > 0 \quad \Rightarrow \Delta P_{Gen} > 0$. Hence, the active power supply from the substation will decrease with a reduction in voltage for all composite load models.

This work was supported by the U.S. Department of Energy under grant DOEDE-FG36-08GO88149.

## III. Impact of Temperature on Line Loss, Load and Generation

We know that at a higher temperature the resistance of a line will increase and consequently line loss ($I^2R$) will increase, but with the voltage-dependent loads such as constant impedance and constant current, load will decrease because the line drop (IZ) increases with the increase in resistance at a higher temperature thus leading to a decrease in the node voltage, and finally, the voltage-dependent load will consume less power at a higher temperature. As the voltage drops at a higher temperature, the reduced voltage again affects the line losses, and whether line losses will increase or decrease at that reduced voltage depends on the type of load as shown in Table I. For the system with a dominant constant impedance load, line losses decrease at a reduced voltage caused by a rise in temperature, and again, line losses increase for an increase in resistance due to temperature rise, but an increment in line losses for an increase in resistance due to temperature rise is greater than a decrement in line losses due to voltage reduction caused by a temperature rise, so the line losses will increase at a higher temperature. For the system with a dominant constant power load, line losses increase at a reduced voltage caused by temperature rise, and again line losses increase for an increase in resistance due to temperature rise; therefore, line losses will increase to a greater degree. Similarly, for the system with a dominant constant current load, due to a temperature rise, line losses will increase by an amount that is less than the increment in line losses for the system with a dominant constant power load but greater than the increment in line losses for the system with a dominant constant impedance load. A comparison in the increase in line loss is shown in (3)

$$\Delta P_{Loss}^{Z} < \Delta P_{Loss}^{C_Z} < \Delta P_{Loss}^{C_P} < \Delta P_{Loss}^{P} \quad (3)$$

**Impact of temperature on generation:** $\Delta P_{Gen} = \Delta P_{Load}\downarrow + \Delta P_{Loss}\uparrow$. Generation will increase if, $\Delta P_{Loss}\uparrow > \Delta P_{Load}\downarrow$, or decrease if $\Delta P_{Load}\downarrow > \Delta P_{Loss}\uparrow$. System with dominant constant power load, $\Delta P_{Loss}^{P}\uparrow > \Delta P_{Load}^{P}\downarrow$, therefore generation increases. System with dominant constant impedance load, $\Delta P_{Load}^{Z}\downarrow > \Delta P_{Loss}^{Z}\uparrow$, therefore generation decreases. For the system with dominant constant current load, $\Delta P_{Loss}^{C}\uparrow > \Delta P_{Load}^{C}\downarrow$, therefore generation increases.

## IV. Joint Effect of Voltage and Ambient Temperature

The interaction effect of temperature and voltage is given by (4).

$$SS_N = \frac{\left[\sum_{i=1}^{a}\sum_{j=1}^{b} y_{ij} y_{i.} y_{.j} - y_{..}\left(SS_A + SS_B + \frac{y_{..}^{2}}{ab}\right)\right]^2}{abSS_A SS_B} \quad (4)$$

with 1 degree of freedom.

# Adaptive PI Control of STATCOM for Voltage Regulation

Yao Xu and Fangxing Li
The Department of Electrical Engineering and Computer Science, the University of Tennessee (UT), Knoxville, TN 37996, USA,
Email: yxu25@utk.edu and fli6@utk.edu

*Abstract*—**STATCOM can provide fast and efficient reactive power support to maintain power system voltage stability. In the literature, various STATCOM control methods have been discussed including many applications of proportional–integral (PI) controllers. However, these previous works obtain the PI gains via a trial and error approach or extensive studies with a tradeoff of performance and applicability. Hence, control parameters for the optimal performance at a given operating point may not be effective at a different operating point. This paper proposes a new control model based on adaptive PI control, which can self-adjust the control gains during disturbance such that the performance always matches a desired response, regardless of the change of operating condition. Since the adjustment is autonomous, this gives the plug-and-play capability for STATCOM operation. In the simulation test, the adaptive PI control shows consistent excellence under various operating conditions such as different initial control gains, different load levels, change of transmission network, and consecutive disturbances. As a comparison, the conventional STATCOM control with tuned, fixed PI gains usually perform fine in the original system, but may not perform as efficient as the proposed control method when there is a change of the system conditions.**

## I. Key Equations

Voltage regulator PI gains can be computed by the following equations:

$$K_{p\_V}(t) = \frac{k_V \times \Delta V(t)}{\left(\Delta V(t) + m_V \times \int_t^{t+T_S} A dt\right)} \quad (1)$$

$$K_{i\_V}(t) = m_V \times K_{p\_V}(t) \quad (2)$$

Current regulator PI gains can be obtained by:

$$K_{p\_I}(t) = \frac{k_I \times \Delta I_q(t)}{\left(\Delta I_q(t) + m_I \times \int_t^{t+T_S} B dt\right)} \quad (3)$$

$$K_{i\_I}(t) = m_I \times K_{p\_I}(t) \quad (4)$$

## II. Key Figures

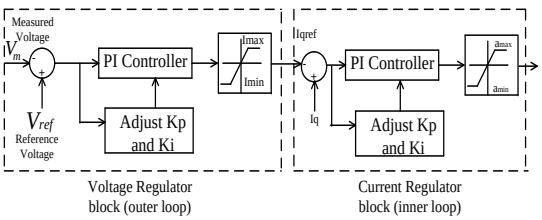


Fig. 1. Adaptive PI control block for STATCOM.

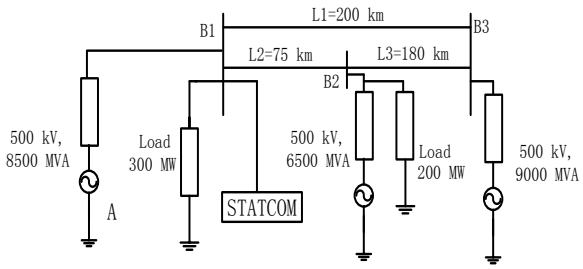


Fig. 2. The studied system.

## III. Key Results

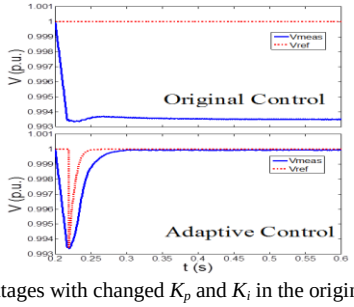


Fig. 3. Voltages with changed $K_p$ and $K_i$ in the original control.

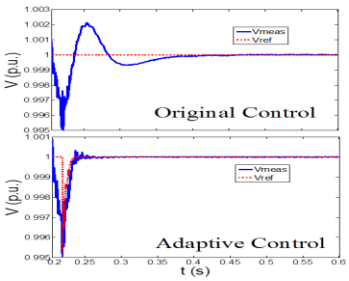


Fig. 4. Results of measured voltage with change of transmission network.

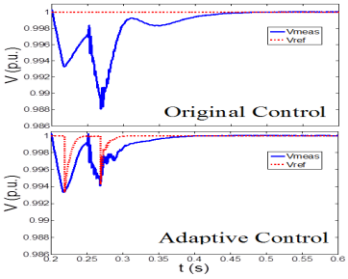


Fig. 5. Results of measured voltage in two consecutive disturbances.

# Control of Hybrid Tripole HVDC Based on LCC and F-MMC

Feng Xu, Zheng Xu
Department of Electric Engineering, Zhejiang University, Hangzhou 310027, Zhejiang Province, China
Email: xuf_1988@zju.edu.cn; xuzheng007@zju.edu.cn

***Abstract*—In order to overcome some inherent defects of the conventional tripole HVDC, a hybrid tripole HVDC structure is proposed, which replaces the thyristor converters of pole 3 with the modular multilevel converters (F-MMC) based on cascaded full bridge sub-modules (FBSM). To increase the transmission capacity, a special current modulation is adopted. In order to meet the demands of the reactive power (voltage) balance, the DC current balance and the sub-module capacitor voltage balance in the transition process, the corresponding control strategies are also proposed. The performance of the proposed hybrid tripole HVDC structure is evaluated through time-domain simulation studies in PSCAD/EMTDC. The results show that a satisfactory response of the system can be achieved with the proposed control strategies.**

## I. Key Figures

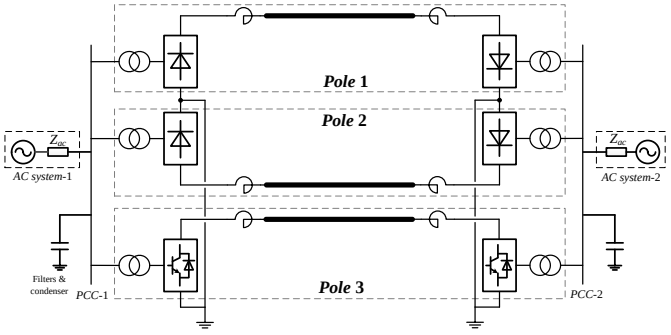


(a) Proposed hybird HVDC structure

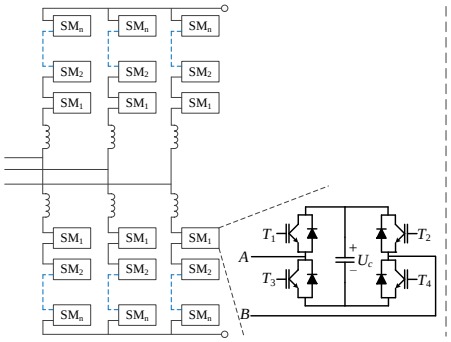


(b) Topology of F-MMC

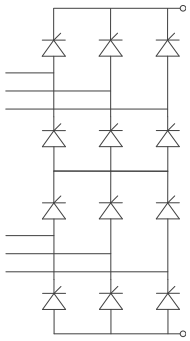

(c) 12-pulse LCC

Fig. 1. Proposed hybrid tripole HVDC system.

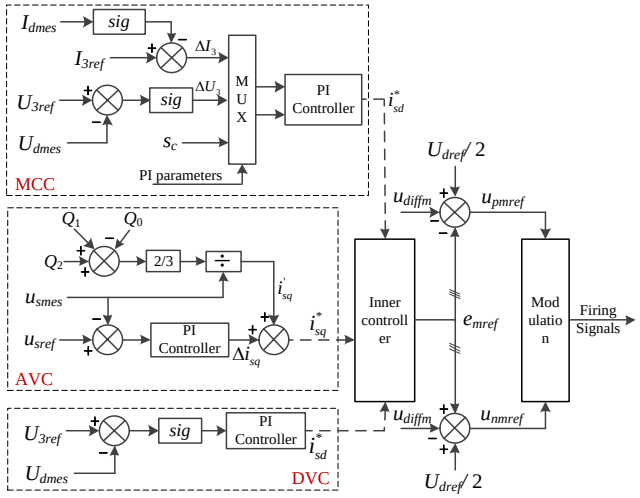


Fig. 2. Control block diagram of the F-MMC.

## II. Key Results

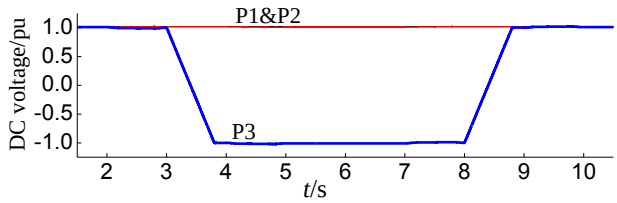


Fig. 3. DC voltages of three poles.

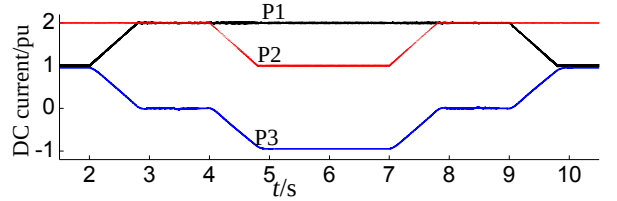


Fig. 4. DC currents of three poles.

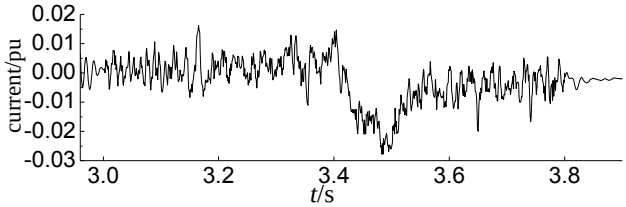


Fig. 5. Ground current.

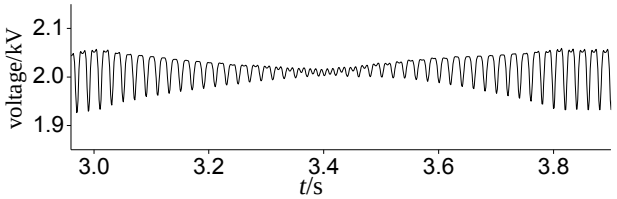


Fig. 6. Capacitor voltage.

# A Total Harmonic Distortion (THD) computation using improved Shunt Active Power Filter Design in Energy Management Systems

Ranganath Vallakati, IEEE Student Member, Prakash Ranganathan, IEEE Senior Member
*Email:* ranganath.vallakati@my.und.edu
Department of Electrical Engineering, University of North Dakota, Grand Forks, ND 58202

*Abstract*—Power factor correction is an important task in power system field. The advent of power electronics and nonlinear converters in recent days has increased the consumption of non-sinusoidal current significantly. The modern day power electronic devices with a very high switching frequency represent a significant amount of reactive power and harmonic components compared to traditional linear loads. Harmonic or sub-harmonic components need to be reduced in the power system, because they create additional problems such as voltage harmonics, and disturbances affecting equipment and sub-systems interconnected to the power network. The consumption of reactive power by nonlinear loads presents critical problems such as higher Root Mean Square (RMS) current value; increase in temperature of transmission lines and equipment causing losses and larger inefficiencies in the system.

This research work studies a filter named 'Shunt Active Power Filter' (SAPF) based on a PQ theory for reducing such harmonics caused due to non-linear loads. Our implementation uses a MATLAB/Simulink modeling technique to design the SAPF and PQ theory concepts. The filter models the active and reactive powers in time domain. Through our simulation and analysis, we observe that the results show significant reduction in harmonic components and can eliminate the power system stability problems yielding better efficiency.

**Keywords: Shunt Active Filter, Harmonics, PQ theory**

## I. Introduction

The use of non-linear loads in power electronic (PE) devices has been increasing continuously from the past 3 decades. With more and more dependency on PE devices, power system is being subjected to dynamic oscillations due to the non-linearity conditions. Traditionally, many types of solutions were proposed and they were somewhat helpful in reducing the level of impact on the system [1][2]. Some of them include in-line reactors, Static compensators, Passive filters, resonant filters and high pass filters. Power quality problem requires continuing monitoring and new methods to reduce the percentage of harmonics or inter-harmonics in the network.

Due to the limitations of classical filters and capacitors, active power filters are now seen as a viable alternative to compensate harmonics and reactive power in non-linear loads.

The objective of this active power filter design is to compensate the harmonic currents and voltages in addition to selective reactive power compensation such that the grid current or voltage waves can conserve the sinusoidal form.

## II. Key Figure

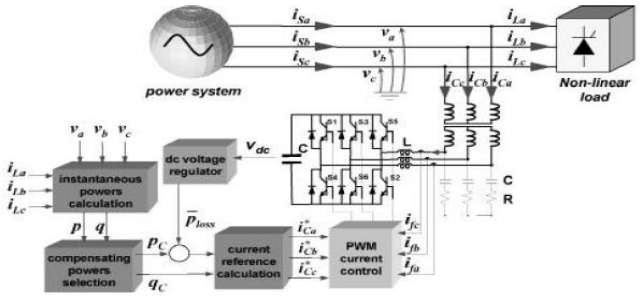


Figure 1. System Block Diagram of SAPF [1]

## III. THD Computation & Simulation

In the simulink design, we modeled the sources using virtual elements and bridge rectifier is treated as a non-linear load. The shunt active power filter is connected in parallel to the transmission line as shown in Figure 1. The simulation ran for a total period of 0.5 seconds, during which the SAPF is connected to the grid after 0.1 seconds. Thus, we understand the system behaviors in two conditions; 1) THD calculation with SAPF and 2) THD computation without SAPF. For the simulated model without SAPF, THD is 30.90% at t=0.3 seconds. With SAPF included, the computed THD is 2.91%.

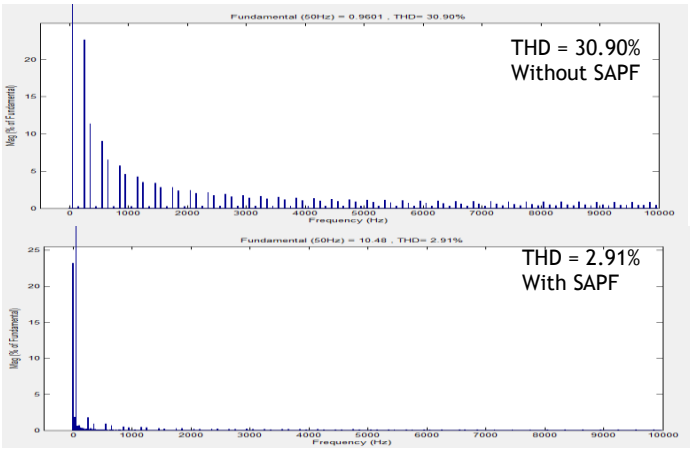


Figure 2. THD Simulation

## References

[1]. "Instantaneous Power Theory and Applications to Power Conditioning" by Hirofumi Akagi, Edson Hirokazu Watanabe and Mauricio Aredes.

[2]. H. Akagi, Y. Kanazawa and A. Nabae, "Generalized Theory of Instantaneous Reactive Power and its Applications," Transactions of the IEE-Japan, Part B, vol. 103, no.7, 1983

# PV Current Harmonic Suppression Under Unbalanced Fault Based on Factor Selection Control

Niancheng Zhou, Xiaoxuan Lou, *Student Member, IEEE,* David Yu, *Member, IEEE,* Qiang Fu, Qianggang Wang.

***Abstract*—Fault ride-through operation of three-phase photovoltaic (PV) inverters will produce apparent current harmonics under unbalanced grid fault. This paper mainly researches on power control of PV under unbalanced voltage, and has analyzed the total harmonic distortion (THD) and the feature of each order of the harmonics in the inverter currents. Then the analytic formulas of power fluctuation, current THD and odd harmonics in the current of the PV inverter were derived, and two algorithms of the adjustment coefficients of PV power control were proposed. The control strategy model of current harmonic suppression under unbalanced grid voltage was built. In addition, the feasibility of this method is verified by the simulation result produced by PSCAD/EMTDC.**

***Index Terms*—unbalanced voltage; photovoltaic; harmonic suppression; power fluctuation; odd harmonic**

## I. Introduction

The grid-connected PV system and its power control structure are shown in figure 1.

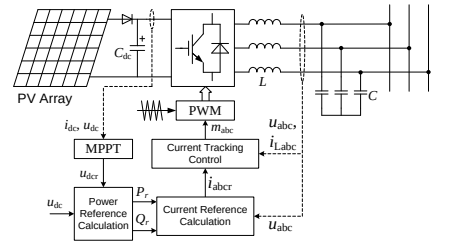


(a) The Structure of PV Generation System

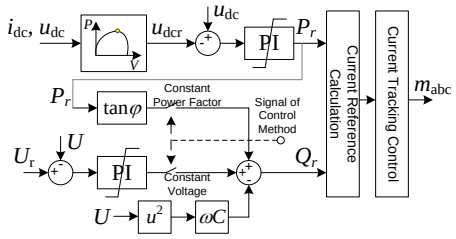


(b) Power Control of PV system

**Fig. 1 Grid-connected photovoltaic system**

This work was supported by National Natural Science Foundation of China (51277184); Scientific Research Foundation of State Key Lab. of Power Transmission Equipment and System Security (2007DA10512711209)...

## II. Key Expressions

The current reference with coefficients can be expressed as,

$$\boldsymbol{i}_{\mathrm{r}}(t)=\frac{P_{\mathrm{r}}[\boldsymbol{u}^{+}(t)+\alpha\boldsymbol{u}^{-}(t)]+Q_{\mathrm{r}}[\boldsymbol{u}_{\perp}^{+}(t)+\alpha\boldsymbol{u}_{\perp}^{-}(t)]}{|\boldsymbol{u}^{+}(t)|^{2}+(1+\alpha)\beta\boldsymbol{u}^{+}(t)\boldsymbol{u}^{-}(t)+\alpha|\boldsymbol{u}^{-}(t)|^{2}} \tag{1}$$

### A. Power Fluctuation Suppression

$$\Delta p=\left[\frac{\tilde{p}(t)}{p(t)\text{-}\tilde{p}(t)}\right]_{\max}=\frac{(1-\beta)(1+\alpha)n}{1-\beta(1+\alpha)n+\alpha n^{2}} \tag{2}$$

$$\Delta q=\left[\frac{\tilde{q}(t)}{q(t)\text{-}\tilde{q}(t)}\right]_{\max}=\frac{(1-\alpha)n}{1+\alpha n^{2}} \tag{3}$$

### B. Odd Harmonics and THD Suppression

$$THD=\sqrt{\frac{I^{2}}{I_{1}^{2}}-1}=\sqrt{\frac{A^{2}}{2C(B-C)}-1} \tag{4}$$

Where A=β(1+α)n, B=1+αn$^2$ and C=$\sqrt{B^{2}-A^{2}}$.

$$I_{3}=\frac{1}{\sqrt{2}}\sqrt{E_{3}^{\,2}+F_{3}^{\,2}}=\frac{P_{\mathrm{r}}(1+\alpha n)}{3U^{+}}\left[\frac{2B/A+1}{\sqrt{C(A+B)}}-\frac{2}{A}\right] \tag{5}$$

$$I_{5}=\frac{P_{\mathrm{r}}(1+\alpha n)}{3U^{+}}\left[\frac{4B^{2}/A^{2}+2B/A-1}{\sqrt{C(A+B)}}-\frac{4B}{A^{2}}\right] \tag{6}$$

$$I_{7}=\frac{P_{\mathrm{r}}(1+\alpha n)}{3U^{+}}\left[\frac{8B^{3}/A^{3}+4B^{2}/A^{2}-4B/A-1}{\sqrt{C(A+B)}}+\frac{2}{A}-\frac{8B^{2}}{A^{3}}\right] \tag{7}$$

The international standard for the PV generation system with a rated voltage of 380V and a rated capacity of 10MVA has formulated that odd current harmonics from 3rd to 9th should be lower than 0.0041pu、0.0041pu、0.0029pu and 0.0014pu.

Then the selection region of the coefficients $\alpha$ and $\beta$ should be in the shadow area, shown in figure 2:

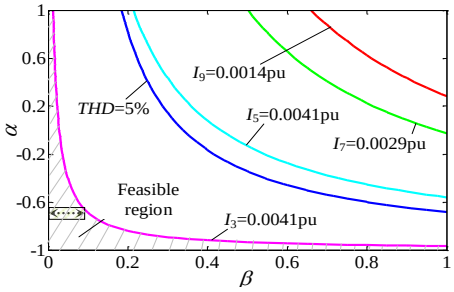


Fig. 2 The contour lines of odd current harmonics and current THD

## III. Simulation

The control method is verified in PSCAD/EMTDC with a rated capacity of 2.5kVA, L=12mH, C=0.7μH, Cdc=1800μH.

# Harmonic filtering phenomenon in single phase induction motors

Gaurav Singh, *Student Member, IEEE,* and E.R.(Randy) Collins, Jr., *Senior Member, IEEE*

***Abstract*—Single phase induction motors are widely used in household applications. This follows from their various attributes such as their simple and rugged construction, wide availability and low cost. For use in household devices such as refrigerators, air conditioners and pumps, capacitor start capacitor run motors are preferred, because of their higher efficiency and lower acoustical noise. This, coupled with the increasing usage of single phase rectifier front end devices in recent years, leads to an interesting scenario where single phase capacitor run motors are connected in shunt with a single phase full wave rectifier across a common feeder bus. Intuitively it is expected that this motor-rectifier combination will draw an extremely distorted harmonic rich current. However, recent work by the authors has shown that this is not the case. It has, in fact, been observed that the single phase induction motor absorbs a large quantity of the harmonic current, leading to a relatively harmonic free current being absorbed by the combination. This poster attempts to outline this harmonic filter like behaviour of the single phase capacitor run motor and it's implications for the power grid.**

***Index Terms*—Single phase, Induction motor, Rectifier, Filter, harmonics.**

## I. Introduction

TRADITIONALLY utilities have considered single large loads to be the main contributors to harmonics in the power grid. Household loads were not considered to be a serious threat to power quality. However, the recent advent of devices such as Compact Fluoroscent Lamps (CFL), personal computers and other consumer electronic devices, which utilize rectifier front ends has changed this scenario drastically. Single phase full wave rectifiers, employed by these devices, are rich sources of odd harmonics. The growing numbers of these devices is causing an accumulation of harmonics in distribution systems.

Another electrical device present in abundance in a modern household is the single phase capacitor run Induction motor. This leads to an interesting scenario where the single phase Induction motor is connected to a supply voltage which is rich in harmonics. This scenario was simulated in the laboratory and it's results have been shown here.

### A. Experimental work and results

The experimental setup utilized for this scenario has been shown in Fig. 1.

We expect this motor rectifier combination to draw a huge amount of harmonic current. However, the results obtained were unexpected in that the total current drawn by the combination is relatively harmonic free. The experimental work was done using three motors of representative sizes. Results from an experiment carried out with a 2HP motor have been shown in Fig. 2

Gaurav Singh and E.R.Collins, Jr. are with the Department of Electrical and Computer Engineering, Clemson University

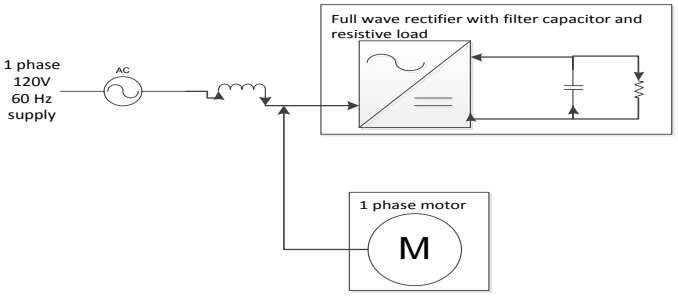


Fig. 1. Experimental circuit showing single phase cap run motor connected in parallel with single phase full wave rectifier

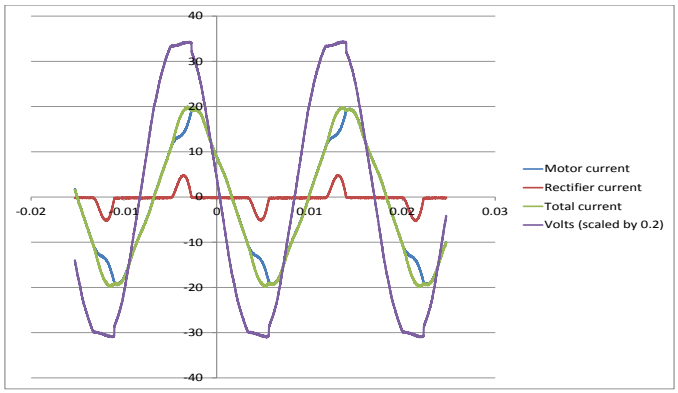


Fig. 2. Plot of voltage, motor current, rectifier current and total current when a 2HP motor is connected into the circuit. Note that voltage has been scaled down by a factor of 0.2 for illustration purposes.

## II. Conclusion

Because of the presence of a running capacitor, the auxiliary winding circuit of a single phase induction motor is essentially an RLC circuit with a resonant point. As a result, at dominant harmonic frequencies in households, the single phase induction motor represents a much lower impedance for harmonic currents produced by rectifier front end devices, as compared to source impedance. This causes harmonic cancellation in the total current absorbed by the house load. Cheap single phase motor drives that are sometimes employed by these devices, negate this characteristic. Thus, it turns out that single phase motor drives end up doing more harm than good to the power quality of a household.

# Modeling and Simulation of a High-Head Pumped Hydro System

Hang Li, Student Member IEEE, Gregory Parker
Brian K. Johnson, Senior Member IEEE,
Joseph D. Law, Member IEEE
Department of Electrical and Computer Engineering
University of Idaho
Moscow, Idaho USA
b.k.johnson@ieee.org

Kyle Morse
Donald F. Elger
Department of Electrical and Computer Engineering
University of Idaho
Moscow, Idaho USA

***Abstract*— Increasing penetration of intermittent renewable generation, such as solar or wind, will lead to the deviation of the power grid frequency from normal due to the randomness of the output renewable energy sources. Pumped storage can be used to balance the renewable output in a manner to regulate the frequency of the grid. This paper presents a feasibility study of a proposed pumped storage system used to regulate the frequency of power grid to meet the NERC CPS2 standard in response to variable renewable energy output. Studies are performed using dynamic electrical and hydraulic models of the pumped hydro system.**

## I. Overview

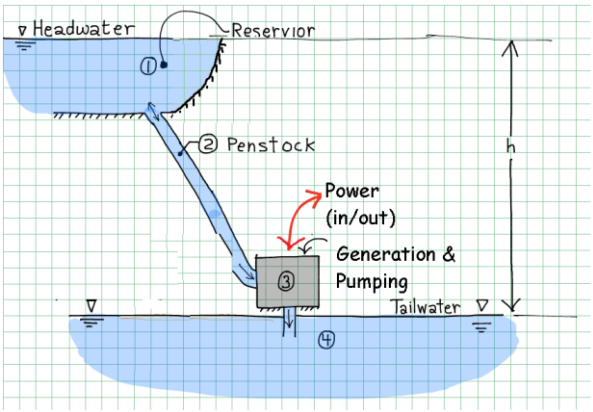


Fig. 1 Pumped storage system diagram

Fig. 1 shows a diagram of the pumped storage system. The points listed below illustrate the operation of the pumped storage system.

1) Energy is stored in the upper reservoir in the form of potential energy associated with the increased elevation of the water in the reservoir relative to the elevation of the tail water.
2) When the system is generating power, water flows down the penstock. When the system is pumping water, the water flows up the same penstock. Only one penstock is used to simplify the pump storage system design.
3) Electric machine located at the bottom of the penstock for generation and pumping
4) The tail water can be a lake or river at a lower elevation.

## II. Modeling

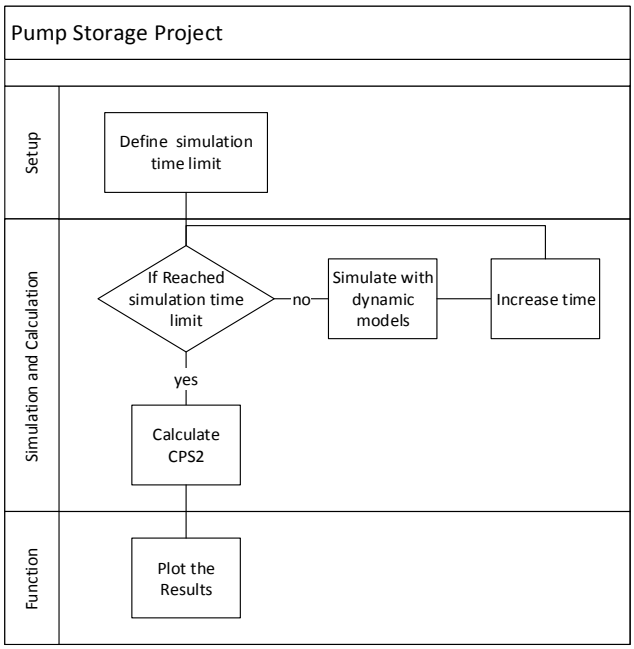


Fig. 2 Overall simulation flow diagram

## III. Simulation Results

There were four CPS2 violations during the total time period, giving a mean score of 92%.

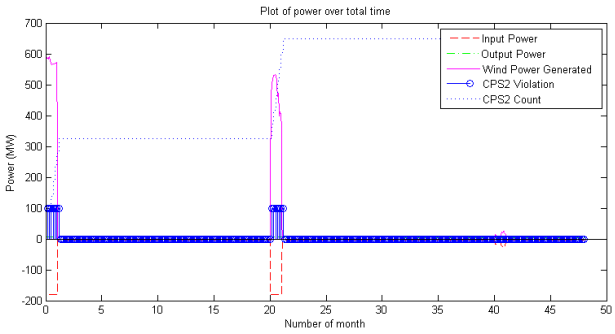


Fig. 3 Simulation result

# Developing Integrated Load Modeling Framework for Campus Microgrids with Large Buildings

Sayonsom Chanda, *Student Member, IEEE* and Anurag K Srivastava, *Senior Member, IEEE*
Smart Grid Demonstration and Research Investigation Lab (SGDRIL)
Washington State University, Pullman, WA, USA
sayonsom.chanda@email.wsu.edu

***Abstract*--- With ongoing smart grid efforts, electricity consumers of the future are expected to opt for energy conservation through demand response, establishing energy consumption patterns for trending analysis and microgrid implementation for higher reliability. Customers may also have an option to choose from which utility they draw their power. All these ongoing changes may lead to significant changes in distribution system power flows. To analyze and understand consumer behavior, it is required to develop detailed load models. This will help with the smart grid implementation process, and will provide better insights for developing global or local control systems.**

***Index Terms*--- ETP Model, ZIP Model, microgrid, SynerGEE, GridLAB-D, energy usage**

## I. Introduction & Motivation

Load modeling is critical for analyzing the functionality of the electrical grid, as loads eventually drive the need for power generation, transmission and distribution. The advent of smart grid and bilateral information exchange, has also brought newer kinds of power sources like fuel cells, and newer kinds of loads like electric vehicles, which will become increasingly mainstream. This raises a need of a framework to better organize the task of load modeling to expedite the process of development of detailed load models to help with power flow studies, planning, development and implementation of modern distribution systems. Developing a detailed load model is usually a tedious process, and requires inputs from contractors, maintenance and construction engineers. Hence, most campuses or large buildings do not have detailed load models, despite its evident benefits. However if a systematic automated approach, as shown in this poster (Fig.1), can be followed - detailed load models of campuses with large buildings can be developed.

## II. Methodology

The task is carried out using Open Source software, GridLAB-D, developed by Pacific Northwest National Laboratories (PNNL) [1]. Currently, utilities model their distribution systems using proprietary software like SynerGEE. So, the first step of this work is to develop a *converter* to translate the SynerGEE files (detailed enough to include building transformers or building data) into GridLAB-D.

To this "Detailed Load Model Developer" program, civil engineering data about building construction, weather data, obtained from different sources may be added. Additionally, information about distributed storage and distributed on-campus generators may be added in appropriate fields. All this information will be put in the correct syntax, and added to the existing one-line power distribution model converted from SynerGEE, to obtain the detailed GridLAB-D model. For future needs, several buildings or other information can be added as and when necessary.

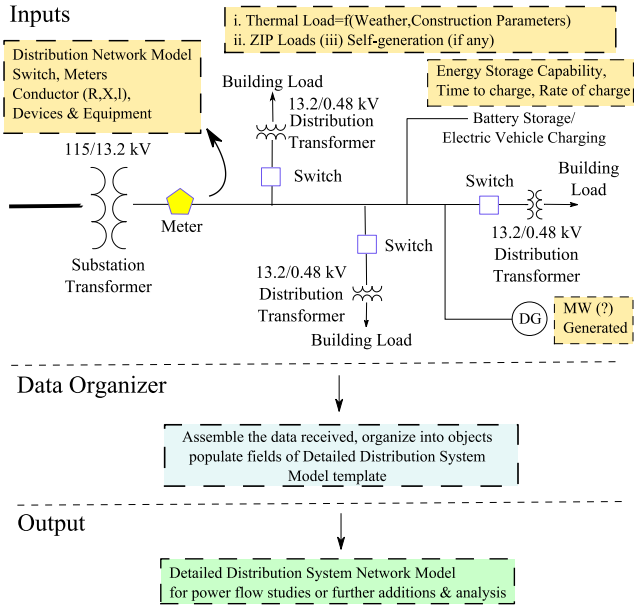


**Figure 1. Detailed Load Modeling Developer Framework**

## III. Applications of This Work

(i) Developing and testing of restoration strategies for higher reliability of power supply. (ii) This work may be extended to large commercial buildings as well. (iii) Modeling of generators and distributed energy resources for peak shaving, islanded microgrid operation. (iv) Facilitate the development of better control systems and algorithms to optimize the distribution system. (iv) Studying of newer kinds of distributed energy storage options like battery charging, electric vehicles and their impact on distribution system power flow.

## Reference

[1] Chassin, D.P, Schneider, K., Gerkensmeyer, C., "GridLAB-D: An open-source power systems modeling and simulation environment", *Transmission and Distribution Conference and Exposition, 2008. T&D.*

# Dynamic Modeling and Analysis on Cut-in Grid of Doubly-fed Induction Wind Power System

Sibei Mi [1, 2], *Student Member IEEE*, Jingqi Su and David Yu [1], *Senior Member IEEE*
1. College of Engineering and Applied Science, University of Wisconsin Milwaukee, WI, USA;
2. School of Electrical Engineering, Chongqing University, Chongqing, China
Email: sibeimi@uwm.edu

This poster introduces doubly-fed induction generator in the rotary $dq$ coordinate system dynamic mathematical model based on the basic principles of wind turbines. By studying on the grid control strategy of Doubly-fed induction generator, analysis vector control technology for dual PWM, and adopt PSCAD / EMTDC to establish the dynamic simulation model.

From (1), when wind speed remains unchanged, the output power of wind turbine varies while the wind speed changes. To track $P_{\max}$, the adjustments of $\omega_m$ must be in time when wind speed changes, and maintain the optimal tip speed ratio. Fan speed $\omega_m$ can be adjusted by varying the pitch of wind turbine blades or by controlling the output power of the generator.

$$P_{\max} = \frac{1}{2} C\mathrm{p}_{\max} A\rho v^3 = \frac{1}{2} Cp_{\max} A\rho (\frac{R}{\lambda_{opt}})^3 \omega_m{}^3 \qquad (1)$$

There is the rotary $dq$ coordinate system dynamic mathematical model of the doubly-fed induction generator. Equations of the rotor

$$T_l - T_e = \frac{T_J}{N_P}\frac{d\omega_r}{dt} = T_1 - \frac{3N_P}{2} L_m (I_{sd} I_{rq} - I_{sq} I_{rd}) \qquad (2)$$

When study the electromechanical transient of the parallel-operate doubly-fed induction wind turbines, the dynamic process of the stator winding circuit can be not taken into consideration.

Therefore, the voltage equations of the stators turn into:

$$\begin{cases} U_{sd} = R_s(-I_{sd}) - \omega_1 L_s^{'}(-I_{sq}) + E_d \\ U_{sq} = R_s(-I_{sq}) - \omega_1 L_s^{'}(-I_{sd}) + E_q \end{cases} \qquad (3)$$

Differential equation of stator inner potential:

$$\begin{cases} \frac{dE_d}{dt} = -\frac{R_r}{L_r}\left[E_d - \omega_1(L_s - L_s^{'})I_{sq}\right] + s\omega_1 E_q - \frac{L_m}{L_r} U_{rq} \\ \frac{dE_q}{dt} = -\frac{R_r}{L_r}\left[E_d + \omega_1(L_s - L_s^{'})I_{sd}\right] - s\omega_1 E_d + \frac{L_m}{L_r} U_{rd} \end{cases} \qquad (4)$$

(2),(3)and(4)constitute the dynamic model of the doubly-fed induction generator. From (3) we can get the equivalent circuit of the doubly-fed induction generator showing in Figure 1.

Under the state of different energy flow of the rotor, the two converter achieve the functions of rectifier and inverter alternatively. For AC excited generator, when it operates in sub-synchronous state, rotor winding absorbs slip power, and grid side converter operates in PWM Rectifier state while the rotor-side converter operates in PWM inverter status. When it operates in super-synchronous state, part of the slip power drives back from the exciter rotor winding through grid, and rotor-side converter operates in PWM Rectifier state while the grid side converter operates in PWM inverter status

Simulation analysis of operating characteristics shows in Figure 2. Before 0.5 seconds, generator is controlled by the speed, and after that it is controlled by pitch angle. In steady-state operation, set the voltage to be 0.69p.u.. As showing in Figure 2, the simulation result is between 0.6p.u.and 0.7p.u. which is quite close to the set-point. Grounding fault happened at 3rd second, and the voltage dips to about 0.25p.u.. After 0.2 seconds, failure is excluded. Then after a very short time of oscillation, the voltage quickly runs back to the normal working value. The simulation shows that the unit has a strong resiliency.

## KEY FIGURES

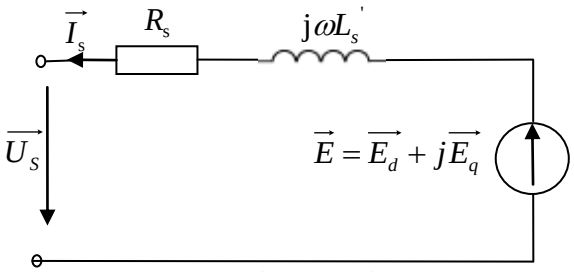


Figure 1. Equivalent circuit of the doubly-fed induction generator

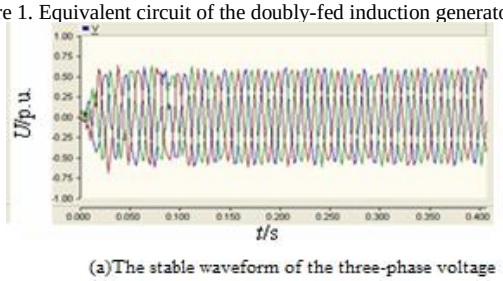


(a)The stable waveform of the three-phase voltage

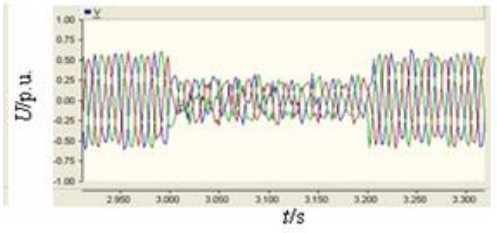


(b) The fault waveform of the three-phase voltage

Figure 2. Three-phase voltage of generator outlet